To the Graduate Council:

I am submitting herewith a thesis written by Benan Basoglu entitled "Analysis of a Hypothetical Criticality Accident Involving Damp Low-enriched UO_2 Powder." I have examined the final copy of this thesis for form and content and recommend that it be accepted in partial fulfillment of the requirements for the degree of Master of Science, with a major in Nuclear Engineering.

H.L. Dodds, Major Professor

We have read this thesis
and recommended its acceptance:

Paul N Stevens

Belle R Upadhyaya

Accepted for the Council:

Associate Vice Chancellor
and Dean of the Graduate School

Analysis of a Hypothetical Criticality Accident Involving Damp Low-enriched UO_2 Powder

A Thesis

Presented for the

Master of Science

Degree

The University of Tennessee, Knoxville

Benan Basoglu

August 1992

DEDICATION

This thesis is dedicated to the memory of my grandfathers, Hüseyin Coşkun Güvenç *(Ankara, b.1925-d.1985)* and Müştak Başoğlu *(Erzurum, b.1888-d.1972)*. May the mercy of God be upon them.

Bir katredir ancak aldığım hep,
Derya yine durmada lebalep.

The things I've chosen are a drop, no more,
The undiminished sea still crowds the shore.

Ziya Pasha (Ottoman Poet, b.1829-d.1880)

ACKNOWLEDGEMENT

The work in this research could not have been completed successfully without the invaluable supervision and support of my advisor, Dr. H.L. Doods, Jr. I would like to express my deepest gratitude to him.

I would also like to extend my gratitude to the other members of my committee, Dr. P.N. Stevens, Dr. B.R. Upadhyaya for their suggestions and for serving on my committee, and Dr. P.F. Pasqua for his priceless advice and help throughout the course of my work.

I would like to thank the many present and former members of the Nuclear Criticality Safety group of the University of Tennessee who contributed through their discussion and help, particularly: W.D. Newmyer, D.L. Hollenbach, C.F. Haught, R.W. Brewer and A.D. Wilkinson.

The use of SCALE-IV system would not have been possible without constant help given by Mike Westfall, Bill Herman, Nancy Landers, and the other staff members in Building 6011 of the Oak Ridge National Laboratory.

I also appreciate the cooperation of the personnel of the Westinghouse Fuel Fabrication Plant in Columbia, South Carolina. Specifically, the help of W.L. Goodwin, R. D. Montgomery, and N. A. Kent during various phases of this work was truly exceptional.

In addition, I wish to express my appreciation to Evren Eryurek, system manager of U.T.N.E. VAX Workstations, for his patience and technical assistance; to

T.D. Radcliff for helpful technical discussions; to L.H. Tsoukalas for motivating and helping me to write a paper on Nuclear Criticality Safety; to the U.S. Nuclear Regulatory Commission for financial support for this research via R.E. Wilson; and to the University of Tennessee for providing my education.

Finally, I would like to thank all of my fellow colleagues, the academic and technical staff in the Department of Nuclear Engineering, especially, W. Yan, B. Dange, and L. Holbrook for their support.

ABSTRACT

In this work, we report on the development of a computer model for predicting the excursion characteristics of a postulated criticality accident involving a homogeneous mixture of low-enriched UO_2 powder and water contained in a cylindrical blender. The model uses point neutronics coupled with simple lumped-parameter thermal feedback. The reactivity feedback coefficients, reactivity driving force function, and the mean generation time are computed *a priori* using Criticality Safety Analysis Sequences No.1(CSAS1X) and No.2(CSAS25) in the SCALE-IV system. The temperature of the system is calculated using a simple time-dependent energy balance where two extreme conditions for the thermal behavior of the system are considered which bound the real life situation. These extremes are zero and infinite heat transfer coefficients(0-HTC and ∞-HTC, respectively) between the major components(i.e., the powder and the water) of the system. Using these extremes, three different models are developed where the first model assumes the 0-HTC. The second model utilizes the ∞-HTC where the system is assumed to be vented(i.e., open at the upper end) under constant atmospheric pressure with any steam produced leaving the system instantly. The third model also assumes ∞-HTC but the system is not vented(i.e., closed at the upper end and the total volume of the system remains constant). The resulting time-dependent coupled set of ordinary differential equations is solved numerically using the Livermore Solver of Ordinary Differential Equations(LSODE). To evaluate the models, we compared our results

with the results of the POWDER code which was developed by CEA/UKAEA(France/UK) for damp powder systems. The agreement in these comparisons is quite satisfactory.

Results of the excursion studies in this work show that approximately 10^{19} fissions occur as a result of accidental water ingress into powder blenders containing 5000 kg of damp low-enriched(5%) UO_2 powder.

TABLE OF CONTENTS

SECTION **PAGE**

LIST OF TABLES

TABLE **PAGE**

LIST OF FIGURES

FIGURE **PAGE**

FIGURE **PAGE**

FIGURE **PAGE**

FIGURE **PAGE**

FIGURE **PAGE**

FIGURE **PAGE**

FIGURE **PAGE**

Chapter 1

INTRODUCTION

1.1. Background

Nuclear Criticality Safety plays a major role in any step of the nuclear fuel cycle if an accidental criticality is possible [1]. A generic fuel cycle involves facilities for mining, milling, processing, enrichment, fuel fabrication, reactor, interim storage, reprocessing, and final disposition. Facilities for mining and milling of uranium have no plausible criticality safety concerns. Criticality in the reactor core usually does not present criticality safety concerns. Enrichment plants do present a criticality safety concern where the major focuses are the production of the solidified uranium fluoride compounds, accidental moderation of slightly enriched systems, and dry criticality for highly enriched systems. Criticality control strategies are applied in reprocessing, interim storage, transportation, and final disposition facilities.

Nuclear fuel fabrication for Light Water Reactors (LWR) involves a variety of physical and chemical processes for low-enriched uranium (LEU). First of all, the LEU in the form of UF_6 is received from the enrichment facility whose maximum output is ~ 5 wt% U^{235} for LWR systems. Conversion of UF_6 to UO_2 powder can be a challenging step in terms of criticality safety since this process involves aqueous substances. Thus, appropriate moderation control measures are taken in order to prevent an accidental criticality.

Similarly, UO_2 powder is milled, blended, pressed, and sintered into a final pellet. All these processes as well as interim powder storage are maintained dry since accidental moderator ingress into the components may make the system critical. However, accidental water flooding is usually a credible contingency for all of the steps and is, therefore, the basis for most of the criticality safety limits.

In fuel fabrication facilities, blending systems have been identified as one of the most hazardous components which may result in accidental criticality involving low-enriched damp uranium oxide powders [2]. A blender is a large conically shaped container used to blend dry oxide powder to attain uniform physical and chemical characteristics as required by product and process specifications and relies principally on moderation control for nuclear criticality safety [3,4]. The blending system consists of a powder feed hopper contained inside a ventilation hood, a transfer system, and a dispensing hopper with a discharge screw. It is also provided with a ventilation system equipped with a dual HEPA filter and a powder mixing mechanism. Actual sizes and a schematic of a 5000 kg orbital screw blender are shown in Figures 1.1 and 1.2, respectively [2,5,6].

The operation of blenders is subject to criticality reviews since accidental ingress of water might cause a criticality. Figure 1.2 also shows the input/output lines which can provide potential water leakage routes into the blender. Westinghouse has performed some criticality safety studies for large cone blenders [5,6,7]. Their work includes criticality calculations for dry material mixing. They also studied the effects of several different moderator materials such as water and ammonium oxalate.

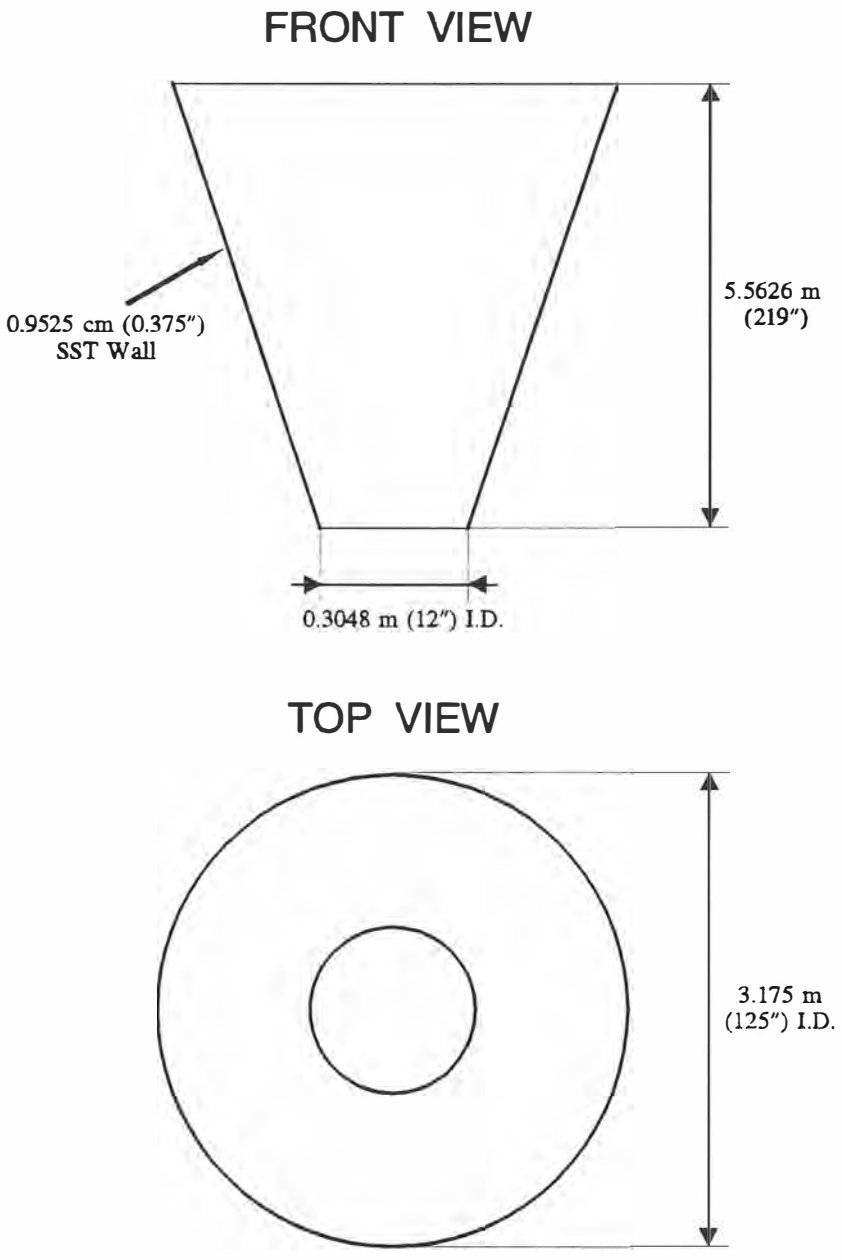

FIGURE 1.1 Dimensions for the 5000 kg Orbital Screw Blender (Not to Scale).

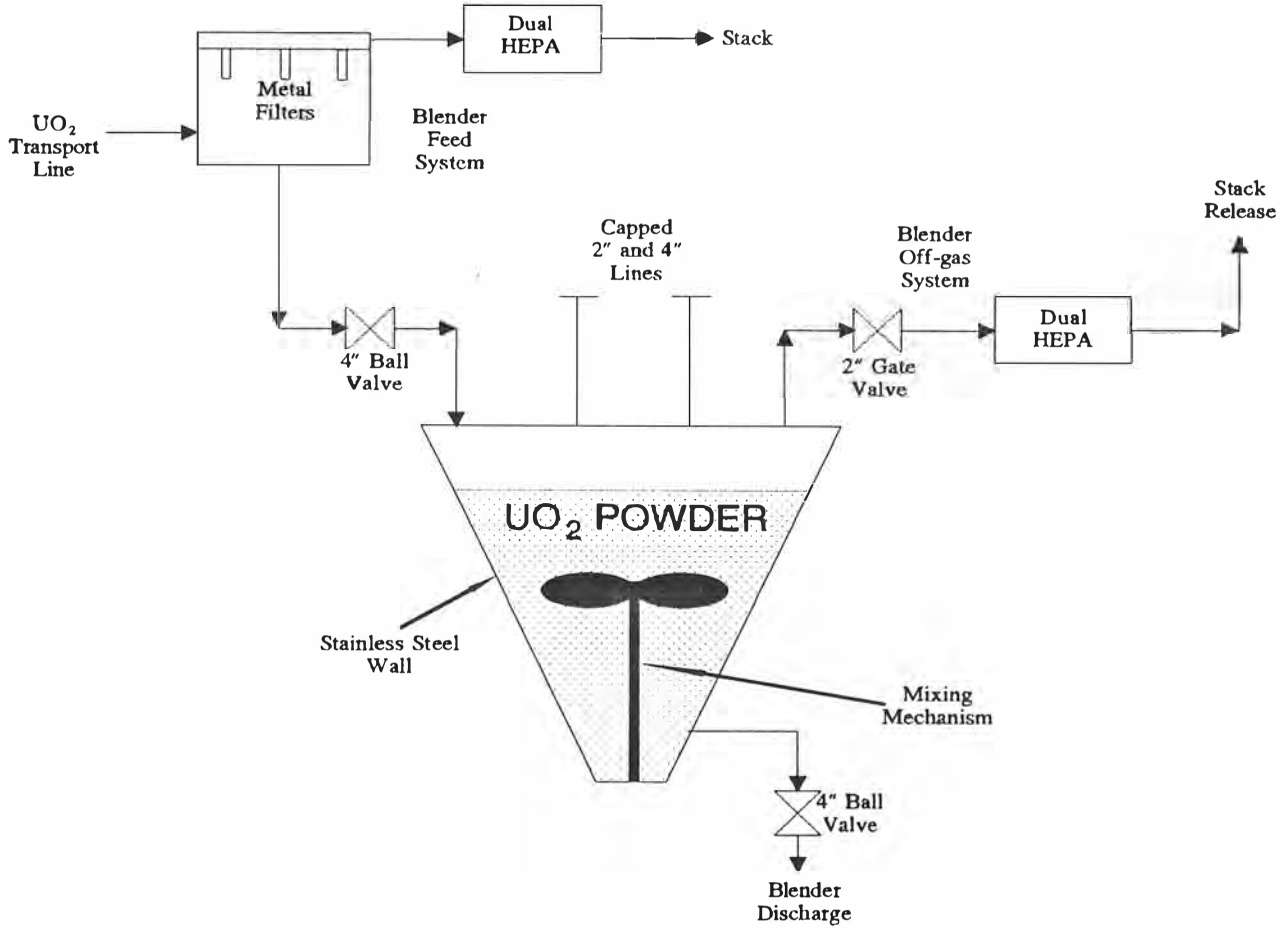

Figure 1.2 Potential Water Ingress Routes into Blender (Not to Scale).

According to Westinghouse documents, each 5000 kg capacity blender contains up to 120 potential critical masses of low-enriched uranium oxide if accidentally moderated [4]. However, there is no information available in the literature on the transient characteristics of postulated hypothetical criticality accidents in the operation of blending systems.

Moreover, the U.S. Department of Energy (DOE) has released two safety notices regarding lessons learned in nuclear criticality safety with respect to the operational experience in governmental and commercial facilities. The first notice was issued in September 1991 entitled "Criticality Safety Moderator Hazards" (*DOE-NS-0003, Issue No. 91-1*). It describes an event where water from an air conditioning system was inadvertently introduced into a portion of a dry process area containing highly enriched uranium (HEU) causing a potential criticality safety problem. This event took place on June 6, 1991 at the DOE Y-12 plant near Oak Ridge, Tennessee. The second notice was distributed in February 1992 with the title of "Criticality Safety Hazards Associated With Large Vessels" (*DOE-NS-0006, Issue No. 92-1*). It reports an event in which 150 kg of LEU solution was accidentally introduced into a large waste treatment vessel on May 28, 1991 at the General Electric (GE) Nuclear Fuel and Component Facility located near Wilmington, North Carolina. These events illustrate the importance of considering accidental water leakage in large vessels such as powder blenders. Powder blenders may also experience criticality system control violations as well as these real-life examples. Also, U.S. Nuclear Regulatory Commission (NRC) statistics indicate that every commercial facility experiences

some type of water flooding incident at least once every ten years.

To illustrate the importance of accidental water ingress into a blender, consider a rate of water ingress of 0.5 l/sec (0.1321 gal/sec) through the UO_2 transport line or the ventilation system shown in Figure 1.2 while the blender operates with 5000 kg of UO_2 powder at a density of 2.2 g/cm^3. The system achieves delayed critical after approximately 16 minutes with an H/U ratio of ~ 3. At delayed critical, the power starts to rise resulting in a criticality excursion. However, knowledge on the characteristics of such an excursion accident in a blender is very limited.

1.2. Survey of Previous Work

The evaluation of off-site and on-site effects of criticality accidents requires an understanding of the potential consequences of such accidents. For any proposed accident, it is the fission energy estimate that ultimately determines the dose at the plant boundary. The fission energy release from criticality accidents involving liquid and metal assemblies has been well established from both experimentally induced excursion data and computational analysis [8,9].

A good example is the CRAC experiments which were performed from 1968 through 1971 by Commissariat à l'Énergie Atomique (CEA)[a] using highly-enriched uranium fissile solutions [10]. During these experiments, 40 excursions were observed for a wide range of solution concentrations and ramp reactivity additions.

DOSAR and SHEBA experiments were performed at the Oak Ridge National

[a] French Atomic Energy Commission

Laboratory (ORNL) and the Los Alamos National Laboratory (LANL), respectively, for the assessment of the minimum criticality accident of concern [11]. Also, the SLOPULS code was developed to simulate a slow rising power pulse associated with a minimum criticality accident. DOSAR experiments were performed to determine the thermal cycling characteristics of low-power events. SHEBA experiments were performed with the 5% U^{235} enriched solution to define the pulse characteristics of a low-power criticality in a solution. The SHEBA work also included a qualitative comparison of LOPCA and SPIKE accidents.[b]

Other examples of criticality experiments with fissile solutions include KEWB and SILENE [12]. KEWB stands for Kinetics Experiment Water Boiler where spherical and cylindrical unreflected or graphite reflected cores were used to measure the excursion characteristics of fissile solutions. The excursions were initiated by a fast moving horizontal pulse rod. The fuel for all experiments was uranyl sulfate solution with a ~93 wt% U^{235} enrichment at uranium concentrations from 57 to 203 g of U^{235}/l. Similarly, SILENE is the French small solution pulsed reactor where the excursion is initiated by a vertical rod [13]. SILENE experiments were done to study fission gas release rates during excursions, boiling type-experiments, and the pressure wave associated with radiolotic gas formation due to the first pulse.

---

[b] LOPCA stands for LOw Power Criticality Accident where it is defined as an accident having long initiation period(20-30 minutes) with insignificant temperature rise, long oscillatory period(several hours) and a low peak power(less than 10 kilowatts). SPIKE represents the accidents which have a very short(less than 5 seconds) initiation period with a fast temperature increase, a short oscillatory period and a high peak power(several thousand kilowatt-hours). SPIKE accidents can result in violent reactions such as bubbling and splashing.

Also, the transient behavior of moderated solid cores has been studied in the SPERT and TRIGA experimental programs, while very fast transients in simple, unmoderated systems are well understood as a result of GODIVA and other fast-burst reactors [14]. The SPERT experiments were performed to investigate the transient behavior of light and heavy water moderated and cooled, highly-enriched, uranium-aluminum and UO_2-stainless steel fueled plate type reactors [15]. The results of all these experiments are frequently used to validate computer codes on the excursion characteristics of fissile systems.

Furthermore, a considerable amount of theoretical and computational study has been done to simulate the physical phenomena occurring in criticality excursions. The analysis of postulated, moderated criticality accidents at ORNL involving fissile liquid systems were considered in Reference 16. This work calculated the initial fission pulse due to a hypothetical excursion and the resulting on-site and off-site radiation doses using a combination of Hansen's and Tuck's methods. Hansen's method contains a theoretical model for fissile systems having a weak inherent neutron source where the transient behavior of the system may significantly depart from the one predicted by conventional point kinetics [17]. It provides the probability of the first persistent chain reaction occurring in a given time interval and the fission yield of the fissile assembly undergoing a ramp or a step reactivity addition. Tuck's method provides simple correlations for the maximum number of fissions in the first fission pulse, the specific fission rate in the first pulse, and the total fission yield of the accident based on experimental data as well as computational results [18]. These

correlations are developed for vertical cylindrical vessels, 28 cm to 152 cm in diameter and separated by more than 30 cm from the bottom reflecting surface. Additions of up to 500 g/l of solutions of U^{235} and Pu^{239} to the vessel are considered at rates from 2.65 l/min to 28.39 l/min. Also, a simple technique developed by Lutz can be used to implement Hansen's method into numerical calculations [19]. This technique is described in Section 2.5.

The CRITEX, CREST, FELIX, and EXCUR computer codes were developed by United Kingdom Atomic Energy Authority (UKAEA), Mitsubishi Atomic Industries Inc.-Japan, GRS-FRG[c], and Rocky Flats, Colorado respectively, to model criticality excursions for fissile solutions using point kinetics model with simple thermal hydraulic feedback [20,21,22,23].

Other computer codes exist to perform a wide range of criticality transients which include SKINATH, PAD, CHATEAU and SARTEMP. SKINATH (Simple KINetics And Thermal-Hydraulics) is a computer code for solving the reactor point kinetics equations coupled with a simple thermal-hydraulic feedback model for a reactor in the shape of a long horizontal cylinder which is cooled externally by an ideal gas via natural convection [24]. It essentially incorporates the theoretical foundations developed for the SLOPULS code. PAD stands for PAjarito Dynamics program which was developed to model dynamic systems with interactive neutronics, thermal-hydraulics, and hydrodynamics in one-dimensional spherical, cylindrical, and planar

[c] Gesellschaft für ReaktorSicherheit Forschungsgelände (Institute for Reactor Safety Research), the Federal Republic of Germany.

geometries [25]. It has been applied to critical excursions in various fissioning systems such as solution, metal, LMFBR etc. where the thermodynamics of solids, liquids, and vapors as well as phase transitions are considered. CHATEAU and SARTEMP were developed by CEA and UKAEA, respectively, to analyze hypothetical accidents involving irradiated fuel elements [26]. Also, the SKINATH-DP code has been developed for the analysis of a hypothetical criticality accident involving dry high-enriched uranium (HEU) of UO_3 and UF_4 [27,28].

More recently, the CEA/UKAEA performed a transient analysis of wetted UO_2 powder systems which included both model development (i.e., POWDER code) and some experimental work [29,30,31]. Their hypothetical scenario considers the introduction of water at 0.5 l/s at the top of a cylindrical vessel containing 500 kg of 5 wt% U^{235} enriched UO_2 powder. POWDER is the only code of this nature where the results are reported in the open literature.

Hence, since very little computational work has been performed on the excursion characteristics of near-dry or damp powder assemblies, new models and computer codes are needed to help understand the consequences of such accidents. Finally, a statement by E.R. Woodcock from Reference 32 regarding criticality accidents further provides the motivation for this research:

> We have discussed powder/liquid systems. This estimate is rather a shot in the dark. Nevertheless, it is certain that exceptional efforts should be made to avoid this type of situation.

1.3. Research Objectives

This study provides a theoretical model for evaluating the consequences of accidental water leakage into a large blender containing low-enriched UO_2 powder. The research consists of developing a computer simulation model which predicts the time-dependent history of the accident scenario. The model consists of a coupled system of neutronic and thermal-hydraulic equations which are solved numerically using the Livermore Solver of Ordinary Differential Equations (LSODE).

The results of this simulation will be useful in calculating the data required to understand and evaluate the off-site and on-site effects of such accidents; i.e. the fission burst, the energy released, the subsequent power history, the powder and water temperature histories, etc.

1.4. Scope and Organization

This thesis contains seven chapters. The first chapter provides some background including a sample accident scenario as well as a survey of previous work and the research objectives.

Chapter 2 discusses neutronic modelling. In Chapter 2, the reader will also find discussions on the identification and calculation of the physical phenomena which may result in significant reactivity changes for a damp powder system. Chapter 3 illustrates thermal-hydraulic modelling along with the heat transfer correlations used in SKINATH-WP.

Chapter 4 contains a description of the SKINATH-WP code. Chapter 5 considers the verification efforts of SKINATH-WP and also presents a brief description of the POWDER code developed by France and the United Kingdom.

Chapter 6 describes the results of this research including sensitivity and parametric studies regarding the transient characteristics of potential hypothetical criticality accidents in the operation of a powder blender. Finally, conclusions and recommendations are presented in Chapter 7.

Chapter 2

ACCIDENT MODELLING: NEUTRONICS

2.1. Point Kinetics

The general kinetics equations can be derived from transport theory by assuming the flux can be written in the form [33]

$$\Phi(x,t) = \psi(x,t)\,n(t), \tag{2.1}$$

where $\psi(x,t)$ is a time-dependent shape function, $n(t)$ is time-dependent amplitude function, and x represents all variables other than time (i.e., space, direction, and energy). This amplitude function satisfies the kinetics equations

$$\frac{dn(t)}{dt} = \{\frac{\rho(t)-\beta}{\Lambda}\}n(t) + \sum_{i=1}^{M}\lambda_i C_i(t) + S(t) - W(t)\,n(t) \tag{2.2}$$

and

$$\frac{dC_i(t)}{dt} = \frac{\beta_i}{\Lambda}n(t) - \lambda_i C_i(t) - W(t)\,C_i(t). \qquad i=1,2,..,m \tag{2.3}$$

$W(t)$ arises due to the general normalization and is given by

$$W(t) = \frac{d}{dt}\{\ \ln\int dx\,\psi_0^*(x)\frac{1}{v}\psi(x,t)\ \}, \tag{2.4}$$

where $\psi_0^*(x)$ is the arbitrary flux for a reference critical configuration, and v is the neutron speed. If the shape function obeys the restriction (i.e., by assuming the time

dependence of the flux is truly separable from the other variables) [34,35]

$$\frac{d}{dt}\{ \int dx \psi_0^*(x) \frac{1}{v} \psi(x,t) \} = 0. \qquad (2.5)$$

Equations (2.2) and (2.3) reduce to the traditional kinetics equations

$$\frac{dn(t)}{dt} = \{\frac{\rho(t) - \beta}{\Lambda}\} n(t) + \sum_{i=1}^{M} \lambda_i C_i(t) + S(t) \qquad (2.6)$$

and

$$\frac{dC_i(t)}{dt} = \frac{\beta_i}{\Lambda} n(t) - \lambda_i C_i(t). \qquad i=1,..,m \qquad (2.7)$$

The physical interpretation of the various parameters appearing in these equations depends on the normalization condition which is arbitrary. The formal definition of these parameters may be carried out if we assume that the neutron balance in the system can be approximated by one-group, age-diffusion theory [34]. Therefore, $\psi_0^*(x)$ is replaced by the steady-state shape function since the flux $\phi(x,t)$ becomes independent of energy and direction. From these assumptions, the quantities β, Λ, and $\rho(t)$ are interpreted as the total delayed neutron fraction, neutron mean generation time (sec), and total system reactivity ($(k_{eff}(t)-1)/k_{eff}(t)$), respectively. The one-group, age-diffusion theory approximation may be satisfactory for large homogeneous damp powder systems; however, age theory is more appropriate for describing the slowing down of neutrons in heavy moderators. It can still provide useful information regarding the moderation of neutrons in water (i.e., hydrogen) [36].

Hence, in the modelling described herein, the point kinetics equations are used

as an approximation because of the interpretation of the parameters in Equations (2.6) and (2.7), and because of the restriction given in Equation (2.5). Moreover, the separability of the time variable also involves some assumptions where the reader may refer to Reference 34 for further discussion. For all of the applications in this work, it is assumed that Equation (2.6) and (2.7) provide a satisfactory estimate of the neutronics excursion for damp low-enriched powder systems. The extraneous source neutron generation rate $S(t)$ in Equation (2.6) is taken to be zero [28]. $C_i(t)$ and $n(t)$ are interpreted as the quantity proportional to the precursor concentration for group i and the time dependent system power (fissions/sec), respectively. Furthermore, in the context of the above assumptions, the neutron density has a fixed spatial distribution when the reactivity changes.

2.2. Delayed Neutron Data

In fissile systems, most of the fission neutrons are released essentially instantaneously with the fission event. However, a very few neutrons appear with a considerable time delay. These delayed neutrons originate from the decay of fission fragments which, after a beta decay, are unstable with respect to number of neutrons in their nuclei. At least 45 species have been identified in neutron-induced fission as producing delayed neutrons. It is customary to group these precursors in six groups where each group is characterized by an approximate decay constant λ_i. The fraction of the total neutron population which appears in the i^{th} group is β_i [37]. Also, the number of delayed neutron precursor groups, m in Equations (2.6) and (2.7), is equal

to six for the present analysis.

Although these delayed neutrons are of minor importance in steady-state critical systems, they are extremely important during transients. In Table 2.1, we have listed the λ_i and β_i values for a thermal U^{235} system which are used as the delayed neutron data in this work. These data are calculated for each precursor group characterizing the principle isotope U^{235} (since in thermal low-enriched UO_2 systems, practically only one isotope fissions) as recommended by ENDF/B-IV and Reference 38. The total delayed neutron fraction can be calculated using Table 2.1 as

$$1 = \sum_{i=1}^{6} \frac{\beta_i}{\beta} \quad \leftarrow \quad \beta = \sum_{i=1}^{6} \beta_i \,. \tag{2.8}$$

TABLE 2.1
Delayed Neutron Decay Constants and Yields from
Thermal Fission of U^{235}

i	λ_i	β_i/β
1	0.0124 ± 0.0003	0.033 ± 0.003
2	0.0305 ± 0.0010	0.219 ± 0.009
3	0.111 ± 0.004	0.196 ± 0.022
4	0.301 ± 0.011	0.395 ± 0.011
5	1.14 ± 0.15	0.115 ± 0.009
6	3.01 ± 0.29	0.042 ± 0.008

2.3. Reactivity Changes

The total system reactivity $\rho(t)$ can be written as the sum of external and feedback reactivities:

$$\rho(t) = \rho_{external}(t) + \rho_{feedback}(t). \tag{2.9}$$

The estimation of the external reactivity requires the calculation of an algebraic function of reactivity with respect to water concentration (driving force function). The Monte Carlo method is the most accurate method for calculating reactivity feedback coefficients and the reactivity driving function for conically shaped systems. However, the computational cost increases with an increase in accuracy which constitutes a significant drawback for this method. On the other hand, the discrete ordinates method solution of the one-dimensional transport equation is much more economical for generic calculations for a wide range of problems.

Therefore, the reactivity driving force function is calculated using Criticality Safety Analysis Sequence No.1 (CSAS1X) with 27 group ENDF/B-IV cross sections in the SCALE-IV system developed at the Oak Ridge National Laboratory [39]. The CSAS1X control sequence activates the cross-section processing codes BONAMI-S and NITAWL-S to provide resonance corrected cross-sections and XSDRNPM-S to calculate the effective multiplication factor (k_{eff}) of the system [40]. XSDRNPM-S code utilizes the discrete ordinates method for solving the neutron transport equation and is applicable only to problems which can be described by simple one-dimensional geometry. Thus, the cone blender was approximated as a buckled cylinder where the approximated cylindrical system and the original conical system have the same

density, volume, and height. We used a buckled one-dimensional radial model of the cylinder as depicted in Figure 2.1 which shows the dimensions for the original conical and the approximated cylindrical systems.

Figure 2.2 presents the results of the external reactivity driving force calculations using SCALE-IV/CSAS1X where the driving force is the change in the homogeneous water content in g/cm^3. According to Westinghouse documents, *a normal operating condition* would consist of an H/U ratio of 1 with a density of 1 g UO_2/cm^3. A density of 2.2 g UO_2/cm^3 is the most reactive for 5 w/o U^{235} enriched UO_2 [6,41]. Thus, the density of UO_2 was assumed to be constant, namely 2.2 g/cm^3, and the H/U ratio was varied between 0 to 10.86 for the driving force calculations. The upper limit for the H/U ratio was established by a parametric study as the ratio when the water content fills all the void space of the UO_2 porous powder body. Figure 2.2 also shows a 9th order polynomial fit of the calculated data is used as the driving force function in the transient calculations. This function can be formulated as

$$\rho_{external}(t) = C_1 x(t)^9 + C_2 x(t)^8 + \ldots + C_i x(t)^{(10-i)} + \ldots + C_9 x(t) + C_{10} , \qquad (2.10)$$

where $x(t)$ is the water concentration (g/cm^3) at time t. Constants C_1 to C_{10} for Equation (2.4) are given in Table 2.2 for 5000 kg of 5 w/o U^{235} enriched UO_2 powder loaded into the cylindrical system described above.

The reactivity feedback effects caused by system temperature changes are moderator evaporation, powder thermal expansion, and a change in resonance absorption due to a change in temperature (i.e., the doppler effect). Thus, the

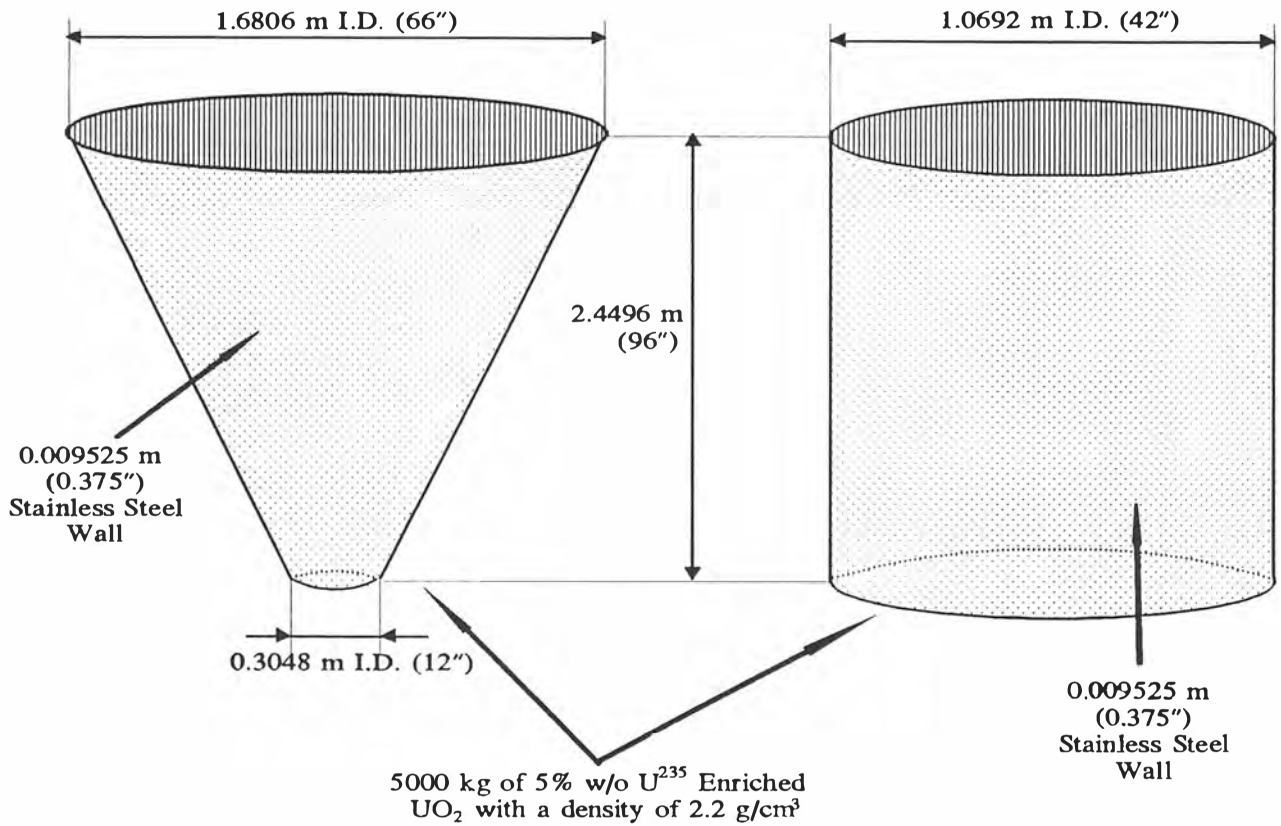

Figure 2.1 Dimensions for the Original Conical and the Approximated Cylindrical Shaped Systems (Not to Scale).

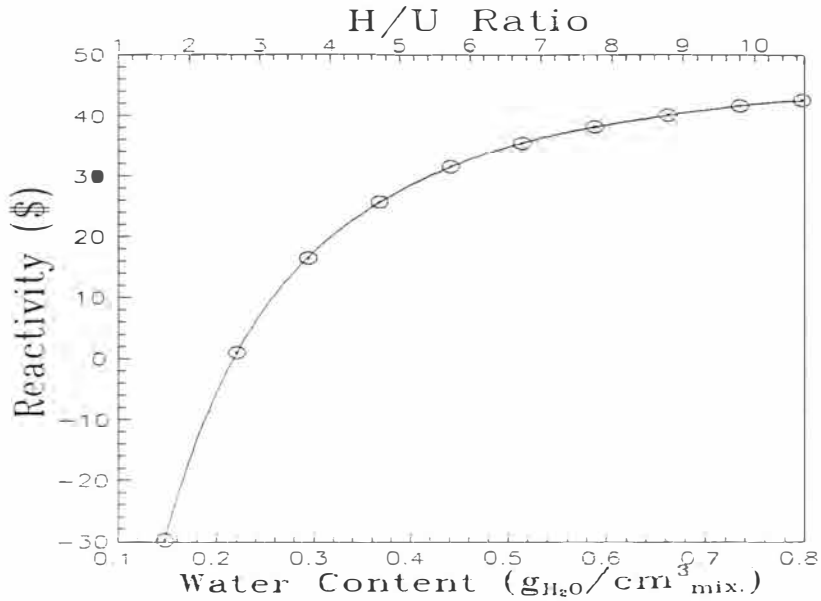

FIGURE 2.2 Results of Reactivity Driving Force Calculations.

TABLE 2.2
Constants C_1 to C_{10} for 5000 kg of 5% w/o U^{235} Enriched UO_2 Powder Loaded into a Cylindrical Blender (Diameter = 106.92 cm, Height = 244.96 cm) with a Density of 2.2 g/cm^3.

CONSTANT	VALUE
C_1	1.09180×10^6
C_2	-4.45837×10^6
C_3	7.83921×10^6
C_4	-7.77543×10^6
C_5	4.79032×10^6
C_6	-1.90423×10^6
C_7	4.92226×10^5
C_8	-8.16329×10^4
C_9	8.39353×10^3
C_{10}	-4.34888×10^2

feedback reactivity can be stated as

$$\rho_{feedback} = \frac{\partial \rho}{\partial D}(D(t)-D_0) + \frac{\partial \rho}{\partial H}(H(t)-H_0)+\frac{\partial \rho}{\partial T}(T(t)-T_0) + \rho_{evap}\,, \qquad (2.11)$$

where D = powder density (kg/m^3),

H = height of powder-water mixture (bulk) (m),

T = average temperature of powder-water mixture (°C),

ρ_{evap} = feedback reactivity due to water evaporation ($).

Reactivity effects of moderator thermal expansion and the formation and migration of vapor bubbles are not, at present, considered in our model. In Equation (2.11), subscript (**0**) is used to denote the initial values, and $\partial\rho/\partial$D, $\partial\rho/\partial$H, and $\partial\rho/\partial$T are the reactivity feedback functions with respect to the thermodynamic and geometric variables density, temperature, and height, respectively. The relationship between these variables and corresponding reactivity changes is non-linear. However, for small relative changes in these variables, the non-linear relation between a particular variable and reactivity can be approximated by a linear relation such that

$$\begin{aligned} \alpha_{dens} &\cong \frac{\partial \rho}{\partial D} \\ \alpha_{dopp} &\cong \frac{\partial \rho}{\partial T} \\ \alpha_{height} &\cong \frac{\partial \rho}{\partial H}\,, \end{aligned} \qquad (2.12)$$

where α_{dens}, α_{dopp}, and α_{height} are the reactivity feedback coefficients due to change in powder density, change in height, and doppler effect of powder/water mixture

respectively. These feedback coefficients are calculated by fitting 1st order polynomials to the CSAS1X or CSAS25 computed data where the slope of the polynomials are interpreted as the reactivity feedback coefficients. A summary of the results of the reactivity feedback coefficient calculations is shown in Table 2.3. CSAS1X is used to calculate the density and doppler reactivity feedback coefficients (α_{dens} and α_{dopp}) where the results are shown in Figures 2.3 and 2.4. CSAS25 is the Criticality Safety Analysis Sequence No.2 of the SCALE-IV system and it activates the three-dimensional Monte Carlo program KENO Va instead of XSDRNPM for k_{eff} calculations [42]. CSAS25 is used to calculate the reactivity feedback coefficient due change in height, α_{height}. XSDRNPM (in CSAS1X) is only a one dimensional calculation which approximates the leakage in the second dimension (i.e. height) using a buckling term from diffusion theory. CSAS25 results are provided in Table 2.4 and Figure 2.5. The Monte Carlo uncertainty

TABLE 2.3
Results of Reactivity Feedback Coefficient Calculations

PHYSICAL PHENOMENON	FEEDBACK COEFFICIENT
Change in powder density	~ 0.006 \$/(kg/m^3) (CSAS1X)
Change in height (i.e. leakage)	~ 0.845 \$/m (CSAS25)
Doppler effect	~ -0.011 \$/°K (CSAS1X)

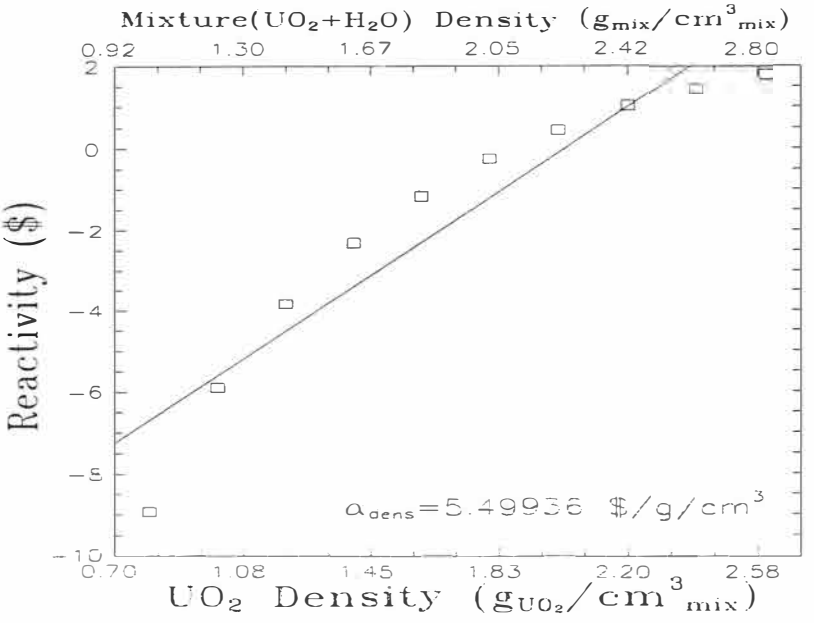

FIGURE 2.3 Reactivity Feedback Coefficient Due to Change in Powder Density.

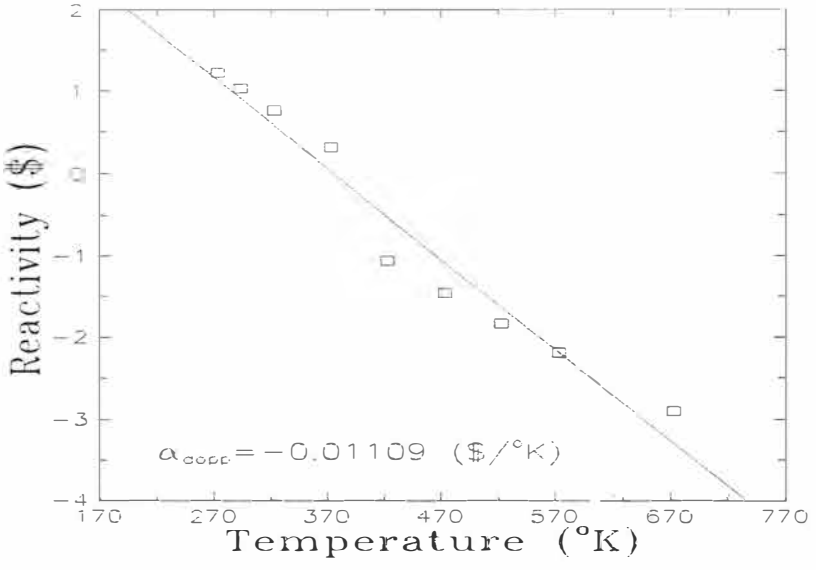

FIGURE 2.4 Reactivity Feedback Coefficient Due to Doppler Effect.

TABLE 2.4
CSAS25 Results for Reactivity Feedback Coefficient Calculations due to Change in Height.

Height (m)	Effective Multiplication Factor
2.45	1.00174 ± 0.00388
2.50	1.00421 ± 0.00434
2.67	1.00468 ± 0.00361
2.83	1.00452 ± 0.00490

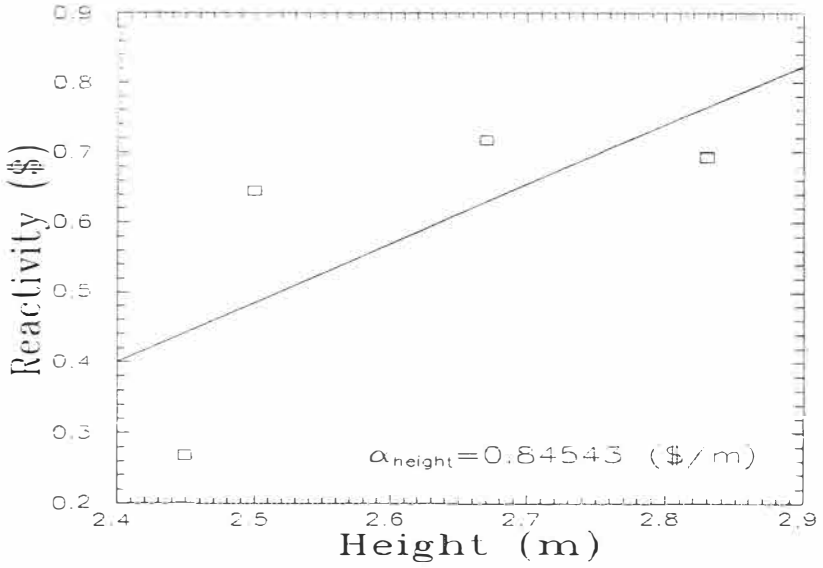

FIGURE 2.5 Reactivity Feedback Coefficient Due to Change in Height.

corresponding to each result is ignored in α_{height} calculations. Also, ρ_{evap} in Equation (2.11) can be evaluated using Equation (2.10) if the evaporation rate is known.

2.4. Neutron Mean Generation Time

The neutron mean generation time Λ used by the point kinetics equations is defined as the average time between the birth of a neutron and subsequent absorption inducing fission. Evaluation of the neutron mean generation time can be obtained using *perturbation theory* where the final expression involves complex volume and energy integrals (over terms containing the adjoint flux of the shape function) as described in Reference 34. These integrals can be evaluated using a multi-group approximation where the integrals over energy are replaced by sums over groups. Similarly, the volume integrals can be evaluated by summing over spatial meshes. There are several codes available which can solve both the continuous equations and the discretized equations to compute these integrals. The Monte Carlo code KENO-Va also calculates a number which may be interpreted as the generation time [42]. It is effectively the average time between successive generations averaged over all generations but the first three in a Monte Carlo calculation. Thus, CSAS25 is used to calculate Λ which is found to be $\sim 2.41 \times 10^{-5}$ sec (with an insignificant uncertainty) for the blender system described in the previous sections. The time dependence of Λ is neglected due to our constant shape function assumption.

2.5. Initial Neutron Source Strength

The early increase of the power, $n(t)$, within a supercritical system of fissile material is stochastic in nature. It may depart significantly from the estimate given by the point-kinetics equations depending on the strength of the neutron source that is present. If the criticality of the fissile system is established in the presence of a "strong" neutron source, point kinetics can provide a meaningful but approximate solution for the system power following the initial power growth period. However, if the neutron source is "weak", the first persistent fission chain reaction takes place at time t_1 (the initiation time), and the value of t_1 may vary due to the statistical nature of the phenomenon. Furthermore, the amount of energy release can be significantly higher than that predicted by the point kinetics if the neutron source is "weak". Hansen developed the following criteria which is valid for a fissile system having a "weak" neutron source; [17]

$$\frac{2S\tau}{\bar{\nu}\Gamma_2} < 1 \qquad (2.13)$$

where S = neutron source strength (neutron/s),

τ = the mean neutron lifetime (s),

$\bar{\nu}$ = the average number of neutrons emitted per fission,

and where

$$\Gamma_2 = \frac{\overline{\nu(\nu - 1)}}{\bar{\nu}^2} . \qquad (2.14)$$

Γ_2 is noted to be ~ 0.8 by Hansen for various fissile nuclides. Hansen also defines

a "strong" neutron source as

$$S\tau > 1. \tag{2.15}$$

Since $2/\bar{\nu}\,\Gamma_2 \approx 1$ for most practical situations involving U^{235}, Equation (2.13) can be used to obtain a simplified expression for a fissile system having a "weak" neutron source, that is [16]

$$S\tau < 1. \tag{2.16}$$

Equation (2.15) and (2.16) can be used to investigate the stochastic nature of the excursion associated with the strength of the inherent neutron source. The SCALE-IV/ORIGEN-S code can be used to calculate the inherent neutron source strength for damp low-enriched powders systems. ORIGEN-S computes time-dependent concentrations and source terms of a large number of isotopes which are simultaneously generated or depleted through neutronic transmutation, fission, radioactive decay, input feed rates, and physical or chemical removal rates [43]. The primary source of neutrons in low-enriched damp UO_2 powder systems is from spontaneous fission of U^{238}. Low enriched uranium is primarily composed of U^{234}, U^{235}, U^{236}, and U^{238}, and all are alpha particle emitters. Neutrons are generated when the alpha particles are absorbed by oxygen atoms. Tables (2.5) and (2.6) shows the results of ORIGEN-S calculations where the total neutron source term was found to be $5.05\text{x}10^4$ neutron/sec for 5 tons of 5% enriched UO_2 powder with an H/U ratio of approximately 3 (i.e., for $k_{eff} \cong 1$, see Figure 2.2). The mean neutron lifetime is estimated using KENO-Va and is equal to $\sim 1.95\text{x}10^{-5}$ sec (with an insignificant

TABLE 2.5
(α,n) Neutron Source per 100 g of Powder-water Mixture.

Isotope	Neutron Source (n/sec)
U^{234}	6.42×10^{-2}
U^{235}	2.79×10^{-3}
U^{236}	9.03×10^{-4}
U^{238}	6.63×10^{-3}
TOTAL	7.45×10^{-2}

TABLE 2.6
Neutron Source due to Spontaneous Fission per
100 g of Powder-water Mixture.

Isotope	Neutron Source (n/sec)
U^{234}	9.66×10^{-5}
U^{235}	2.09×10^{-4}
U^{236}	1.69×10^{-4}
U^{238}	9.38×10^{-1}
TOTAL	9.39×10^{-1}

uncertainty). Thus, Equation (2.16) becomes

$$S\tau = 5.05\times10^{4}\times1.95\times10^{-5} \cong 0.98 \ . \qquad (2.17)$$

Hence, the criteria condition for a "weak" neutron source, Equation (2.16), is not satisfied. However, Equation (2.15) also informs us that we do not have a "strong" source and, therefore, statistical fluctuations in the values predicted by the point-kinetics may be important for our system. The above result requires further investigation by conducting calculations to determine the most likely (expected) initiation times for several reactivity addition rates. These calculations are performed using the equation derived by Hansen for the fissile systems having a weak neutron source

$$\langle t_1 \rangle = \sqrt{\frac{\pi \bar{\nu}\Gamma_2}{4\dot{\alpha}S}} \ . \qquad (2.18)$$

Equation (2.18) is developed for a fissile system near critical and $\langle t_1 \rangle$ is the most likely time location for the first persistent chain reaction. For Equation (2.18), the fissile system attains delayed criticality (i.e., $k_{eff} = 1$) at time $t=0$ while it is undergoing a ramp reactivity addition at the rate of $\dot{\alpha}$ ($\Delta k_{eff}/s$). The standard deviation of the most likely value is given by Lutz as [19]

$$\sigma_1 = \sqrt{(1-\frac{\pi}{4})\frac{\bar{\nu}\Gamma_2}{\dot{\alpha}S}} \ . \qquad (2.19)$$

Hence, Equations (2.18) and (2.19) are evaluated for ramp reactivity addition rates from 0.1 ¢/sec to 10 $/sec and results are presented in Table 2.7. This table also

TABLE 2.7
Results of Initiation Time Calculations

Reactivity Addition Rate ($/sec)	Most Likely Initiation Time (sec)	Standard Deviation	Early Initiation Time (sec)	Late Initiation Time (sec)
0.001	2.147	±1.122	0.711	3.583
0.01	0.679	±0.355	0.225	1.133
0.1	0.215	±0.112	0.071	0.359
1.0	0.068	±0.035	0.023	0.113
10.0	0.021	±0.011	0.007	0.035

reports the early and the late initiation times analogous to the initiation times recommended by Lutz [19]. It is assumed that the most likely initiation time, $\langle t_1 \rangle$, will lie within $\langle t_1 \rangle \pm 1.28\sigma_1$ where $\langle t_1 \rangle - 1.28\sigma_1$ and $\langle t_1 \rangle + 1.28\sigma_1$ are interpreted as the early and the late initiation times, respectively [16]. Thus, the early, the most likely, and the late initiation times are the 10%, 50%, and 90% plausible initiation times corresponding to a gaussian (normal) probability distribution.

Table 2.7 results show that these three initiation times are small and the point kinetics equations should provide a meaningful solution for the system power following the initial power growth period. Thus, the fluctuations in the neutron population and the fluctuation in the time location of the first persistent fission chain reaction may be ignored for our system. For further discussions on weak neutron source considerations and the assumptions involved in the derivation of Equations (2.13) and (2.18), the reader is referred to References 16 and 17.

Chapter 3

ACCIDENT MODELLING: THERMAL HYDRAULICS

3.1. Introduction

To estimate the system temperature during the excursion, an overall energy balance for the system is used. The system may be defined as two separate homogeneous regions for the energy balance, namely, the bulk and the container walls[a]. The first region consists of a homogeneous mixture of the blender contents including the major components: the powder and the water, and also the air (i.e., the bulk). This bulk is assumed to be blended uniformly by the mixing mechanism. It is surrounded by the container walls which is taken as the second region. Energy and mass balances will be performed for each of these regions as follows.

3.2. Region 1 Energy and Mass Balances

The energy generation takes place in the powder particles. A portion of this energy is absorbed within the system and raises the temperature of the system components. Another portion is transferred to the container walls by conduction. To model the energy transfer rates between the components within the system

[a] In fact, a separate energy balance may not be needed for the container wall because it is very thin comparing to the diameter of the approximated cylindrical system.

(namely, the powder particles, the water, and the air in the homogeneous porous medium) requires an understanding of the heat transfer mechanisms within the system including such phenomena as the effects of the mixing mechanism on the heat transfer coefficient, capillary effects in a porous body, and the effects of the partially water saturated porous medium [44]. It is therefore difficult to estimate heat transfer rates between the powder particles, the water, and the air.

During realistic accident scenarios, the bulk temperature may rise above the saturation temperature of water causing the water to boil. Boiling phenomenon further complicates the modelling of the system.

One way of treating this problem is to assume a heat transfer model(e.g. conduction, nucleate boiling, etc.) and calculate the heat transfer rates using appropriate correlations available in the literature [29]. But, results of such a model are not exact due to the reasons given above and also because the effective heat transfer areas from the powder surface to water/air are unknown.

On the other hand, bounding estimates of the above phenomena may be obtained by considering extreme conditions for the thermal behavior of the system which bounds the real life situation. For a damp powder system where the heat transfer mechanism from powder to surrounding water/air mixture is unknown, the extremes of zero and infinite heat transfer coefficients may be considered between the major components(i.e., the powder and the water) of the system. Because these extremes are relatively easy to model and the real life situation should lie somewhere in between, models using these extremes can produce meaningful results. Using these

extremes, three different models have been developed as described below.

3.2.1. Model 1

The first model assumes a zero heat transfer coefficient between the powder particles and the other components (i.e., water and air) in the system. Energy is removed from the region only by means of conduction through the container walls and the water temperature stays constant at room temperature. Since there is no heat transferred to the water, no energy and moderator is lost due to boiling. However, this approximation calculates higher powder temperatures and the doppler effect is maximized due to rapid heat up of the powder. This model also neglects the air in the system and assumes a constant pressure process (i.e.,atmospheric) within each time interval.

To study the energy balance, we use the concept of a control volume as shown in Figure 3.1. This volume is a region in the blender space to be observed with respect to the matter and energy which cross its boundaries. Considering the entire blender contents as a single control volume, the energy balance may be described by the following equation:

$$\frac{dT^B(t)}{dt} = \frac{1}{[c^B(t)\, m^B(t)]}\{\, Q_{gen}(t) - Q_{con}(t) \,\}, \qquad (3.1)$$

where $Q_{gen}(t)$ = energy generation rate (J/s),
$Q_{con}(t)$ = rate of energy loss by conduction to the container walls (J/s),
$c^B(t)$ = specific heat of bulk (J/kg.°C),

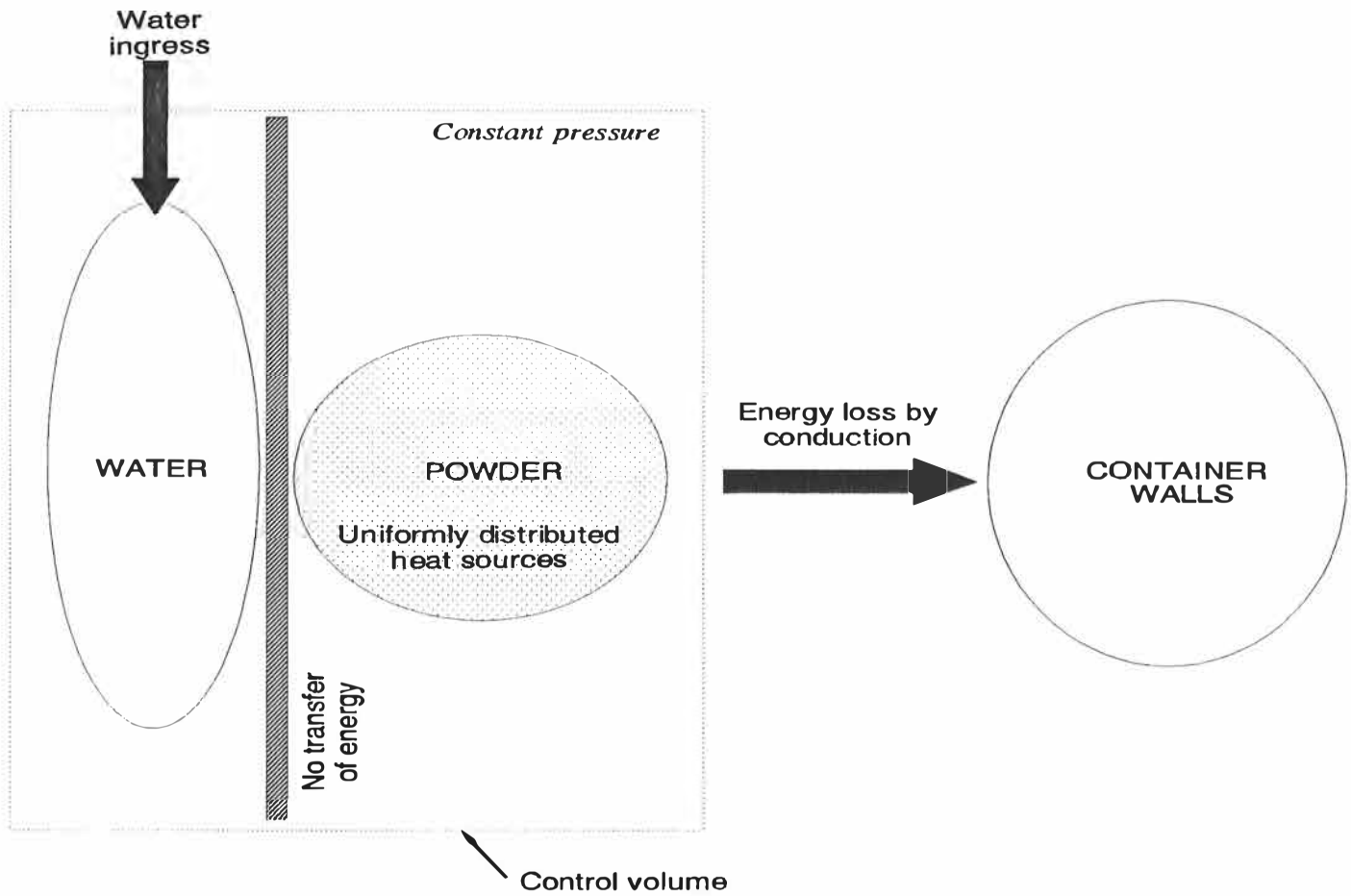

Figure 3.1 Model 1 Mass and Energy Balances for Region 1.

$m^B(t)$ = bulk mass (kg),
$T^B(t)$ = bulk temperature (°C).

Since the heat transfer coefficient between the water and the powder is assumed to be zero in this model, we can replace $T^B(t)$, $c^B(t)$, and $m^B(t)$ with temperature $T^p(t)$, specific heat $c^p(t)$, and mass m^p of powder, respectively, in Equation (3.1). Also, the water mass at time t is calculated as

$$m^w(t) = m_0 + \dot{G}\,t \qquad if \quad t \le t_f \tag{3.2}$$

and

$$m^w(t) = m_0 + \dot{G}\,t_f \qquad if \quad t > t_f\,, \tag{3.3}$$

where m_0 = water mass at t=0 (kg),
$\dot{G}$ = water ingress rate (kg/sec),
t_f = time at which the water ingress is terminated (sec).

3.2.2. Model 2

The second model utilizes an infinite heat transfer coefficient between powder particles and water and the system is assumed to be vented(i.e., open at the upper end) under constant atmospheric pressure with any steam produced leaving the system instantly. Realistically, during the excursion, the powder particles would be at a higher temperature than the water. This model assumes that the water temperature and the powder particle temperature are the same. After heating the water to the saturation temperature, the remaining energy deposited in the

system goes into evaporating water and the system components stay at the saturation temperature.[b] This model also neglects air in the bulk with respect its effects on the energy balance and assumes a constant pressure process (i.e., atmospheric) within each time interval. The control volume for mass and energy balances are illustrated in Figure 3.2.

According to this approximation, the differential equation for the time rate of change of the internal energy of the system can be written as

$$\frac{dU(t)}{dt} = \{ \dot{G} h_0 + Q_{gen}(t) - Q_{con}(t) \} , \qquad (3.4)$$

where h_0 is the enthalpy of the ingress water (kJ/kg). The state of water(i.e., subcooled liquid, or saturated liquid) at time t can be estimated by calculating the internal energy of the water and comparing the result with steam tables. Setting the initial condition for $\Delta U(t)$ equal to zero (i.e., $\Delta U(0) = 0$), Equation (3.4) provides the internal energy increase of the bulk mixture from initial time t_0 to the present time t. This internal energy information can be expanded into its components as

---

[b] If the temperature of the liquid in a system comprised of the *pure substance* water is increased while the pressure is held constant at atmospheric, no vapor will form until the temperature reaches to 100°C. Then, no matter how much vapor is formed, as long as both liquid and vapor are present in equilibrium and the pressure is held constant, the temperature will be 100°C. Not until all of the liquid has changed to vapor can the temperature rise above the saturation temperature. The bulk may assumed to be a *physical mixture* which is composed of three *pure substances*, namely, the powder, the water, and the air.

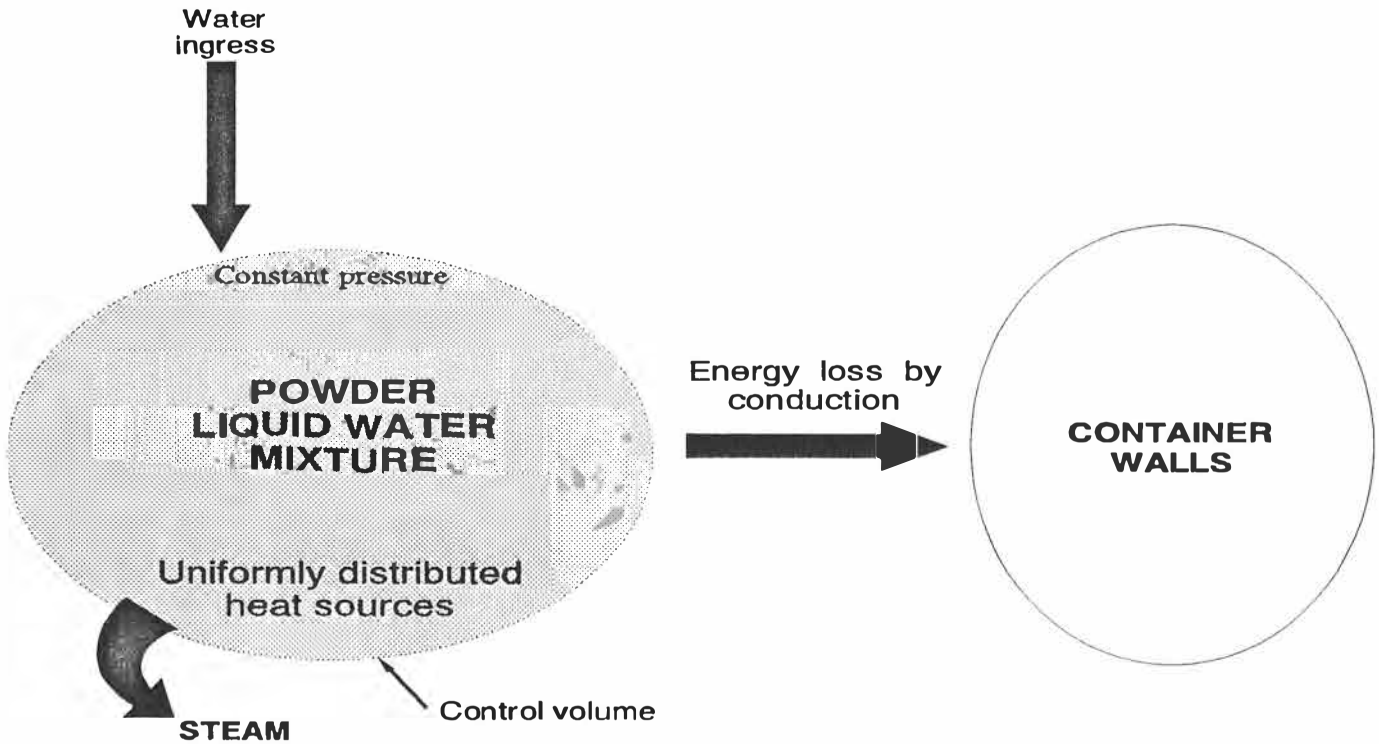

Figure 3.2 Model 2 Mass and Energy Balances for Region 1.

$$\Delta U(t) = \Delta U^w(t) + \Delta U^p(t) \tag{3.5}$$

where $\Delta U(t)$, $\Delta U^w(t)$, and $\Delta U^p(t)$ are internal energy change of the powder/water mixture (bulk) (J), internal energy change of the water only (J), and internal energy change of the powder only(J), respectively, from initial time t_0 to present time t. Therefore, the internal energy change(increase) available to the water at time t can be represented by rearranging Equation (3.5) as

$$\Delta U^w(t) = \Delta U(t) - \Delta U^p(t), \tag{3.6}$$

where

$$\Delta U^p(t) = m^p c^p (T^B(t) - T_0^B). \tag{3.7}$$

In Equation (3.7), T_0^B is the initial bulk temperature (i.e., the room temperature) and $T^p(t) = T^B(t)$. As seen from its defining equation, $\Delta U^p(t)$ depends on the temperature of the bulk mixture, $T^B(t)$. The bulk temperature is not known at the onset of each communication time interval, since it is the basic quantity for which we wish to solve. One possible approach is to assume the most recent bulk temperature value, which is calculated for the previous time interval, for the temperature of powder at time t and then solve Equation (3.6) for $\Delta U^w(t)$; that is, let $T^B(t) = T^B(t-\Delta t)$. We may then, evaluate the specific internal energy of the water as

$$u^w(t) \cong \frac{U_0^w + \Delta U^w(t)}{m^w(t)}, \tag{3.8}$$

where U_o^w is the initial internal energy of water which is the product of initial water

mass and initial specific internal energy which can be found from steam tables. Then, the $u^w(t)$ value can be compared with steam table values of internal energy to estimate the state of liquid water as either subcooled or saturated as described next.[c]

3.2.2.1. Subcooled Mode

For $u^w(t) < u^w_{sat}$, the water is subcooled(i.e., $T^B(t) < T^w_{sat}$) and the temperature of the bulk can be calculated as

$$T^B(t) = \frac{\Delta U(t)}{\Xi} + T^B_0, \tag{3.9}$$

where

$$\Xi = m^w(t)c^w(t) + m^p c^p(t). \tag{3.10}$$

In Equation (3.10), $c^w(t)$ is the specific heat of the water. The mass balance for the subcooled mode is calculated similar to Model 1 using Equations (3.2) and (3.3).

3.2.2.2. Saturation Mode

When $u^w(t) \geq u^w_{sat}$, the model switches into a different calculation mode where the water is assumed to stay at the saturation temperature (i.e., $T^B(t) = T^w_{sat}$

---

[c] The number of independent properties required to specify the thermodynamic state of a system is equal to the number of the possible work modes (volume change, electric and magnetic potentials, etc.) plus one. The *pure substance* water shall assumed to be a simple substance involving only compression (volume change) work mode. Thus, for water only two independent properties are required to define the state of the system. In Model 2, these independent properties are the pressure and the specific internal energy.

$\cong$ *100* °*C* at atmospheric) and the saturation pressure until all water evaporates from the system. Thus, the mass of steam produced during time interval Δt is given by

$$\Delta \hat{m}^s = \frac{\Delta U(t) - \Delta U(t-\Delta t)}{h_{fg}} , \tag{3.11}$$

where h_{fg} is the latent heat of vaporization of water at the saturation temperature corresponding to atmospheric pressure.

The mass of liquid water at time t is then determined as

$$m^w(t) = m^w(t-\Delta t) + \dot{G}\Delta t - \Delta \hat{m}^s \qquad if \quad t \le t_f \tag{3.12}$$

and

$$m^w(t) = m^w(t-\Delta t) - \Delta \hat{m}^s \qquad if \quad t > t_f . \tag{3.13}$$

The saturation mode is used as long as the following criteria is satisfied,

$$\Delta U(t) - \Delta U(t-\Delta t) \ge 0 . \tag{3.14}$$

If the criteria in Equation (3.14) fails, the model switches back to subcooled mode where the temperature is calculated using a modified form of Equation (3.9) as

$$T^B(t) = \frac{\Delta U(t) - \sum_i (\Delta \hat{m}^s h_{fg})_i}{\Xi} + T_0^B \tag{3.15}$$

where the subscript i represents the time intervals for saturation calculation mode.

When $T^B(t) > T^w_{sat}$, the powder temperature is above saturation temperature and there is no water remaining in the system(i.e., dry powder). Preliminary studies have

shown that the energy of the system is not sufficient to evaporate all the water during realistic accident scenarios. Therefore, this case is not important for our research.

3.2.3. Model 3

The third model also assumes an infinite heat transfer coefficient but the system is not vented (i.e., closed at the upper end and the total volume of the system remains constant) [45]. Equation (3.4) is used to calculate the rate of change of the internal energy of the system. The liquid water and vapor is assumed to be in phase equilibria prior to the criticality excursion.[d] Air in the system is assumed to be an inert gas forming an ideal mixture with vapor [46,47]. Thus, the total pressure is the sum of the partial pressures of the water and air where the initial total pressure is standard atmospheric pressure. The contribution of the water to the total pressure is dictated by its temperature and is initially equal to the equilibrium vapor pressure at room temperature. Hence, the initial partial pressure of air can be evaluated by

$$P^a(t_0) = P_{atm} - P^w(t_0), \tag{3.16}$$

where P_{atm}, $P^a(t)$, $P^w(t)$ are standard atmospheric pressure, the partial pressure of air, and the partial pressure of water, respectively.

Using Equation (3.4), we can estimate the internal energy change of the bulk at each time interval which can be expanded into its components as

---

[d] If liquid water is sealed in a vessel at *fixed temperature*, the pressure of the vapor increases (or decreases) until the equilibrium vapor pressure is reached. When an inert gas is introduced, the property of the vapor itself is not altered if the vapor and the gas form an ideal mixture.

$$U(t) - U(t-\Delta t) = \Delta \hat{U}^{w}(t) + \Delta \hat{U}^{p}(t) + \Delta \hat{U}^{a}(t) \tag{3.17}$$

where $\Delta \hat{U}_{w}(t)$, $\Delta \hat{U}^{p}(t)$, and $\Delta \hat{U}^{a}(t)$ are internal energy change of the water (J), powder (J), and air (J), respectively. As described in Section 3.2.2, the subcooled mode of Model 2 uses the internal energy information as the internal energy change from initial time t_0 to present time t for calculational simplicity. On the other hand, Model 3 utilizes the internal energy change at each time interval, namely from time t-Δt to present time t. For clarity, all such quantities are identified by a ***hat***. The internal energy change of the water can be estimated by rearranging Equation (3.17) as

$$\Delta \hat{U}^{w}(t) = [\ U(t) - U(t-\Delta t)\ ] - \Delta \hat{U}^{p}(t) - \Delta \hat{U}^{a}(t) \tag{3.18}$$

where

$$\Delta \hat{U}^{p}(t) = m^{p}\, c^{p}(t)\, [\ T^{B}(t) - T^{B}(t-\Delta t)\ ] \tag{3.19}$$

and

$$\Delta \hat{U}^{a}(t) = m^{a}\, c_{v}^{a}(t)\, [\ T^{B}(t) - T^{B}(t-\Delta t)\ ]\ . \tag{3.20}$$

In Equation (3.20), $c_v^a(t)$ is the specific heat of air at constant volume (J/kg°C). The specific internal energy of the water at time t can be calculated as

$$u^{w}(t) = \frac{U^{w}(t-\Delta t) + \Delta \hat{U}^{w}(t)}{m^{w}(t)}\ . \tag{3.21}$$

Since the system has both liquid and vapor phases of water, the specific internal energy of the water can be written as

$$u^{w}(t) = [1-\chi(t)] \bullet u_{f}^{w}(t) + \chi(t) \bullet u_{g}^{w}(t) \tag{3.22}$$

where $u_f^w(t)$ = specific internal energy of saturated liquid (J/kg),
$u_g^w(t)$ = specific internal energy of saturated vapor (J/kg),
$\chi(t)$ = quality.

Assuming a constant specific volume process within each time interval, the specific volume of an equilibrium mixture of liquid and vapor can be described as follows:

$$v^w(t-\Delta t) \cong v^w(t) = [1-\chi(t)]\cdot v_f^w(t) + \chi(t)\cdot v_g^w(t) \qquad (3.23)$$

where $v_f^w(t)$ = specific volume of saturated liquid (J/kg),
$v_g^w(t)$ = specific volume of saturated vapor (J/kg).

Equations (3.22) and (3.23) utilize properties of saturated liquid and vapor since the process (constant specific volume) is assumed to be taking place (between time t-Δt and time t) on the liquid-vapor line (wet vapor region) of the water phase diagram. A temperature-entropy diagram for water showing a constant specific volume process is given in Figure 3.3. This figure also displays the control volume for the mass and energy balances of Model 3. For a given temperature, $u_f^w(t)$, $u_g^w(t)$, $v_f^w(t)$, and $v_g^w(t)$ can be obtained from steam tables. Moreover, we can calculate $u^w(t)$ using Equations (3.18) to (3.21) since $v^w(t)$ is known from the previous time interval as a result of our assumption(i.e., constant specific volume process). Thus, a line search scheme of the steam tables can be used to determine the temperature which yields the same $\chi(t)$ values for both Equation (3.22) and Equation (3.23). The thermodynamic properties of the system at time t are assumed according to this

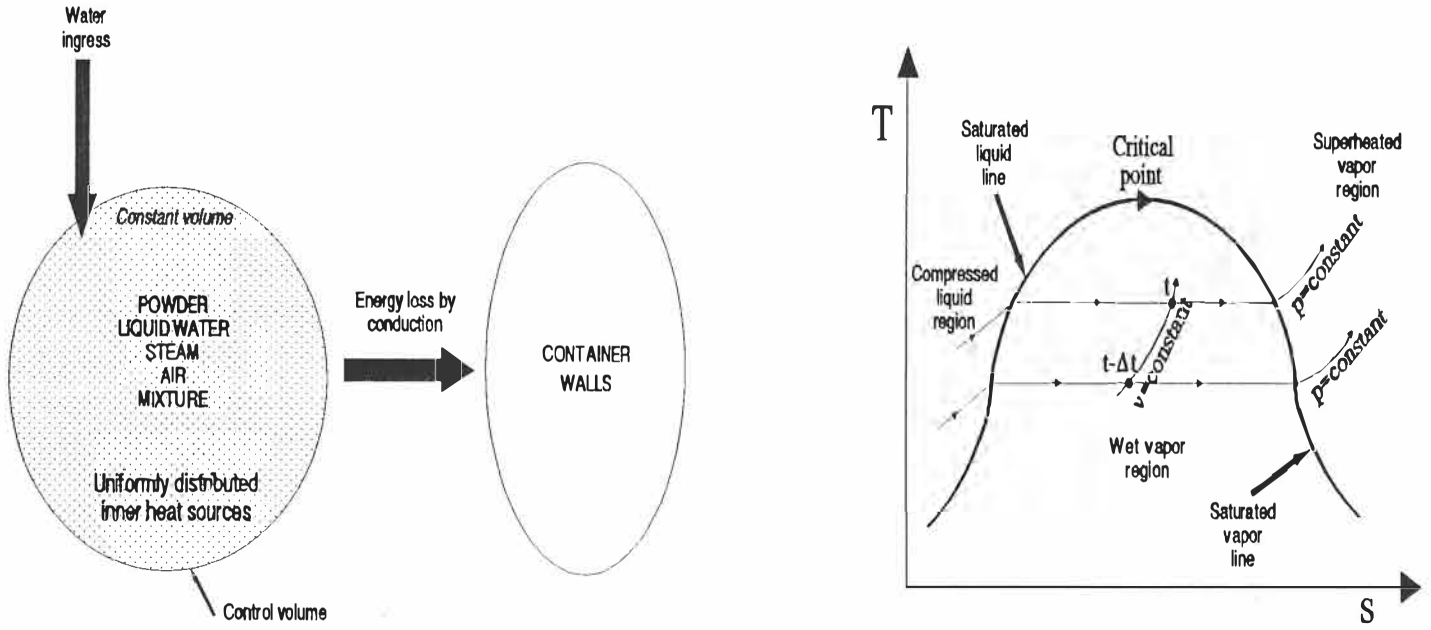

Figure 3.3 Model 3 Control Volume for Mass and Energy Balances for Region 1 and Temperature-Entropy Diagram for Water Showing a Constant Specific Volume Process.

temperature.[c]

The partial pressure of air is calculated using the ideal gas equation as

$$P^a(t) = P^a(0)\left(\frac{T^B(t)+273}{T_0^B+273}\right), \tag{3.24}$$

where the partial pressure of water is the vapor pressure corresponding to the bulk temperature.

In model 3, the water and steam masses at time t can be calculated as

$$\begin{aligned} m^w(t) &= (m_0 + \dot{G}t)(1 - \chi(t)) \qquad if \quad t \le t_f \\ m^s(t) &= (m_0 + \dot{G}t)\chi(t) \end{aligned} \tag{3.25}$$

and

$$\begin{aligned} m^w(t) &= (m_0 + \dot{G}t_f)(1 - \chi(t)) \qquad if \quad t > t_f \\ m^s(t) &= (m_0 + \dot{G}t_f)\chi(t). \end{aligned} \tag{3.26}$$

In all models, the parameters such as $c^s(t)$, $c^w(t)$, and $c^a(t)$ are shown as a function of time, since they are updated at every time step using equations or polynomial fits as a function of $T^B(t)$. However, they are assumed to be constant in the derivation of differential equations which introduces an insignificant error in the final results

---

[c] In Model 3, the specific volume and the specific internal energy are used to define the state of the system (see Footnote c). Thus, if specific volume and specific internal energy of water are specified, the values of all other properties of water such as temperature, density, enthalpy, etc. are fixed since specific volume and specific internal energy may be considered as independent properties. Also, when two phases of water is assumed to exist together in equilibrium, the pressure and temperature depend on each other. Under this condition, pressure is also fixed for a given temperature.

since they change only slightly with respect to time.

3.3. Energy Generation Rate

Energy generation takes place inside the powder particles. Since the rate of energy generation, $Q_{gen}(t)$ is proportional to the power, the energy generation term is the product of the power level $n(t)$, and the fraction of the energy from fission deposited in the system ξ [28],

$$Q_{gen}(t) = \xi\, n(t) \tag{3.27}$$

where ξ can be assumed to be equal to one for most practical situations.

3.4. Region 2 Energy Balance: Heat Conduction in the Container Wall

Heat transfer in the blender container wall from the flat upper and lower surfaces can be described by the one-dimensional heat conduction equation in slab geometry. Also, heat transfer from the curved lateral surface may also be approximated by the same equation since the diameter is large enough and curvature is not a significant factor. Furthermore, the container wall is thin compared to the blender radius. The transient heat conduction equation for one-dimensional slab geometry can be written as

$$\frac{\partial T(t)}{\partial t} = \frac{k^c(t)}{c^c(t)\,\rho^c(t)} \frac{\partial^2 T(t)}{\partial x^2} \tag{3.28}$$

where $\rho^c(t)$ = density of the container wall (kg/m^3),
$c^c(t)$ = specific heat of the container wall (J/kg°C),
$k^c(t)$ = thermal conductivity of the container wall (W/m°C),

Equation (3.28) assumes there is no inner energy source in this region.[f] In this equation, the spatially dependent term is expanded using finite differences as

$$\frac{dT_s(t)}{dt} \cong \left(\frac{k^c(t)}{c^c(t)\,\rho^c(t)}\right)\left[\frac{T_{out}(t)-2T_s(t)+T_{in}(t)}{\Delta x^2}\right] \tag{3.29}$$

or

$$\frac{dT_s(t)}{dt} = -\left(\frac{k^c(t)}{c^c(t)\,\rho^c(t)}\right)\left[\frac{T_s(t)-T_{out}(t)}{\Delta x^2}\right] + \left(\frac{k^c(t)}{c^c(t)\,\rho^c(t)}\right)\left[\frac{T_{in}(t)-T_s(t)}{\Delta x^2}\right] \tag{3.30}$$

where $T_s(t)$ = blender outer surface temperature (°C),
Δx = thickness of the blender container wall (m),

and $T_{in}(t)$ is equal to $T^B(t)$ for a flat temperature distribution inside the container. Also, $T_{out}(t)$ can be calculated using the boundary conditions

$$k^c(t)\,A\frac{\partial T(t)}{\partial t} \cong k^c(t)\,A\,\frac{T_s(t)-T_{out}(t)}{\Delta x} = Q_{fc}(t) + Q_{rad}(t)\,, \tag{3.31}$$

where $Q_{fc}(t)$ = rate of energy loss by free convection (J/s),
$Q_{rad}(t)$ = rate of energy loss by radiation (J/s).

Equation (3.31) can be rewritten as

$$T_{out}(t) = -\frac{\Delta x}{k^c(t)\,A}Q_{fc}(t) - \frac{\Delta x}{k^c(t)\,A}Q_{rad}(t) + T_s(t)\,. \tag{3.32}$$

Substituting Equation (3.32) into Equation (3.30), we get

---

[f] Inner energy source due to radiation is neglected.

$$\frac{dT_s(t)}{dt} = \frac{1}{c^c(t)\,\rho^c(t)\,\Delta x\,A}\left[- Q_{fc}(t) - Q_{rad}(t) + k^c(t)\,A\frac{T_{in}(t)-T_s(t)}{\Delta x} \right]. \quad (3.33)$$

The last term in Equation (3.33) can be defined as the energy loss due to conduction through the container walls

$$Q_{con}(t) = k^c(t)\,A\frac{T_{in}(t)-T_s(t)}{\Delta x} \quad (3.34)$$

and Equation (3.33) can be rewritten as

$$\frac{dT_s(t)}{dt} = \frac{1}{c^c(t)\,\rho^c(t)\,\Delta x\,A}\left[Q_{con}(t) - Q_{fc}(t) - Q_{rad}(t) \right]. \quad (3.35)$$

Equation (3.35) is used to calculate the temperature of the blender's outer surface with respect to time.

The parameters $c^c(t)$, $\rho^c(t)$, and $k^c(t)$ are assumed to be constants in the derivation of the differential Equation (3.28). However, they are shown as a function of time since they are updated at every time step using polynomial fits as a function of $T_s(t)$. The Region 2 energy balance is shown schematically in Figure 3.4.

3.5. Rate of Free Convection Energy Loss

Free convection occurs when a surface is placed in contact with a fluid at a higher or lower temperature than that of the surface [48,49,50]. It originates due to the non-uniform distribution of mass forces in the fluid (i.e., changes in fluid density near the surface) which is caused by gravity as a result of the temperature difference

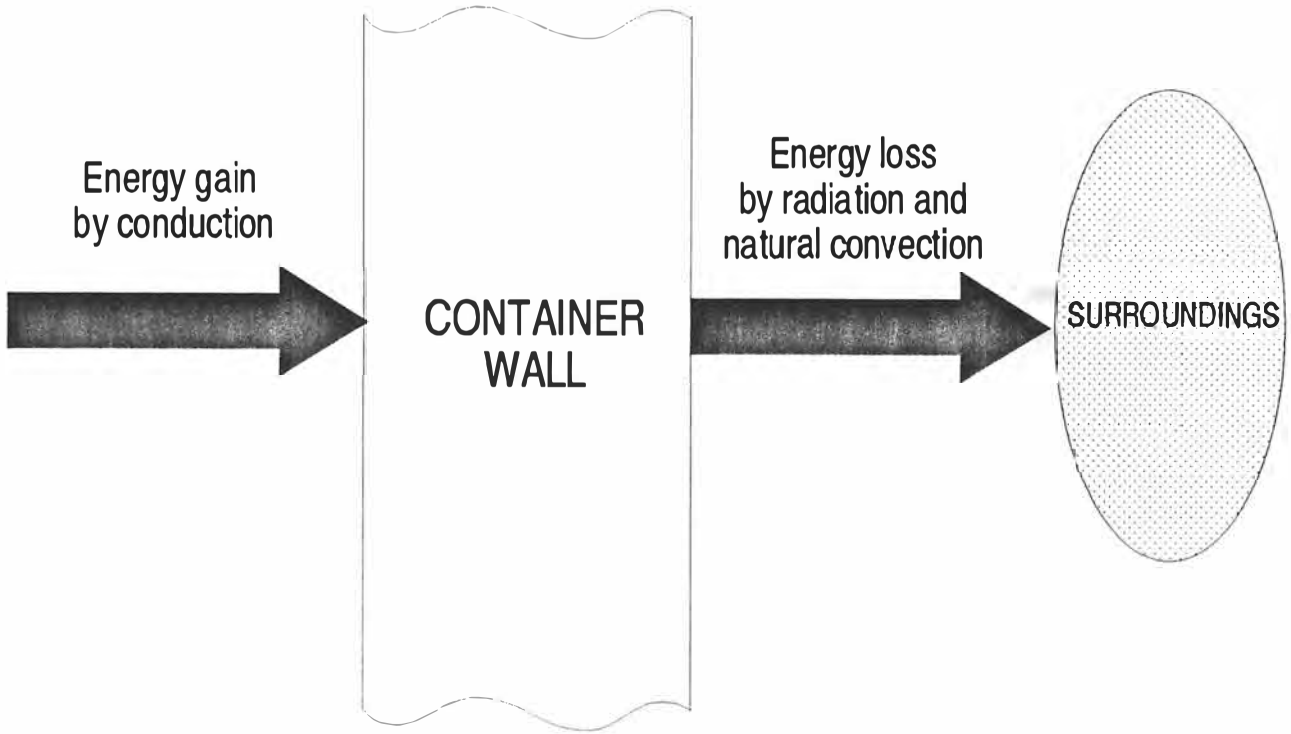

Figure 3.4 Region 2 Energy Balance.

between the fluid and the surface [51]. During a criticality excursion, the blender's surface temperature can rise significantly above the temperature of the surrounding air such that the air in the vicinity of the heated blender outer surface could experience free-convection currents.

The rate of heat transfer by convection between the blender outer surface and the air may be computed by the relation

$$Q_{fc}(t) = hA(T_s(t) - T_\infty) \tag{3.36}$$

where $T_s(t)$ is the blender outer surface temperature and T_∞ is the air temperature outside the blender. The proportionality constant h is the convection heat transfer coefficient ($W/m^2{}^\circ C$) which includes all the effects that influence the convection model such as the surface geometry, the nature of the fluid motion, the fluid thermodynamic and transport properties, etc. Since these quantities are not necessarily constant over a surface, the convective heat transfer coefficient may also vary from point to point. For this reason, we must distinguish between a local and an average convective heat transfer coefficients. The local coefficient is defined by

$$h = \frac{1}{(T_s - T_\infty)} \frac{dQ}{dA} \tag{3.37}$$

and the average coefficient can be defined in terms of the local value by

$$\bar{h} = \frac{1}{A} \int_A h dA \ . \tag{3.38}$$

In the following application, we will be interested in the average values where all

average quantities are identified by a ***bar***. A dimensionless heat transfer modulus, the Nusselt number ***Nu***, has been defined as

$$Nu = \frac{hX}{k}, \tag{3.39}$$

where ***X*** is a dimension that depends on the geometry of the system (m) and ***k*** is the fluid thermal conductivity (W/m°C).

In free convection the Grashof number ***Gr*** and the Prandtl number ***Pr*** are the dominant dimensionless parameters which determine the nature of the flow and the heat transfer coefficient. The Grashof number physically represents the ratio of body forces to viscous forces and is defined as

$$Gr = \frac{\rho^2 c_p g \beta (T_s - T_\infty) X^3}{\mu k}, \tag{3.40}$$

where ρ = density of the coolant (kg/m^3),
c_p = specific heat of the coolant at constant pressure (J/kg°C),
g = standard gravitational constant (m/sec^2),
β = coolant thermal expansion coefficient (1/°C),
μ = coolant dynamic viscosity (kg/m sec).

The Prandtl number is a quantity composed of physical properties of the fluid and it is a measure of the relative magnitudes of momentum and thermal diffusion in the fluid,

$$Pr = \frac{\mu c_p}{k} \tag{3.41}$$

An analytic calculation of average free convection heat transfer coefficient ***h*** can

be made for some systems. For complex situations, it must be determined experimentally. Traditionally, it has been found that h for a variety of circumstances can be correlated by an equation of the type [48]

$$Nu = \phi(Gr)\,\psi(Pr) \tag{3.42}$$

where Φ and Ψ denote functional relationships. However, if the velocities are so small that inertia forces are negligible in comparison with friction and body forces, heat transfer can be correlated with a single variable,

$$Nu = f(Gr, Pr) = f(Ra) \tag{3.43}$$

where Ra, the Rayleigh number is the product of Gr and Pr. In the following section, we summarize appropriate empirical or analytical correlations that have been developed for common geometries relevant to external cooling of a blender during an accidental criticality excursion. The correlations are suitable for most engineering calculations and are of the form given in Equation (3.41) or (3.42). Note that the characteristic dimension X, to be used in the Nusselt and Grashoft numbers for the correlations, is given in the following sections and depends on the geometry of the problem. Also, the fluid properties must be evaluated at the film temperature,

$$T_f(t) = \frac{(T_s(t) + T_\infty)}{2} . \tag{3.44}$$

3.5.1. Vertical Cylinders

For vertical cylinders, it is generally adequate to use correlations for vertical planes if the diameter of the cylinder is large enough so that the curvature is not a significant factor. In practice, it has been found that [49]

$$\frac{D}{L} \geq \frac{35}{Gr^{0.25}} \tag{3.45}$$

is a suitable criterion where D is the diameter of the cylinder and L is its height. This criterion was obtained by Sparrow and Gregg for Pr values of 0.72 and 1.0 for a difference in heat transfer of less than 5% from the flat plate solutions.

For vertical plates, Churchill and Chu recommend a correlation for laminar flow which is in the form [49,50]

$$\overline{Nu}_{plate} = 0.68 + \frac{0.67Ra^{0.25}}{[1+(0.492/Pr)^{9/16}]^{4/9}}, \qquad (0<Ra<10^9) \tag{3.46}$$

where they also give the following correlation which may be applied over the entire range of Ra(i.e., laminar and turbulent regions),

$$\overline{Nu}_{plate} = \{0.825 + \frac{0.387Ra^{1/6}}{[1+(0.492/Pr)^{9/16}]^{8/27}}\}^2 . \tag{3.47}$$

Therefore, slightly better accuracy may be obtained for laminar flow by using Equation (3.46).

From Equation (3.45), it appears that $L/DGr^{-0.25}$ would represent a useful dimensionless parameter for characterizing the deviation of cylindrical heat transfer from planar heat transfer. A formula given by Minkowycz and Sparrow is [49]

$$\overline{Nu}_{cyl} = \overline{Nu}_{plate}[1 + 1.43(\frac{L}{DGr^{0.25}})^{0.9}] \qquad (3.48)$$

The curvature of cylindrical geometry, providing additional volume for fluid moving away from the surface, leads to a higher heat transfer coefficient.

When the diameter to height ratio is not large enough to ignore the effects of curvature, the relevant governing equations must be solved. LeFevre and Ede employ an integral method to solve the governing equations and give the following expression for the average Nusselt number where both ***Nu*** and ***Gr*** are based on the height of the cylinder [52],

$$\overline{Nu} = \frac{4}{3}\left[\frac{7GrPr^2}{5(20+21Pr)}\right]^{0.25} + \frac{4(272+315Pr)L}{35(64+63Pr)D} . \qquad (3.49)$$

The cylinder's height must be used as the length dimension to evaluate the Nusselt number and the Grashof number for a vertical cylinder rather than its diameter.

3.5.2. Horizontal Surfaces

Heat transfer from the upper and lower surface areas of blender to air can be approximated by free convection heat transfer from heated horizontal plates.

For horizontal surfaces, the specific form of the correlation depends on whether the surface is facing up or down and is heated or cooled. The following correlations from Reference 53 are recommended for the upper surface of a heated plate or the lower surface of a cooled plate,

$$\overline{Nu} = 0.54 Ra^{0.25} \qquad (10^4 \leq Ra \leq 10^7) \tag{3.50}$$

and

$$\overline{Nu} = 0.15 Ra^{1/3} . \qquad (10^7 \leq Ra \leq 10^{11}) \tag{3.51}$$

The correlations can be used to calculate the heat transfer coefficients for free convection heat transfer from the upper surface area of the blender to air.

A hot surface facing down will cause the fluid near the surface to expand and thus stimulate some fluid motion. However, gravity does not advance the flow as when the plate faced up. Therefore, the heat transfer coefficient will be lower. Reference 54 gives the following correlation for heated horizontal plates facing downward,

$$\overline{Nu} = 0.27 Ra^{0.25} . \qquad (10^5 \leq Ra \leq 10^{10}) \tag{3.52}$$

This correlation is valid only for laminar flow conditions and can be used to calculate an approximate free convection heat transfer coefficient from the bottom surface area of the blender to air.

Observations to date have led to recommendations that, for a square surface, the characteristic dimension should be the length of one side and, for circular disk (which is the case for a blender) the dimension should be ***0.9D***.

3.5.3. Vertical Cones

For laminar heat transfer from the sides of a cone, Kuiken predicts the following equation for the average Nusselt number for air [55]:

$$\overline{Nu} = (0.564 + 0.412\epsilon + 0.02\epsilon^2)Ra^{0.25}, \quad (3.53)$$

where

$$\epsilon = \frac{2}{Ra^{0.25}\tan(\frac{\phi}{2})} \quad (3.54)$$

and ϕ is the vertex angle of the cone.

Experimental data by Oosthuizen and Donaldson for free convection from vertical cones with vertex angles between 3° and 12° are considerably higher than predicted by Equation (3.53); however, the data are correlated by the following equation [56]

$$\overline{Nu} = 0.63(1 + 0.72\varepsilon)Gr^{0.25}, \quad (3.55)$$

where ***Ra*** number in Equation (3.53) is replaced by ***Gr*** number and the data are obtained for air with a Raleigh number between $2x10^7$ and $4x10^8$.

Rohsenow, Hartnett and Ganic rearranged Equation (3.53) using the measurements of Oosthuizen and Donaldson and give the following equation [57],

$$\overline{Nu} = (0.69 + 0.412\epsilon + 0.020\epsilon^2)Ra^{0.25}. \quad (3.56)$$

Nu, ***Ra***, and ***Gr*** numbers are based on the slant height of the cone.

3.6. Rate of Radiation Energy Loss

The blender contents are at a higher temperatures than its surroundings which is air. For high temperatures, the energy loss from the surface of the blender is not

only by convection but also by radiative heat transfer. The quantity of energy leaving a surface as radiant energy depends upon the absolute temperature of the blender surface. Thermodynamic considerations show that an ideal thermal radiator will emit energy at a rate proportional to the fourth power of the absolute temperature of the body. A more common name for an ideal radiator is blackbody. A blackbody emits and absorbs, at any temperature, the maximum possible amount of radiation at any given wavelength.

Real bodies such as the surface of the blender do not meet the specifications of an ideal radiator. According to Kirchhoff's law, a real surface always radiates less than a blackbody at the same temperature. If they emit, at a temperature equal to that of a blackbody, a constant fraction of blackbody emission at each wavelength, they are called grey bodies. Thus, the blender surface itself can be modelled as a grey body where the blender surroundings may be treated as a blackbody provided all incident radiation is absorbed by the surroundings regardless of wavelength and direction. The net rate of radiative heat transfer from a gray blender surface at a temperature $T_s(t)$ to a surrounding blackbody at T_∞ is given by [51,58]

$$Q_{rad}(t) = \sigma \epsilon A [(T_s(t)+273)^4 - (T_\infty+273)^4)] , \qquad (3.57)$$

where ϵ is the emittance of the blender surface(i.e., container wall) and σ is the Stefan-Boltzmann constant.

Chapter 4

SIMULATION CODE

4.1. SKINATH-WP Code

A FORTRAN computer code, SKINATH-WP, was developed using the models described in Chapters 1 and 2. SKINATH-WP inherited its name from SKINATH, a code developed for calculating criticality excursions for fissile systems having the form of a long horizontal cylinder externally cooled by natural convection [24].

The main program loop and a simplified flow chart of SKINATH-WP are given in Figures 4.1 and 4.2, respectively. SKINATH-WP consists of three major computational subprograms, namely, WPINTGEN, WPDYN, and LSODE. Simplified flow charts for these subprograms are given in Appendix B.

WPINTGEN, which is executed once per program run, conducts the initial calculations to provide starting values of various parameters used in the WPDYN and LSODE. WPDYN contains the statements executed during every communication time interval (i.e., edit interval) such as the mass balance and the temperature calculations. LSODE solves the coupled set of neutronic and thermal-hydraulic differential equations using the August 13, 1981 version of the Livermore Solver of Ordinary Differential Equations [59].

LSODE is a package based on GEAR, GEARB, and the October 23, 1978 version of ODEPACK. It solves the traditional initial value problem for stiff or non-

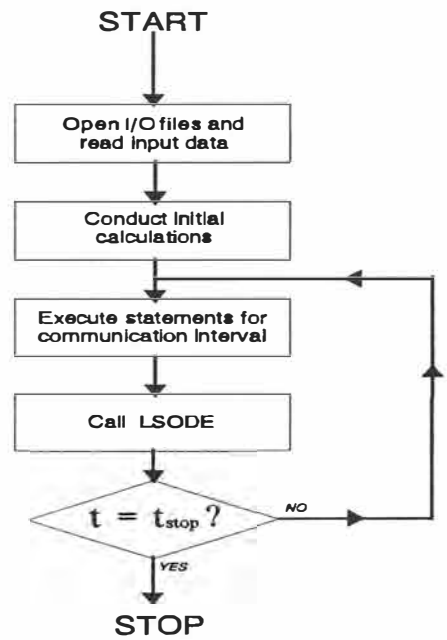

FIGURE 4.1 Main Program Loop of SKINATH-WP.

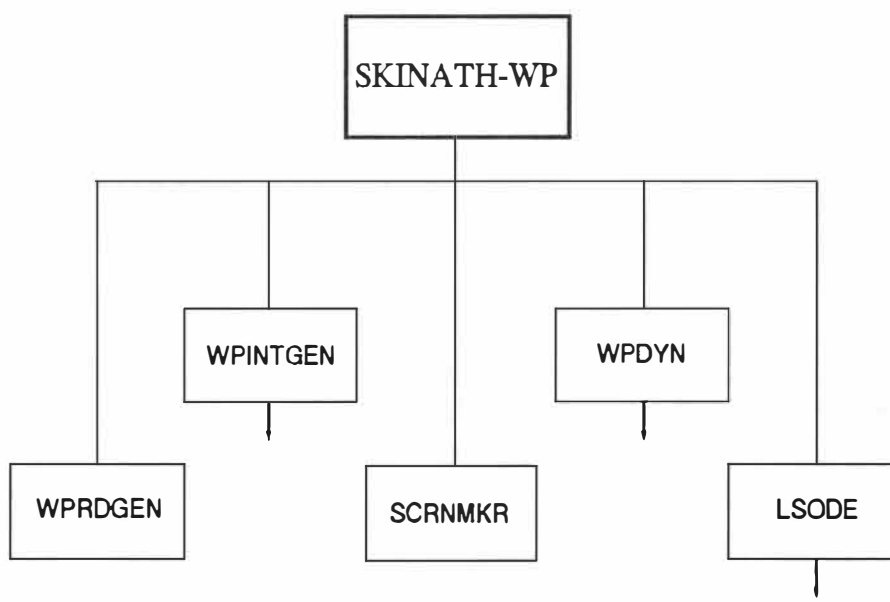

FIGURE 4.2 Flow Chart for SKINATH-WP.

stiff systems by calling a user-supplied subroutine which defines the set of first order differential equations. This subroutine, called ***Subroutine F***, declares neutronic and thermal-hydraulic models for damp powder systems by calling the subroutines shown in its flow chart (see Figure B.2). The coupled set of differential equations is introduced in the form of;

$$\frac{dy(i)}{dt} = f(i) = f(i,t,y(1),y(2),...,y(n)), \qquad i=1,2,...,n \tag{4.1}$$

as required by LSODE. The estimated local error in $y(i)$ is controlled by LSODE so as to be roughly less (in magnitude) than

$$e_{local}(i) = RTOL \times |y(i)| + ATOL \qquad if \quad ITOL = 1 \tag{4.2}$$

or

$$e_{local}(i) = RTOL(i) \times |y(i)| + ATOL(i) \qquad if \quad ITOL = 2, \tag{4.3}$$

where ITOL is an indicator for the type of error control. It is 1 or 2 depending on whether ATOL or RTOL is a scaler or an array where ATOL and RTOL are relative and absolute error tolerance parameters, respectively.

Thus, SKINATH-WP runs WPDYN and LSODE, and outputs results for each communication interval while LSODE solves the differential equations for all integration intervals within a communication interval as shown in Figure 4.3.

SKINATH-WP also calls SCRNMKR to reset the computer screen and WPRDGEN to open I/O files and to read three separate input files. The first file is the general input and the other two files contain saturation data for water.

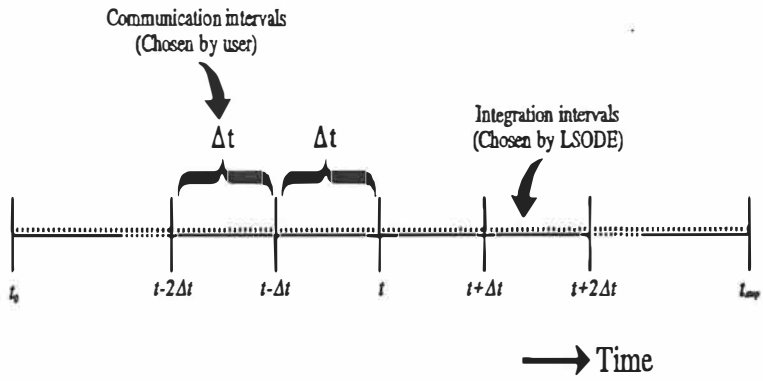

FIGURE 4.3 Hierarchy of time intervals in SKINATH-WP

Appendix B serves as a *user's manual* for SKINATH-WP. It contains simplified flow charts for the major subroutines, brief descriptions of subroutines and input, a table showing the contents of output files, sample screen output, sample input, and the code listing. The code is currently running on the VAX workstation and IBM compatible PCs at the Nuclear Engineering Department of the University of Tennessee.

Chapter 5

CODE VERIFICATION

5.1. Introduction

Several means have been used to verify the subprograms, the equations, and the models used in the SKINATH-WP code. The subprograms associated with the thermophysical properties of the system components (i.e., water, powder, container wall and air) are evaluated by simply comparing the calculated results to those expected from the corresponding listed property data. Also, parametric studies and hand calculations were employed to assure that the equations and parameters have been correctly defined in SKINATH-WP.

Attempting to validate the models is extremely difficult since, to the best of our knowledge, no experimental work has been done involving excursions of damp low-enriched UO_2 powder systems. Previous computational work on such criticality accidents is also very limited [8]. Recent CEA/UKAEA work considers a wet UO_2 system which includes both model development (i.e., POWDER code) and some experimental studies [29,31]. They developed a computer program (i.e. the POWDER code) to model the excursion of a mass of UO_2 powder containing water where the code calculates the variation of the power, the temperature, and the energy deposited with time. The POWDER code is intended for a potentially heterogeneous system without a mixing mechanism, whereas the SKINATH-WP code

assumes a homogeneous system with a mixing mechanism. Thus, the assumptions on the thermal-hydraulic phenomena, and the external and feedback reactivities are slightly different for SKINATH-WP and POWDER. However, it is the only code having the same nature as SKINATH-WP where the results are reported in the open literature and it can be used to verify SKINATH-WP to some degree.

5.2. POWDER Code

The POWDER code uses the conventional point kinetics equations to analyze the excursion characteristics of heterogeneous UO_2 powder systems contained in an open cylindrical vessel [29]. The water is assumed to enter from the top or from the bottom. The axial length is divided for computational purposes into a number of meshes for the powder and the water which surrounds it. In each mesh interval representing the powder region, a spherical powder particle is used for the calculation and represents one of the very many UO_2 particles in that mesh. Each particle is surrounded by the appropriate amount of water. Then, heat flow from the powder particle to the surrounding water is calculated using two different calculation modes, namely the conduction mode and the nucleate boiling mode. The conduction mode is used until vapor is produced. The code numerically solves the heat conduction equation in spherical geometry:

$$\rho c \frac{\partial T}{\partial t} = \frac{1}{r^2} \frac{\partial}{\partial r}\{kr^2 \frac{\partial T}{\partial r}\} + P\rho \ , \qquad (5.1)$$

where T Temperature (°C),

P Power (W),

r Radius vector (m),

k Thermal conductivity (J/m s °C),

ρ Density (kg/m^3),

c Specific heat (J/m^3 °C).

Following the vapor production (at the nucleation point for water),[a] the POWDER code switches to the nucleate boiling mode where the expression used for the heat flux is given as

$$F = 1.45 \times (T_p - T_n)^2 \times (T_p - T_w). \quad (5.2)$$

In Equation (5.2), T_p is the temperature of the particle edge (°C), T_n is the pressure dependent nucleation temperature (°C), and T_w is the average water temperature (°C). The POWDER code treats powder dispersion by solving the hydrostatic equation in each axial mesh, that is

$$\rho_{av} + \frac{\partial^2 z}{\partial t^2} = \frac{\partial p}{\partial z} - g \ , \quad (5.3)$$

where ρ_{av}, p, and g are average density (kg/m^3), pressure (Pa), and standard gravitational acceleration (m/s), respectively. In the POWDER model, the external reactivity driving force has two components, namely, water penetration through the

[a] The nucleation point of water is its saturation temperature. According to the CEA/UKAEA model, water vaporization occurs at a temperature above the normal boiling point of water (i.e., 109°C instead of 100°C). This excess temperature is due to the pressurization caused by mass of UO_2 and water above the point of nucleation.

porous powder body and powder collapse. Experiments were conducted to estimate these components in order to calculate a realistic external reactivity addition rate. They used an apparatus containing UO_2 powder consistent with the proposed scenario where the speeds of water penetration and powder collapse were measured. The results showed that the powder density increases from 1 g/cm^3 to 2.2 g/cm^3 with a powder collapse speed of 1 cm/min and a water penetration speed is 2 cm/min. This resulted in an external reactivity addition rate of ~3.85 ¢/sec [29].

The physical phenomena which resulted in significant reactivity feedback effects were powder temperature change (doppler effect), water temperature change, and system movement due to formation and migration of bubbles. The doppler and water temperature feedback reactivities were formulated as

$$k_i = A_i \log\left(\frac{T_f}{T_{fo}}\right) + B_i (T_f - T_{fo}), \tag{5.4}$$

where A_i and B_i are the constant coefficients depending on H/U ratio, T_f is the average particle temperature initially at T_{fo}, and the subscript i represents the feedback phenomena (i.e., doppler effect and water temperature change). The coefficients in Equation (5.4) were evaluated using the APOLLO (CAE) and WIMS (UKAEA) codes [31]. The POWDER code also has an option to consider the expansion of water. This option was introduced in order to account for the effect of air spaces in the powder body. Such space should allow the water to expand without driving the whole system apart.

The reactivity feedback due to formation and migration of bubbles was calculated

using perturbation theory. Each axial segment provides a reactivity worth per unit mass of material using the expression:

$$K_M = \int_V (\delta\rho)\,\omega\,dV + \int_S \omega\,\rho\,(d \bullet dS)\ , \qquad (5.5)$$

where ω is the worth which is calculated assuming a cosine shape for the flux, and ρ is the density.

The CEA/UKAEA model does not consider the stochastic nature of the excursion associated with the strength of the inherent neutron source present in the system. The reader is referred to Reference 29 for further discussion on CEA/UKAEA work.

5.3. Comparison of Results from SKINATH-WP and POWDER

To evaluate the models, we analyzed the accident scenario described in Reference 29 which involves the introduction of water at a rate of 0.5 l/sec in the center of a cylindrical vessel (r=0.4m, and h=1m) open at the upper end and containing 500 kg of $U(5\%)O_2$ powder with an initial density of 1 g/cm^3. Since SKINATH-WP requires a driving force function with respect to homogeneous water content in g/cm^3, some calculations were performed using CSAS1X with the 27 group ENDF/B-IV cross-sections provided in the SCALE-IV system. Figure 5.1 presents the results of these calculations and the 7th order polynomial fit of the calculated data which can be formulated using an expression similar to Equation (2.10). Table 5.1 shows the constants C_1 to C_7 for a system consistent with the scenario described above. SCALE-IV/CSAS25 was used to calculate the neutron mean generation time

TABLE 5.1
Constants C_1 to C_{10} for ~500 kg of 5% w/o U^{235} Enriched UO_2 Powder Loaded into a Cylindrical Blender (Diameter = 80 cm, Height = 100 cm) with a Density of 1 g/cm³.

CONSTANT	VALUE
C_1	3.46249×10^5
C_2	-1.21651×10^6
C_3	1.77355×10^6
C_4	-1.38959×10^6
C_5	6.33002×10^5
C_6	-1.68984×10^5
C_7	2.50626×10^4
C_8	-1.66420×10^3

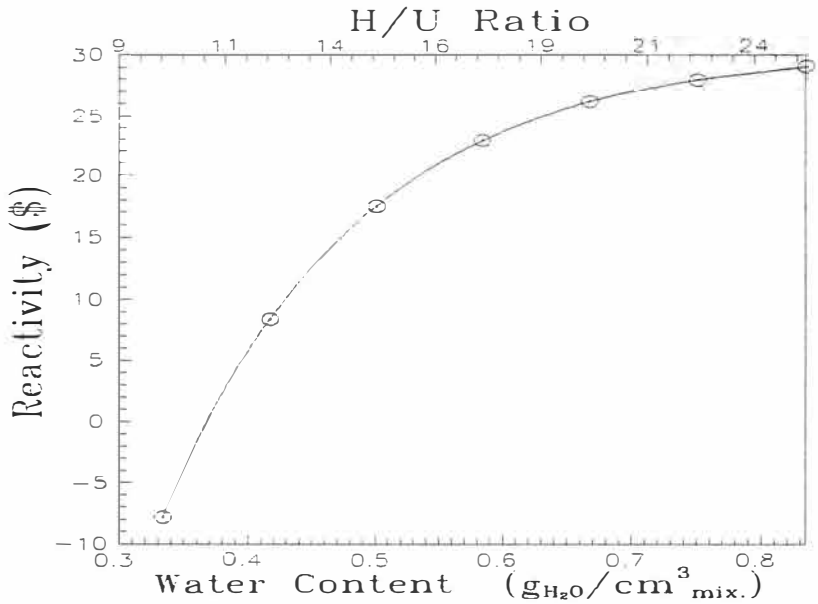

FIGURE 5.1 Results of Reactivity Driving Force Calculations for the System Considered in CEA/UKAEA Work.

which is found to be $\sim 6.25 \times 10^{-5}$s with an insignificant uncertainty. Also ~ -1.38 ¢/°C is used as the lumped feedback coefficient representing the doppler effect of powder and the change in water temperature where this value is reported as the temperature coefficient by Reference 29.[b] The external reactivity addition rate is taken to be ~ 3.85 ¢/sec as described in the previous section.

Also, we did not consider the stochastic nature of the excursion to make our assumptions consistent with the CEA/UKAEA model. However, the criteria given by Equation (2.6) for the systems having a weak neutron source is roughly estimated for ~ 500 kg of $U(5\%)O_2$ powder and it is found to be ~ 0.28.[c] Hence, the statistical properties of weak sources may be important for the system considered in the CEA/UKAEA work.

The results are presented in Figure 5.2 along with the Reference 29 results for the case where moderator expansion effects are included in the Reference 29 calculations. As expected, our results bracket the Reference 29 results because of the bounding nature of our modelling assumptions. The time location of the power peaks are all in excellent agreement; whereas, the power peaks are in agreement to within an order of magnitude. If moderator expansion effects are not included

---

[b] Reference 29 apparently reports ~ -1.3846 ¢/°C as the feedback coefficient for the doppler effect. Reference 29 also mentions the use of separate feedback coefficients for the effects of doppler and neutron spectrum changes due to changes in the water temperature. However, SKINATH-WP assumes a lumped doppler feedback coefficient for the bulk.

[c] The mean neutron lifetime is estimated using SCALE-IV/KENO-Va and is equal to $\sim 5.54 \times 10^{-5}$ sec (with an insignificant uncertainity).

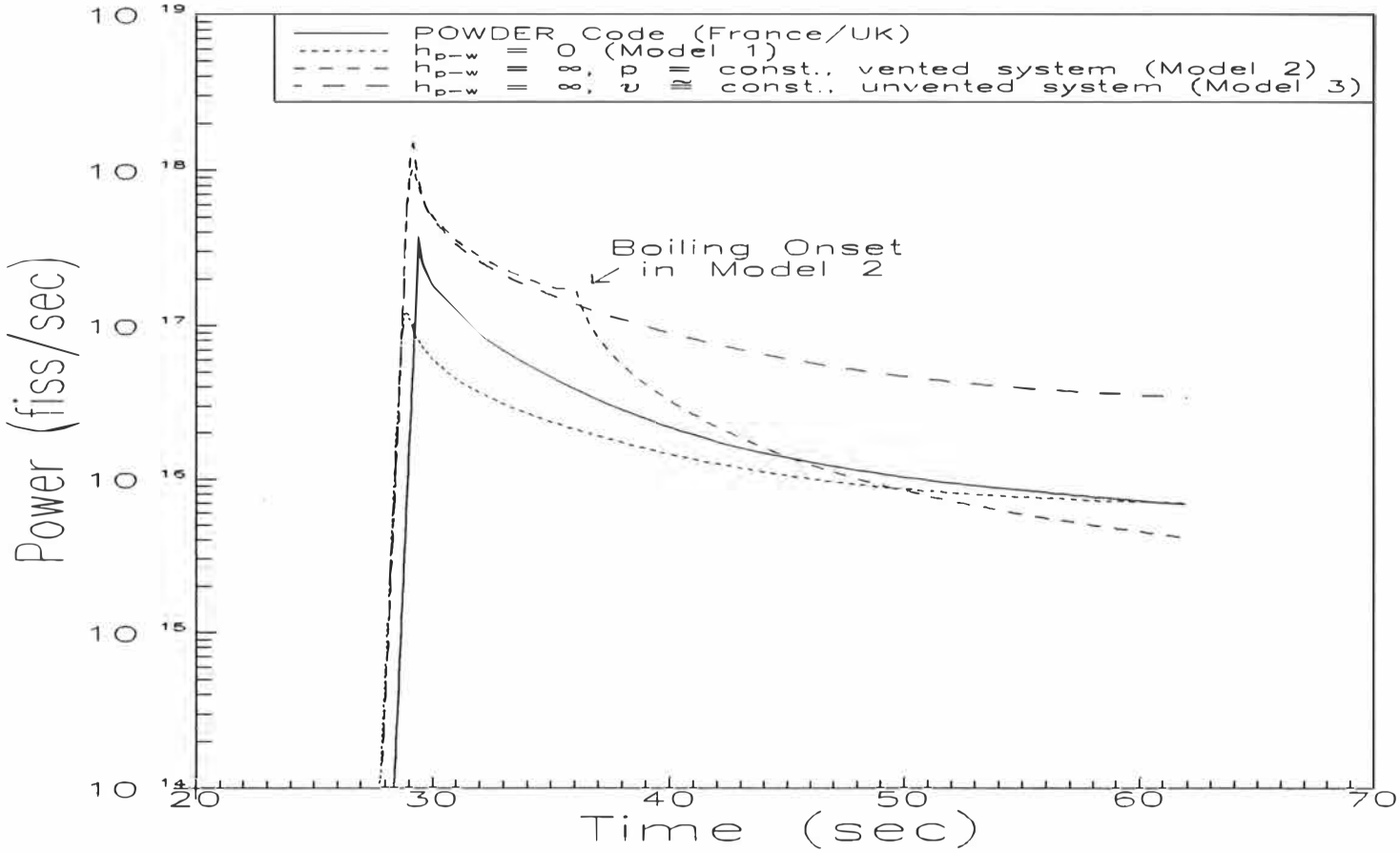

Figure 5.2 Power versus Time: Comparison of SKINATH-WP Results with the Results from the POWDER Code.

in the Reference 29 calculations, the peak power and boiling time predicted by Reference 29 are 7.0×10^{17} fiss/sec and 33.1 sec, respectively, which is in good agreement with our Model 2 results of 10.1×10^{17} fiss/sec and 35.2 sec, respectively.

As seen in the above discussion, Model 2 and Model 3 are capable of producing more conservative results than either Model 1 or the POWDER code. Model 2 is developed for open systems and is in good agreement with the CEA/UKAEA model. However, our blender system is potentially closer to a closed system which is better approximated by the assumptions for Model 3. Moreover, only Model 3 estimates pressure and quality with respect to time which may be valuable information. Hence, Model 3 is used for excursion studies in Chapter 6.

Chapter 6

RESULTS

6.1. Blender Transient Simulations

Transient blender simulations were conducted for a wide range of reactivity addition rates using SKINATH-WP. Model 3 is chosen for the analysis due to several factors. First of all, Model 3 assumes an infinite heat transfer coefficient between major components as described in Section 3.2.3. Preliminary studies and the work described in Chapter 5 have shown that this assumption provides more conservative results than the other bounding model which assumes zero heat transfer coefficient. In other words, Model 2 and Model 3 are superior to Model 1 with respect to conservatism of the results (i.e., total fissions, first fission pulse etc.). Second, Model 3 utilizes an unvented system assumption where all steam generated is trapped in the system increasing its pressure. The actual system is closed at the upper end, and hence, resembles a closed system which is assumed in Model 3. Also, only Model 3 estimates pressure with respect to time which may provide valuable design information.

A comparison of Model 2 and Model 3 (i.e., vented and unvented systems) with respect to total fissions is presented in Section 6.2.6. Since the actual blending system has a ventilation system, such a comparison may be helpful to understand the effect of ventilation during an accident. Thus, the use of Model 3 may be assumed to

accompany the assumption of total blackout (or failure) of the ventilation system as a contingency.[a]

Results for two accident scenarios are given in Tables 6.1 and 6.2 which consist of reactivity addition rates ~1 ¢/sec and ~1 $/sec, respectively. These scenarios involve 5000 kg of dry UO_2 powder in a cylindrical blender. Its dimensions are given in Chapter 2. The material density of the power is taken as 2.2 g/cm^3 at 20 °C. It is postulated that water is pouring continuously into the blender at a constant rate while the mixing mechanism is in operation thus mixing the blender contents homogeneously. The H/U ratio of the system at delayed critical (which is ~3) is taken as the starting point for the excursion calculations. The initial pressure inside the blender is atmospheric and the initial temperatures of the blender contents, container wall, and outside air are set to 20°C. The pressure of the outside environment is assumed to be constant at atmospheric.

Plots of external, feedback and total reactivities, power, total fissions, temperature, and pressure versus time for reactivity addition rates of ~1 ¢/sec and ~1 $/sec are shown in Figures 6.1 and 6.2, respectively. Similar results for reactivity addition rates of ~0.1 ¢/sec, ~6.776 ¢/sec, ~10 ¢/sec, and ~10 $/sec are given in Appendix B. A water ingress rate of 0.5 l/sec suggested by the CEA/UKAEA work for commercial facilities corresponds to a reactivity addition rate of ~6.776 ¢/sec [29]. All of these figures show the results for the case where water addition is

[a] Model 3 assumes that all the steam generated will remain in the blender during the transient. This can only happen if the ventilation system is not in operation.

TABLE 6.1 Summary of Accident Scenario #1.

Water Ingress Rate	0.0681 l/sec (0.0180 gal/sec)
Reactivity Addition Rate	~ 1 ¢/sec
Elapsed Time to Delayed Critical	1.96 hr

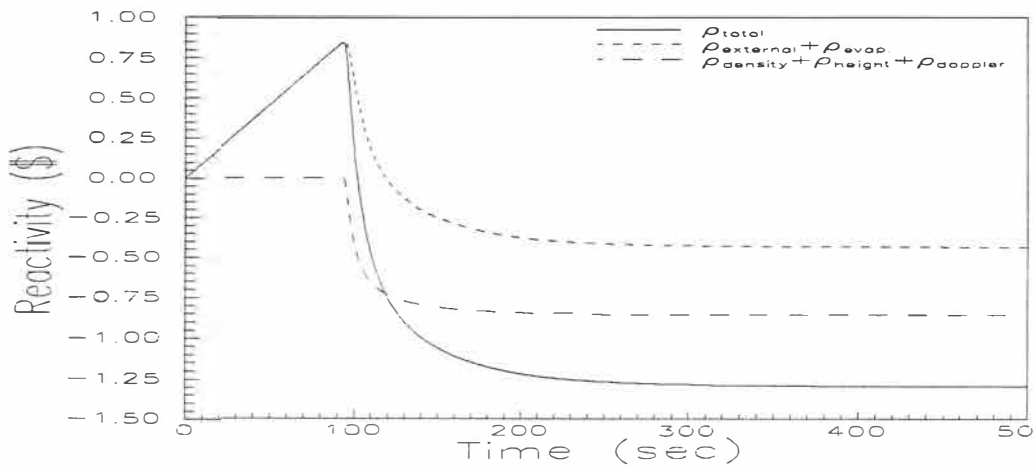

Figure 6.1a Reactivity versus Time for ~1 ¢/sec Reactivity Addition Rate if Water Ingress is Stopped at the First Power Peak.

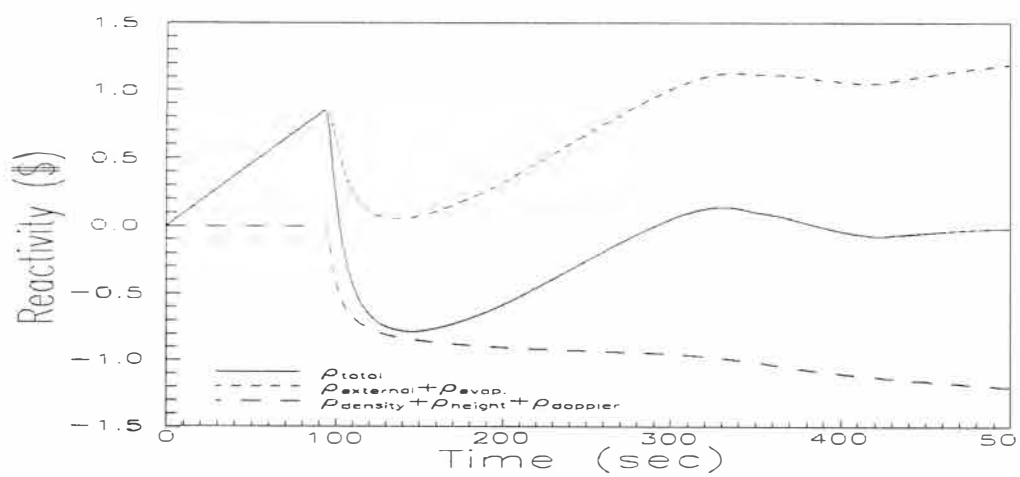

Figure 6.1b Reactivity versus Time for ~1 ¢/sec Reactivity Addition Rate for Continuous Water Ingress.

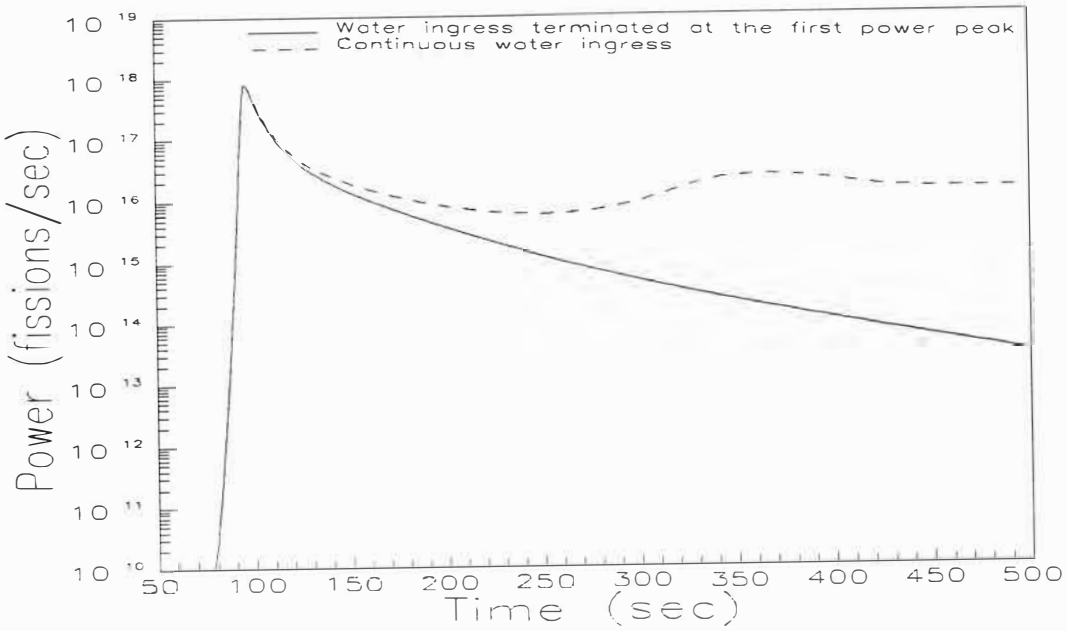

Figure 6.1c Power versus Time for ~1 ¢/sec Reactivity Addition Rate.

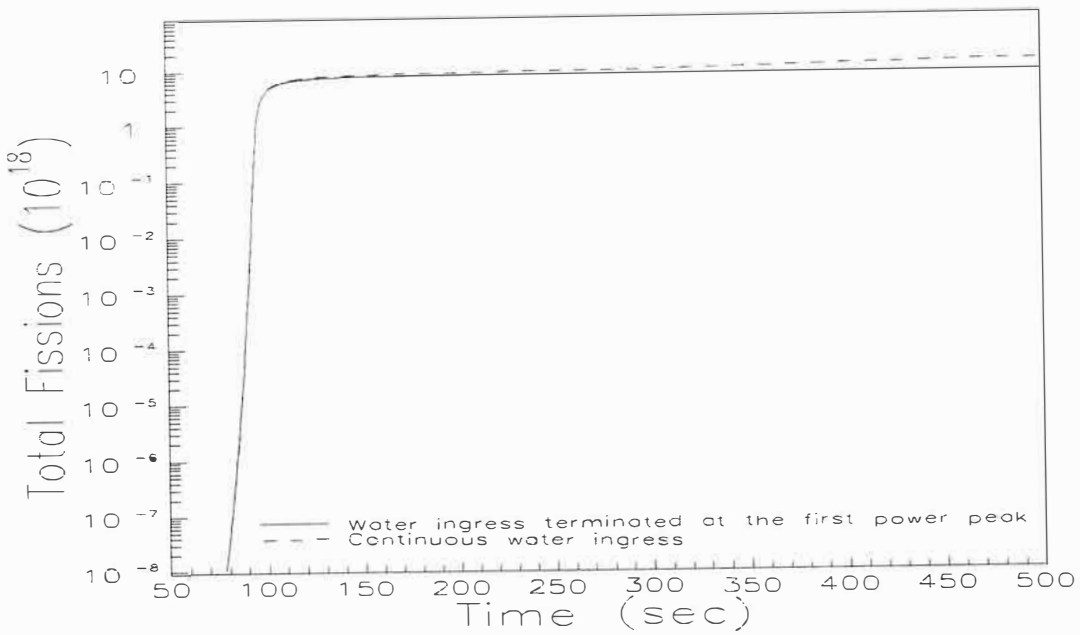

Figure 6.1d Total Fissions versus Time for ~1 ¢/sec Reactivity Addition Rate.

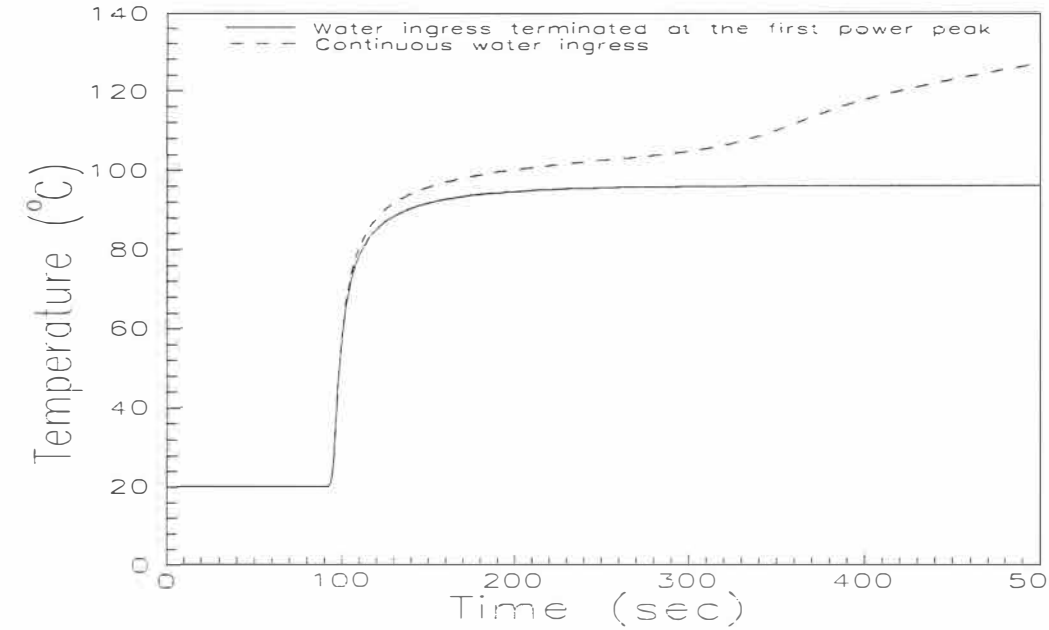

Figure 6.1e Temperature versus Time for ~1 ¢/sec Reactivity Addition Rate.

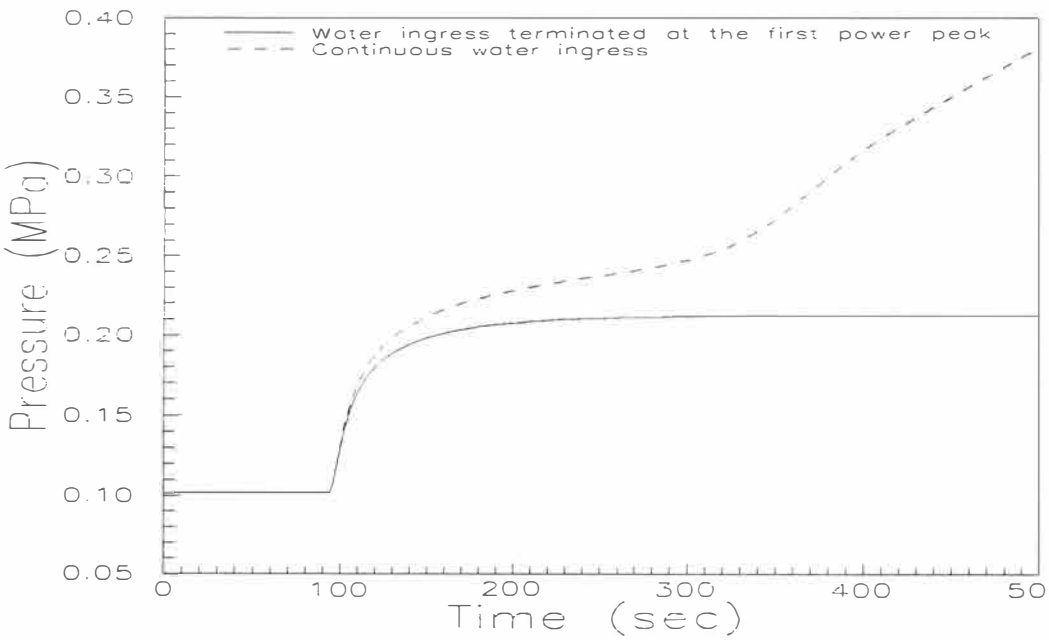

Figure 6.1f Pressure versus Time for ~1 ¢/sec Reactivity Addition Rate.

TABLE 6.2 Summary of Accident Scenario #2.

Water Ingress Rate	7.4753 l/sec (1.9750 gal/sec)
Reactivity Addition Rate	~1 $/sec
Elapsed Time to Delayed Critical	1.07 min

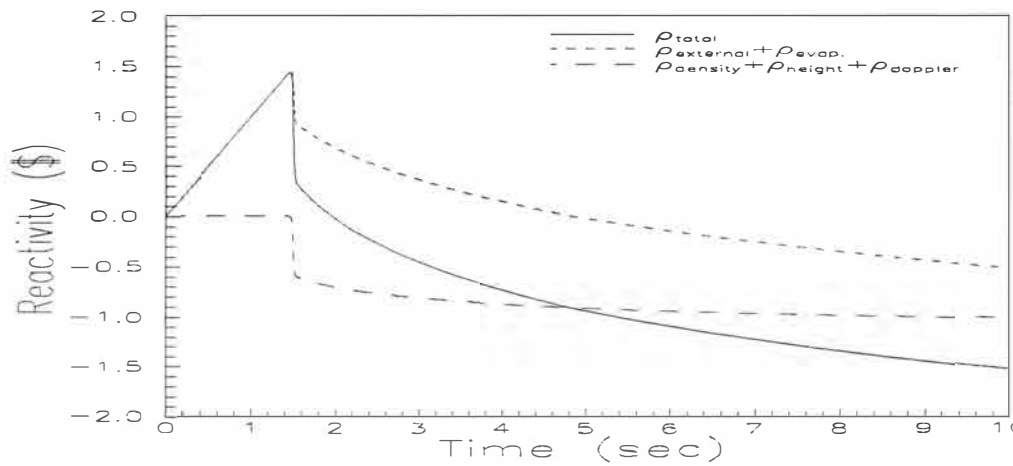

Figure 6.2a Reactivity versus Time for ~1 $/sec Reactivity Addition Rate if Water Ingress is Stopped at the First Power Peak.

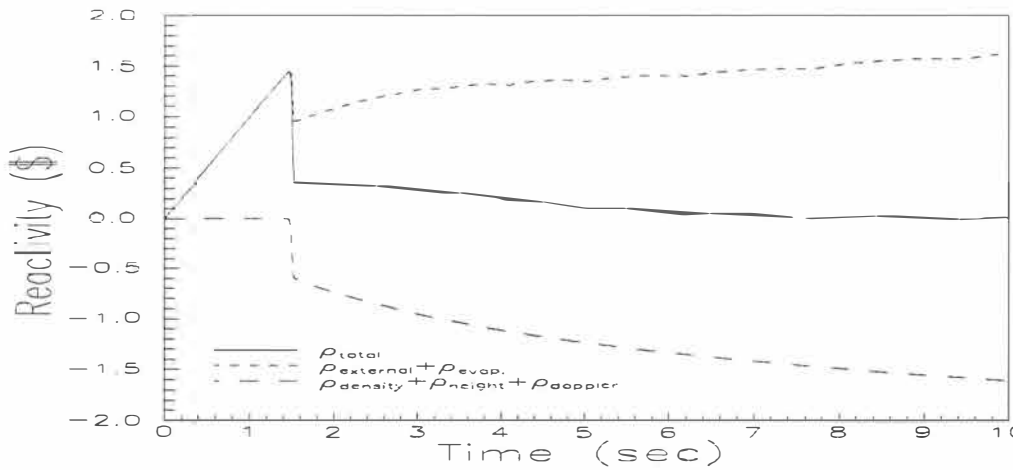

Figure 6.2b Reactivity versus Time for ~1 $/sec Reactivity Addition Rate for Continuous Water Ingress.

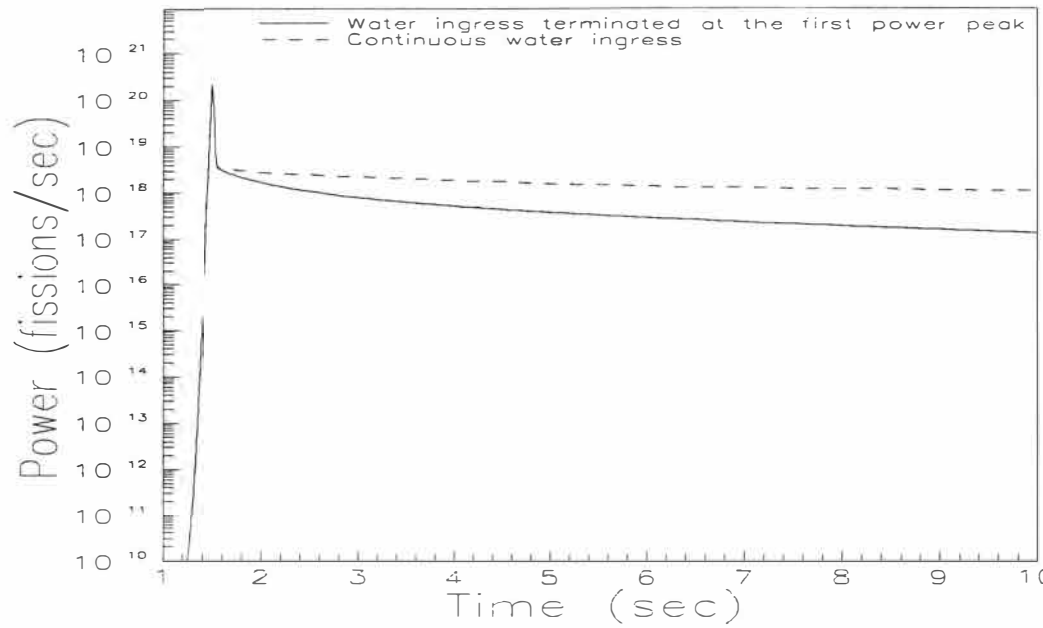

Figure 6.2c Power versus Time for ~1 $/sec Reactivity Addition Rate.

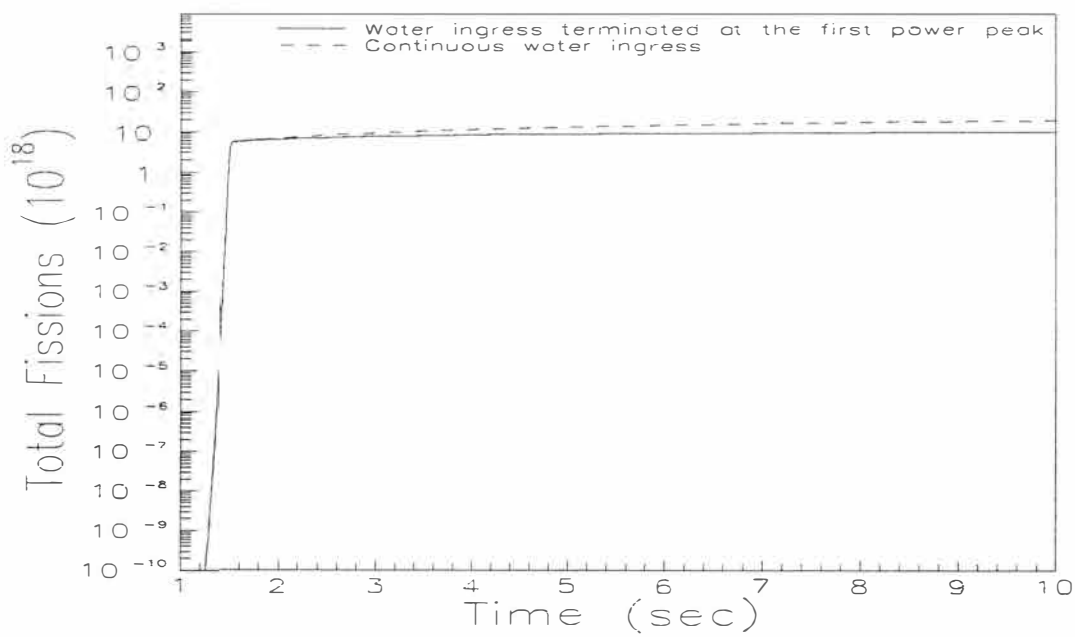

Figure 6.2d Total Fissions versus Time for ~1 $/sec Reactivity Addition Rate.

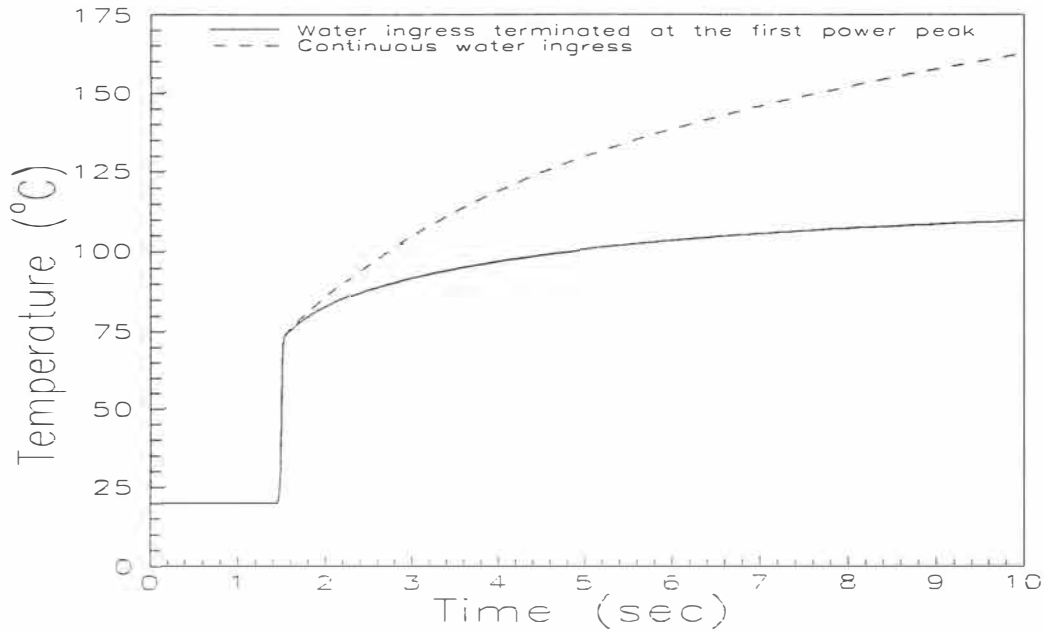

Figure 6.2e Temperature versus Time for ~1 $/sec Reactivity Addition Rate.

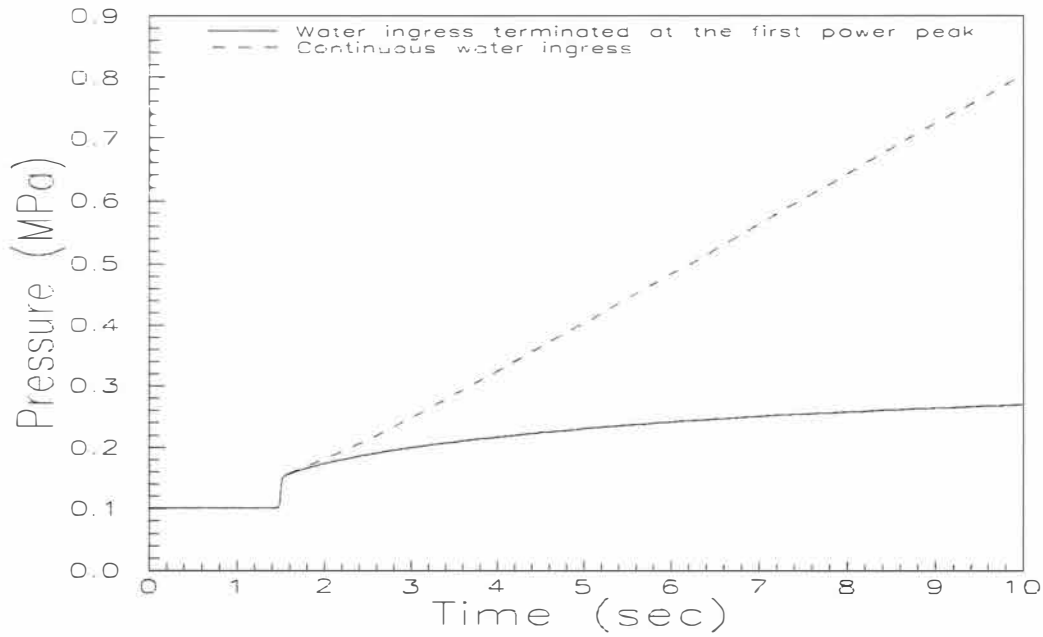

Figure 6.2f Pressure versus Time for ~1 $/sec Reactivity Addition Rate.

stopped at the peak of the first fission pulse (the spike) as well as the results for the case where water addition is continuous.

In all of the accident scenarios, the power curve has two main parts, the spike and the plateau. The spike identified by a high rate of energy release and short time interval. In other words, the spike is the first fission pulse (or first power peak). Then, the curve follows a lower region, the plateau, which is characterized by a long time interval. The plateau region is smooth if the water is added until the peak of the first power peak. For continuous water addition, the plateau region contains a series of pulses of decreasing magnitude and frequency. A discussion of these results are presented in the following sections.

6.1.1. The Spike

The spike generated during a criticality excursion is important because it determines the immediate consequences of the accident such as explosive destruction and dose rates to personnel before emergency evacuation. Figure 6.3 shows the relation between the spike peak value and the reactivity. As seen in this figure, the peak value changes significantly with respect to reactivity addition rate. It increases almost linearly from 2.94×10^{17} fissions/sec to 2.51×10^{21} fissions/sec for reactivity addition rates from ~ 0.1 ¢/sec to ~ 10 \$/sec. It is controlled by thermal feedback effects such as powder thermal expansion, the doppler effect, and moderator boiling. A plot of the spike location in time with respect to reactivity addition rate is shown in Figure 6.4. The spike time can be defined as the elapsed time between delayed

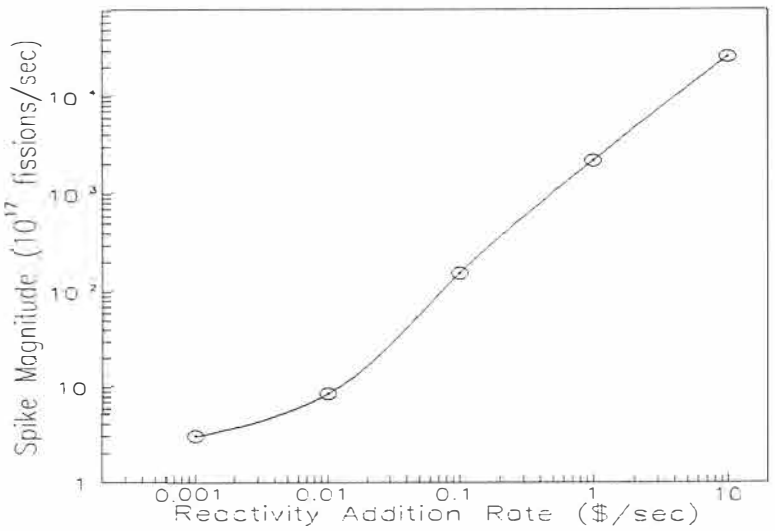

FIGURE 6.3 Spike Magnitude versus Reactivity Addition Rate if Water Ingress is Stopped at the First Power Peak and if Water Ingress is Continuous.

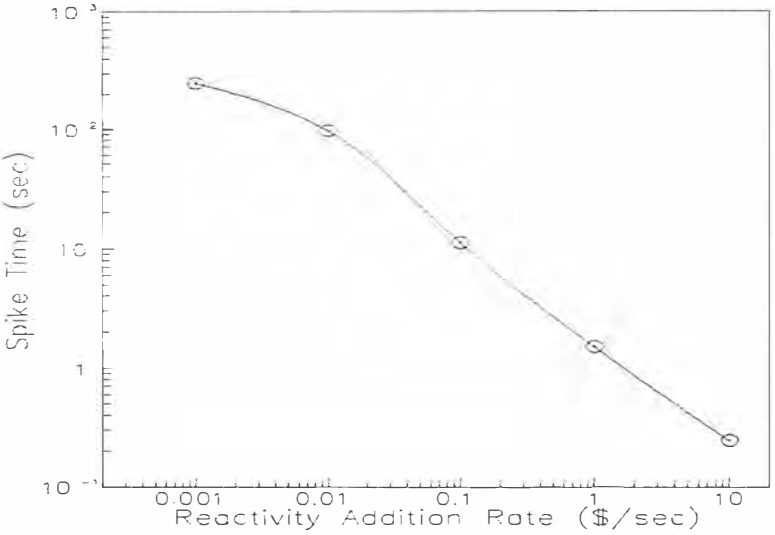

FIGURE 6.4 Spike Time versus Reactivity Addition Rate if Water Ingress is Stopped at the First Power Peak and if Water Ingress is Continuous.

criticality (at t=0) and the time location of the first fission pulse peak. It decreases from 243 sec to 0.24 sec for the same reactivity addition rate range.

For large reactivity addition rates, the height of the spike increases tremendously in a short time interval. The result of such instant energy release is probably severe mechanical damage or disassembly.

6.1.2. Second Fission Pulse

The relationship between the second fission pulse peak value and the reactivity addition rate is shown in Figure 6.5. Subsequent pulses appear following the spike if water ingress continues after the duration of the first fission peak. In general, power pulses continue with decreasing peak value and frequency as long as water is added into the system. Among these pulses, the second pulse is the largest in magnitude and it ranges from 1.61×10^{16} fissions/sec to 1.43×10^{19} fissions/sec for reactivity addition rates from ~0.1 ¢/sec to ~10 $/sec.

Roughly speaking, the second pulse is one order of magnitude less that the spike for small reactivity addition rates. It is two orders of magnitude less if reactivity addition is large. Similar to the spike time, the second fission pulse time can be defined as the elapsed time between delayed criticality (t=0) an the second fission pulse peak. It decreases with respect to reactivity addition rate as shown in Figure 6.6.

Finally, some feedback mechanisms which are not taken into account in SKINATH-WP may be important, and hence, the second fission pulse peak values

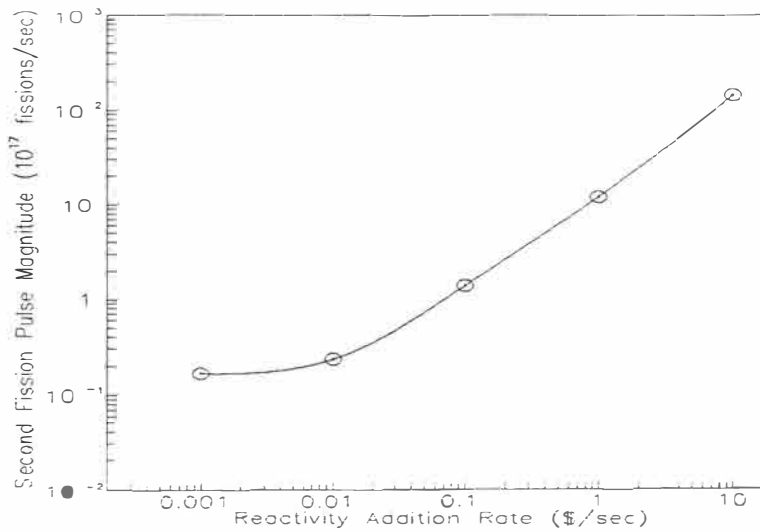

FIGURE 6.5 Second Fission Pulse versus Reactivity Addition Rate for Continuous Water Ingress.

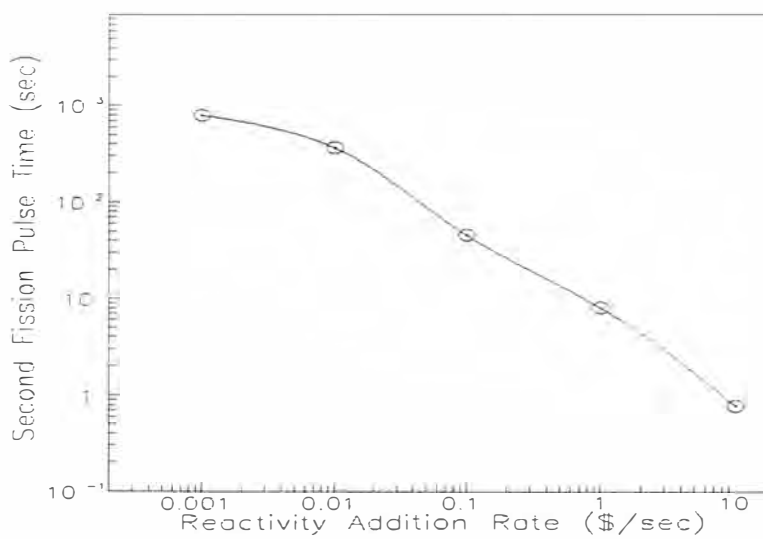

FIGURE 6.6 Second Fission Pulse Time versus Reactivity Addition Rate for Continuous Water Ingress.

presented in this section may not be accurate. Also, the second fission pulse will not happen if the spike mechanically destroys the blender. Such destruction intuitively seems to be likely for large reactivity addition rates.

6.1.3. Maximum Temperature and Pressure

If the water ingress is stopped at the first power peak, the temperature and pressure rise sharply accompanying the power increase up to point the where they reach their maximum value. Then, they decrease due to cooling mechanisms (i.e., natural convection and radiation). A plot of maximum temperature and pressure with respect reactivity addition rate is presented in Figures 6.7 and 6.8, respectively. The maximum value of temperature increases from 85°C to 144°C and the pressure increases from 0.18 MPa to 0.55 MPa when the reactivity addition rate increases from ~0.1 ¢/sec to ~10 $/sec.

If water addition is continuous, the temperature and pressure increase sharply at fission pulses and more gradually between power peaks for small reactivity addition rates. However, the temperature and pressure increases almost linearly following the sharp rise accompanying the spike if the reactivity addition rate is large. The two major assumptions of infinite heat transfer coefficient and an unvented system employed in Model 3 are expected to provide an upper limit on the maximum blender pressure.

The maximum blender temperature and pressure are strictly dependent on the accident scenario. They may differ significantly from the maximum values given in

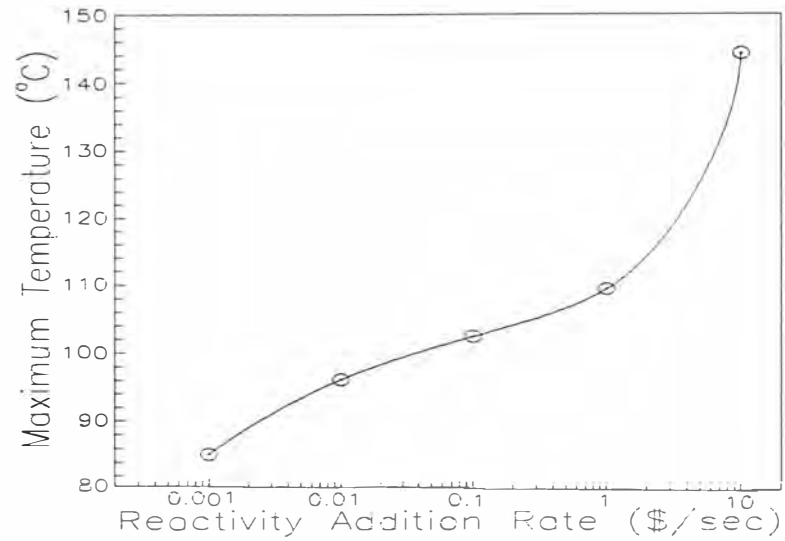

FIGURE 6.7 Maximum Temperature versus Reactivity Addition Rate if Water Ingress is Stopped at the First Power Peak.

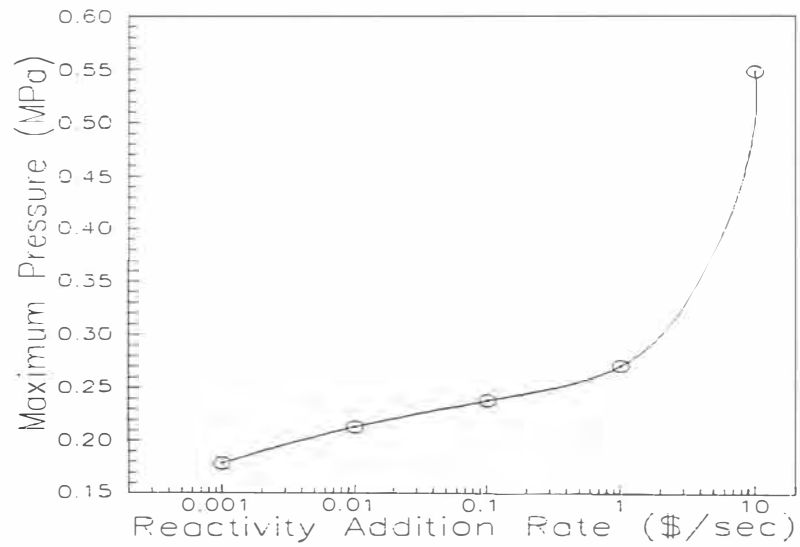

FIGURE 6.8 Maximum Pressure versus Reactivity Addition Rate if Water Ingress is Stopped at the First Power Peak.

Figures 6.7 and 6.8 if water ingress continues after the first power peak. As an example, Figure 6.8 gives a maximum pressure of 0.26 MPa for a reactivity addition rate of 1 \$/sec. However, if water ingress is continuous, the pressure may reach 0.8 MPa only 10 seconds after delayed criticality as shown in Figure 6.2f. Thus, it is 3 times larger than the value given by Figure 6.8.

6.1.4. Total Fissions

The total number of fissions generated is important because it defines the magnitude of the radionuclide source strength available for environmental release. The total fissions at time t is given by

$$Total\ Fissions = \int_0^t n(t')\ dt' \qquad (6.1)$$

where $n(t)$ is the system power at time t (fissions/sec). The total fissions for various reactivity addition rates differ only slightly.

A summary of the transient results is given in Table 6.3. This table also presents a comparison between the two different water ingress stopping criteria, namely continuous water ingress and stopping the water ingress at the first power peak. The total fissions are calculated for both stopping criteria corresponding to an arbitrary reference time. It is found that they differ only slightly for small reactivity addition rates but may differ by an order of magnitude if the reactivity addition rate is large.

The spike seems to be the main contributor to the final total energy release. An analysis for water addition stopped at the first power pulse may provide rough

estimates of the total fission yield for continuous water addition cases. These estimates should be satisfactory if the number of fission pulses following the spike is small. A plot of the total fissions versus reactivity addition rate is given in Figure 6.9.

6.2. Parametric and Sensitivity Studies

Parametric and sensitivity studies were conducted using SKINATH-WP to determine the effects of several factors. An extensive analysis was conducted by varying the following factors: communication time interval, initial power, LSODE integration method, free convection correlation, total water ingress time, reactivity feedback coefficient, and neutron mean generation time. The effect of these factors on the spike, total fissions, maximum temperature and pressure are evaluated. Two base accident scenarios are defined as a 500 kg water ingress at a rate of 0.068 l/sec ($\sim$1¢/sec) and 7.475 l/sec ($\sim$1$/sec). The former represents a small reactivity addition rate while the latter is chosen to illustrate sensitivity for a large reactivity addition rate. Assuming, no water is present in the blender initially (i.e., H/U=0), water is assumed to be pouring in until the total mass of water is equal to 500 kg. The severity of an accident is characterized primarily by the magnitude of the spike and the total number of fissions produced in the accident. In the following sections, the effects on total fissions are primarily discussed since preliminary studies have shown that the sensitivity of the spike to various parameters is consistent with the sensitivity of the total fission yield.

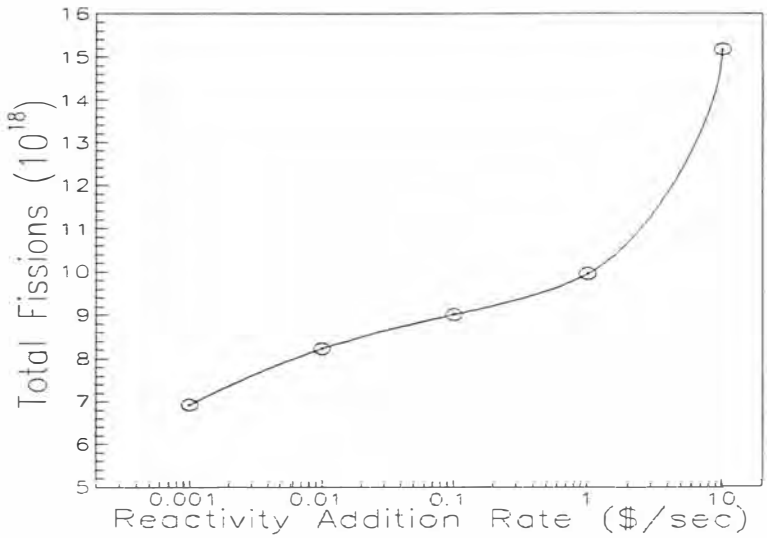

FIGURE 6.9 Total Fissions versus Reactivity Addition Rate if Water Ingress is Stopped at the First Power Peak.

TABLE 6.3
Summary of the Transient Results.

Reac. Addit. Rate ($/sec)	Water Ingress is Stopped at the First Power Peak				Continuous Water Ingress			
	First[b] Fission Pulse[c]	Time (sec)	Total Fiss.	Time (sec)	Second Fission Pulse[c]	Time (sec)	Total Fiss.	Time (sec)
0.001	2.94e+17	243	6.92e+18	1000	1.61e+16	792	9.89e+18	1000
0.01	8.17e+17	96	8.24e+18	500	2.29e+16	366	1.27e+19	500
0.1	1.48e+19	11.1	9.03e+18	50	1.37e+17	45.3	1.35e+19	50
1.0	2.08e+20	1.5	9.97e+18	10	1.18e+18	7.95	1.94e+19	10
10.0	2.52e+21	0.24	1.52e+19	1	1.43e+19	0.77	2.05e+19	1

[b] First fission pulse is same for continuous water ingress case.

[c] Units are fissions/sec.

6.2.1. Initial Power

SKINATH-WP assumes delayed criticality as the starting point for the excursion calculations. The transient analysis may also be started at subcritical. Starting a transient at subcritical requires calculation of a fixed extraneous source term which is used as the source term in the point kinetics equations. However, such a starting concept is not desirable due to several factors. These factors are described in Reference 28 which include Hansen's delay time concept, the potential invalidity of the point kinetics equation at subcritical, loss of flexibility in the units attributed to several parameters in the point kinetics equations, and computation cost. Furthermore, Reference 28 results show that the subcritical and delayed critical starts do not differ significantly.

On the other hand, starting a transient at delayed critical does not involve any of the above listed factors, but it does require the knowledge of initial power in the system at delayed critical. The initial power is not known due to lack of experimental data. Also, to the best of our knowledge, there is no theoretical method in the open literature to estimate the power at delayed critical. Hence, we conducted some calculations to study whether or not the total fission yield is sensitive to initial power assumed at delayed critical. We varied the initial power from 10^{-2} to 10^{4} per 100 g of UO_2-water mixture. The plot of total fissions with respect to initial power is given in Figures 6.10 and 6.11 for the base accident scenarios. The calculations show almost no difference between the total number of fissions for both small and large

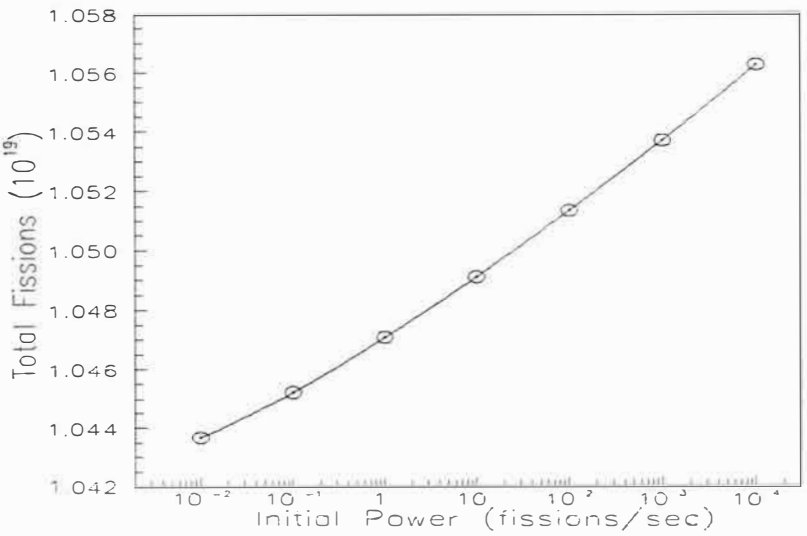

FIGURE 6.10 Total Fissions vs Initial Power per 100 g of UO_2-Water Mixture for Reactivity Addition Rate of ~ 1 ¢/sec

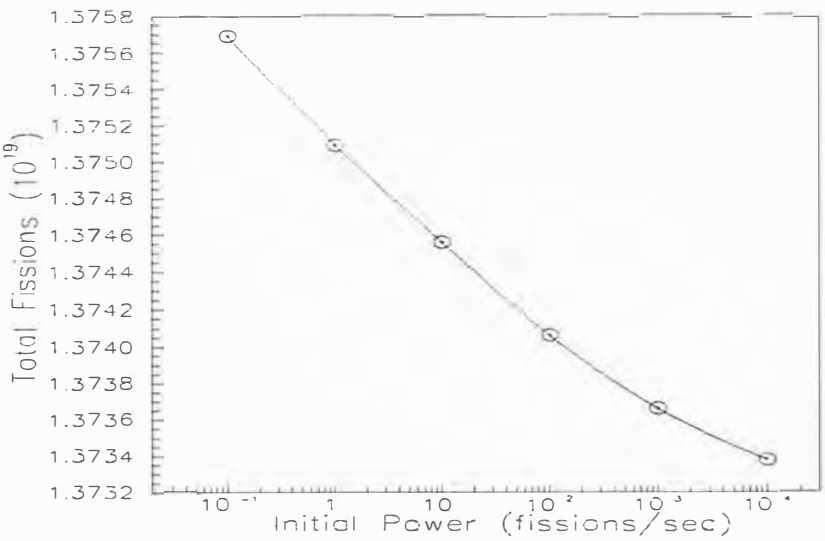

FIGURE 6.11 Total Fissions vs Initial Power per 100 g of UO_2-Water Mixture for Reactivity Addition Rate of ~ 1 $/sec.

reactivity addition rates. Thus, the total number of fissions can be viewed as insensitive to the initial power.

The initial power used in the analysis is calculated by dividing the neutron production rate of spontaneous fission events given in Section 2.5 by the average number of neutrons emitted per fission (≈ 2.43). Then, a lower limit for the initial fission power of the system is calculated to be ~ 19321 fissions/sec. This value is assumed as the initial power in this work.

6.2.2. Communication Time Interval

The sensitivity of the results to the communication time interval is important since SKINATH-WP updates the mass balance and temperature information only once at each communication time interval. We expect better results for smaller communication time intervals. Also, it effects the runtime which is directly related to the computational cost. Specifically small communication time intervals are not desirable due to large runtime and computational cost. Thus, an optimum communication time interval should be chosen considering the trade-off between computational cost and adequate representation of the mass and energy balances.

We conducted a sensitivity study to find an optimum value for the communication time interval. The communication time interval used in the analysis depends on reactivity addition rate. In general, it is taken as 0.1 sec for small reactivity addition rates and 0.001 sec for large reactivity addition rates. This parameter is varied over

the range from 0.001 sec to 1 sec and from 0.0001 to 0.01 for the first and second base accident scenarios, respectively. The effect on the total fissions is shown in Figures 6.12 and 6.13. Both figures demonstrate that there is no noticeable deviations in the results for the considered ranges and the values chosen as the default may be considered as adequate.

6.2.3. Total Water Ingress Time

The total water ingress time is the sum of the elapsed time to delayed critical and the transient time up to the end of water ingress. In other words, it is the total time up to the termination of the external reactivity addition. A parametric study was conducted to study the effect of total water ingress time on total fissions. Figures 6.14 and 6.15 show total fissions versus total water ingress time where it can be seen that total fissions increase almost linearly. These results are expected because more external reactivity is added to the system for larger ingress times. Also, the total water ingress time is linearly proportional to total ingress water mass. Figures 6.16 and 6.17 show the same phenomena but with respect to total ingress water mass instead of total water ingress time.

6.2.4. Reactivity Feedback Coefficients

As described in Chapter 2, reactivity feedback coefficients are calculated using CSAS1X and CSAS25. These parameters will differ slightly for different computer

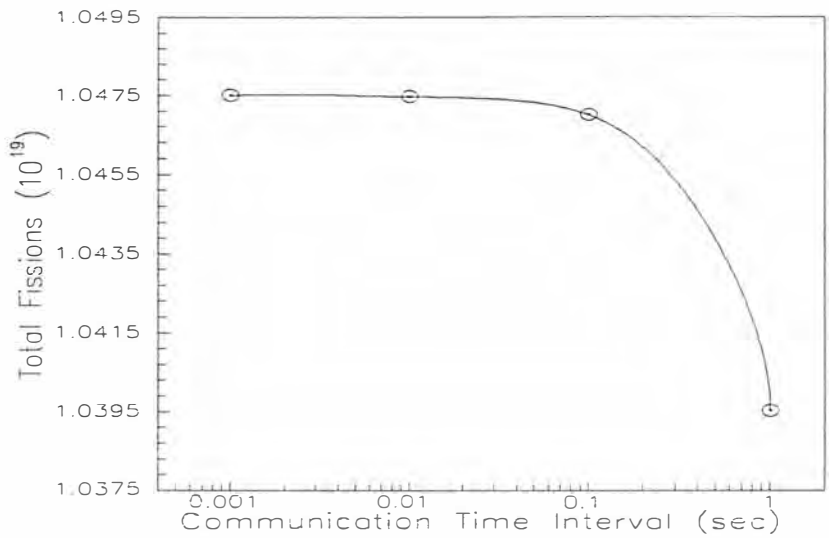

FIGURE 6.12 Total Fissions versus Communication Time Interval for ~1 ¢/sec Reactivity Addition Rate.

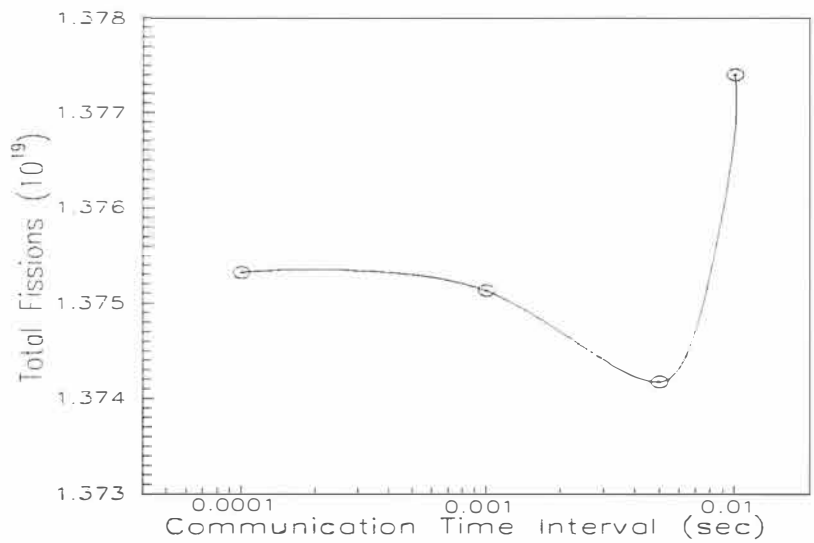

FIGURE 6.13 Total Fissions versus Communication Time Interval for ~1 $/sec Reactivity Addition Rate.

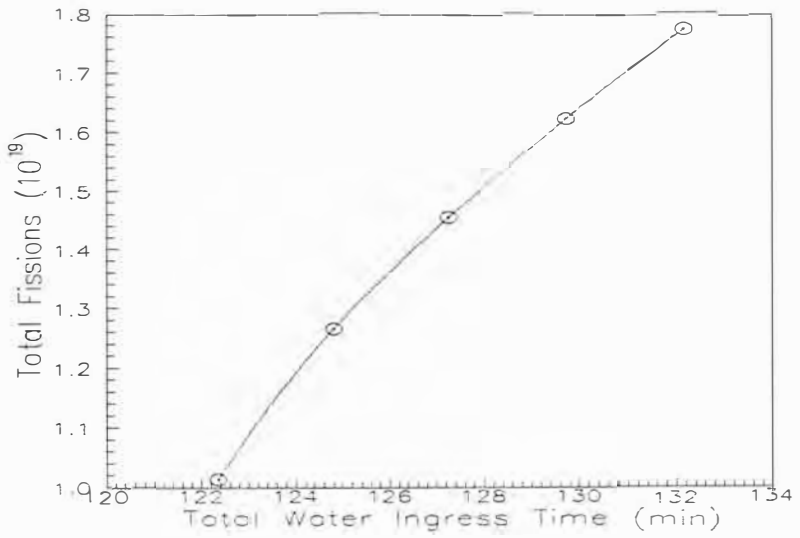

FIGURE 6.14 Total Fissions versus Total Water Ingress Time for ~1 ¢/sec Reactivity Addition Rate.

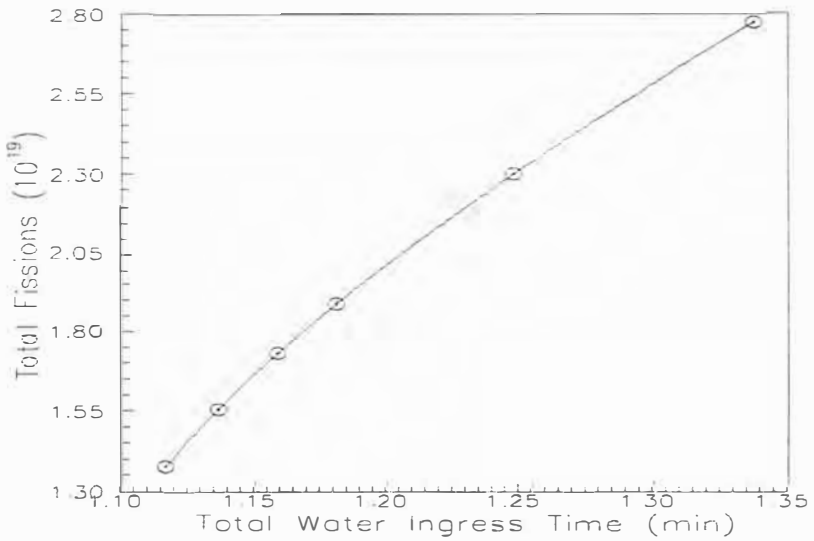

FIGURE 6.15 Total Fissions versus Total Water Ingress Time for ~1 $/sec Reactivity Addition Rate.

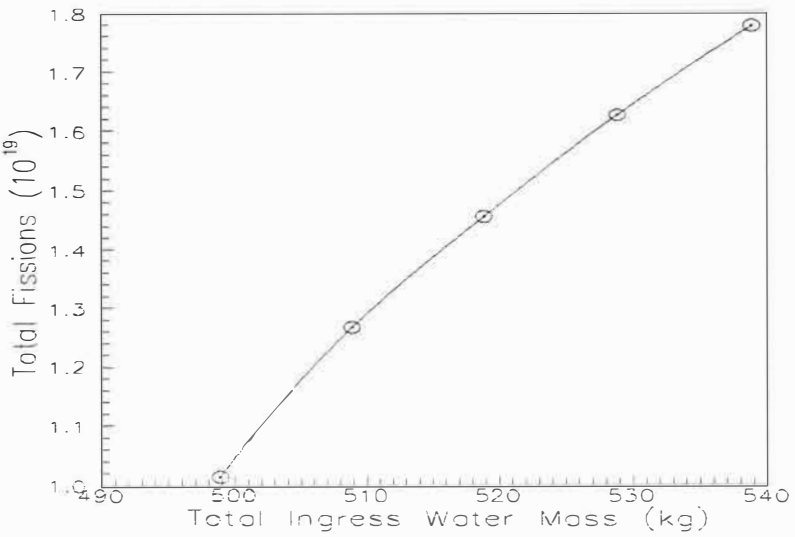

FIGURE 6.16 Total Fissions versus Total Ingress Water Mass for ~1 ¢/sec Reactivity Addition Rate.

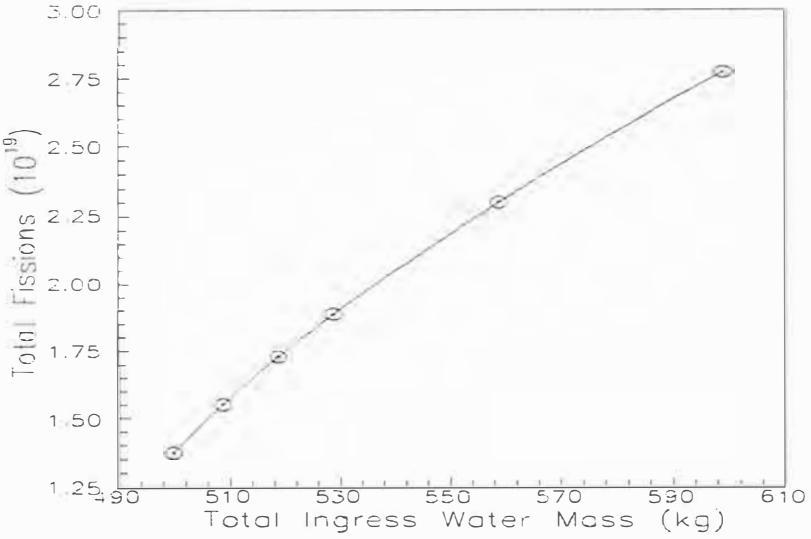

FIGURE 6.17 Total Fissions versus Total Ingress Water Mass for ~1 $/sec Reactivity Addition Rate.

codes (e.g.; two dimensional transport code DOT instead of XSDRNPM). Thus, it is necessary to study the sensitivity of results to changes in reactivity feedback coefficients. The most significant reactivity feedback mechanism is due to the doppler effect. Hence, the doppler reactivity feedback coefficient is considered for the study. This parameter was varied %10 and %50 from the CSAS1X calculated value. Results are obtained for a doppler feedback coefficient that is 10% and 50% too large, and 10% and 50% too small. Plots of total fissions versus the doppler feedback coefficient are given in Figures 6.18 and 6.19 for the base accident scenarios. Both figures demonstrate that the total fissions increase linearly with respect to doppler reactivity feedback coefficient and the results are only slightly affected by changes in the feedback coefficient.

6.2.5. Neutron Mean Generation Time

Sensitivity of results on neutron mean generation time is also considered. This parameter was varied 10% and 50% from the CSAS25 calculated value. The results are obtained with a mean generation time that is 10% and 50% larger, and 10% and 50% smaller. Plots of total fissions versus neutron mean generation time are given in Figures 6.20 and 6.21 for the base accident scenarios. Three more SKINATH-WP runs were done for the first base accident (1 ¢/sec) reactivity addition scenario due to unexpected behavior of the plot as shown in the Figure 6.20. Both figures show that the total fission yield is not effected by these changes in neutron mean generation time.

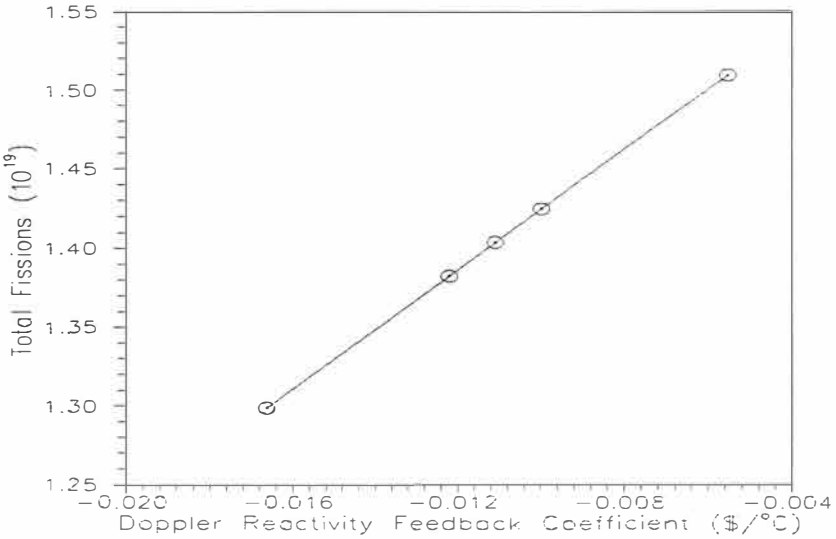

FIGURE 6.18 Total Fissions versus Doppler Reactivity Feedback Coefficient for ~1 ¢/sec Reactivity Addition Rate.

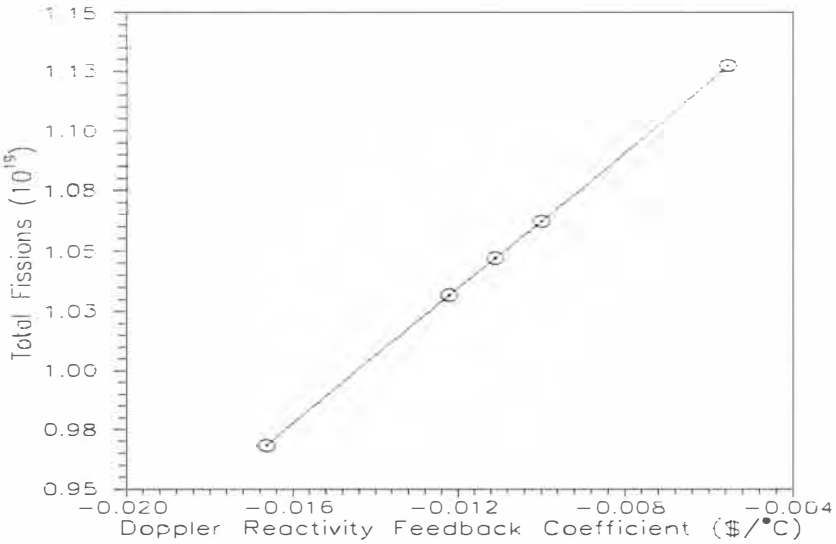

FIGURE 6.19 Total Fissions versus Doppler Reactivity Feedback Coefficient for ~1 $/sec Reactivity Addition Rate.

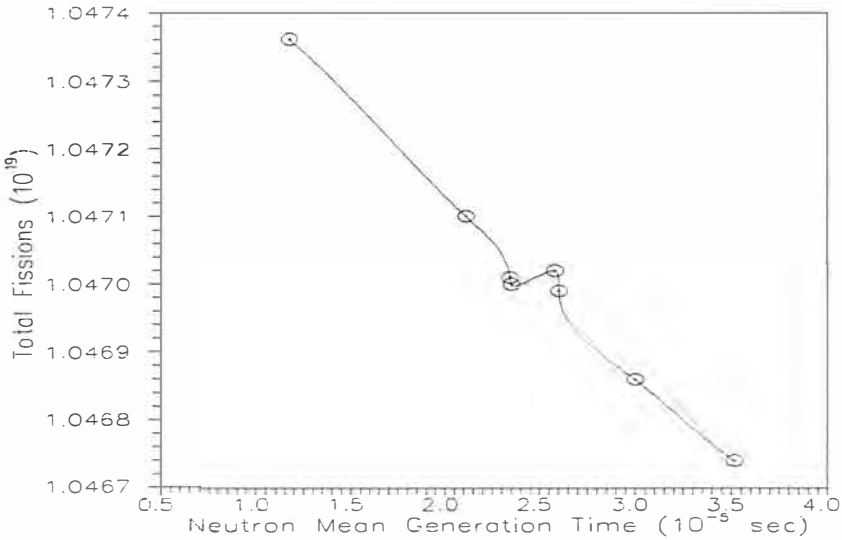

FIGURE 6.20 Total Fissions versus Neutron Mean Generation Time for ~1 ¢/sec Reactivity Addition Rate.

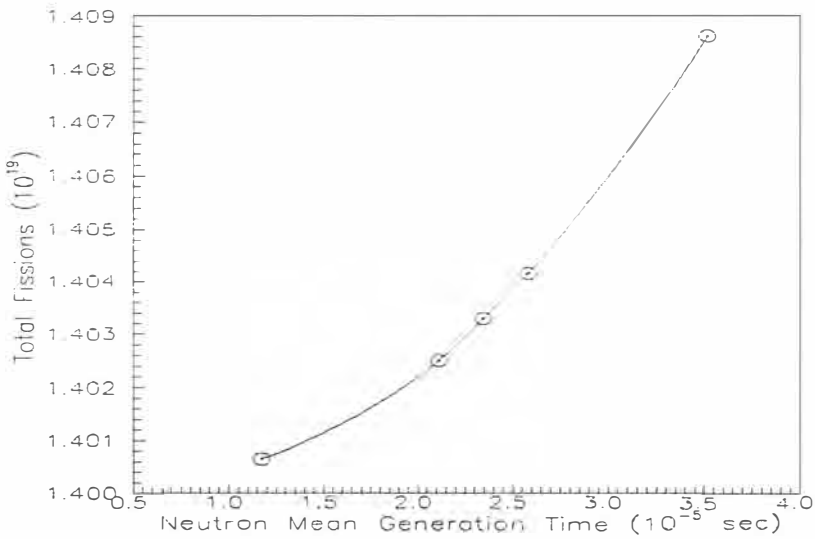

FIGURE 6.21 Total Fissions versus Neutron Mean Generation Time for ~1 $/sec Reactivity Addition Rate.

6.2.6. Model 2 vs Model 3

Figure 6.22 and 6.23 show a comparison of Model 2 (vented system) and Model 3 (unvented system). In these figures, the total fissions with respect to time are shown. Both models estimate almost the same total fission yields for the base accident scenarios. However, the results vary moderately for different accident scenarios, especially for the scenarios involving continuous water leakage.[d]

6.2.7. Continuous Water Ingress

If water ingress is continuous, additional pulses follow the spike as long as the water is added into the system. Plots of power, total fissions, temperature, and pressure versus time on a long time scale are given in Figures 6.24 and 6.25 for the base accident scenarios. Thus, after a delayed critical configuration is achieved, the power increases to a peak (spike). Then, this initial pulse dies out and is followed by a series of pulses of decreasing size and frequency. These pulses are separated by intervals which depend on the reactivity addition rate and none equal or exceed the magnitude of the spike. The subsequent pulses have lower fission yields due to several factors. First of all, the total reactivity of the system is lower for the subsequent pulses because of the feedback mechanisms.

---

[d] Model 2 assumes that any steam produced leaving the system instantly, and, hence, reactivity feedback effect due to water evaporation is larger. Power estimated by Model 2 follows a lower trend than the one estimated by Model 3. Thus, Model 2 and Model 3 estimate moderately different total fission yields for the scenarios involving continuous water ingress.

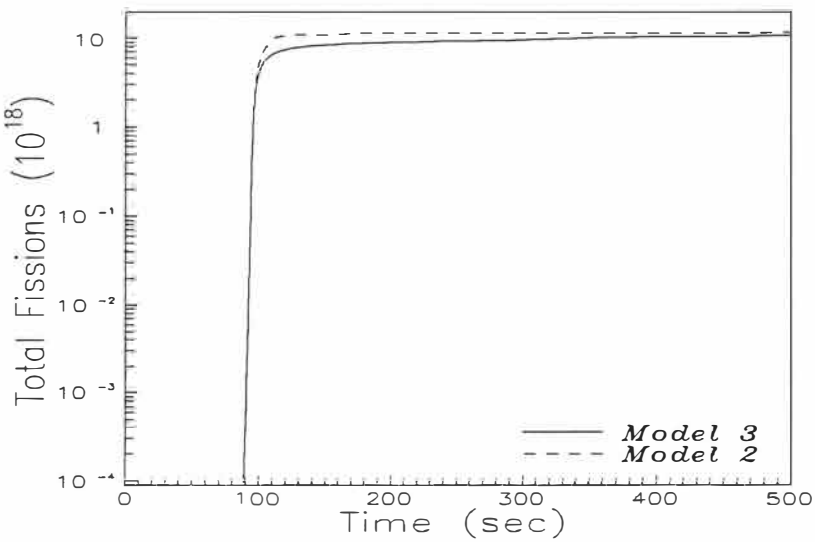

FIGURE 6.22 Comparison of Model 2 (Vented System) and Model 3 (Unvented System) for ~1 ¢/sec Reactivity Addition Rate.

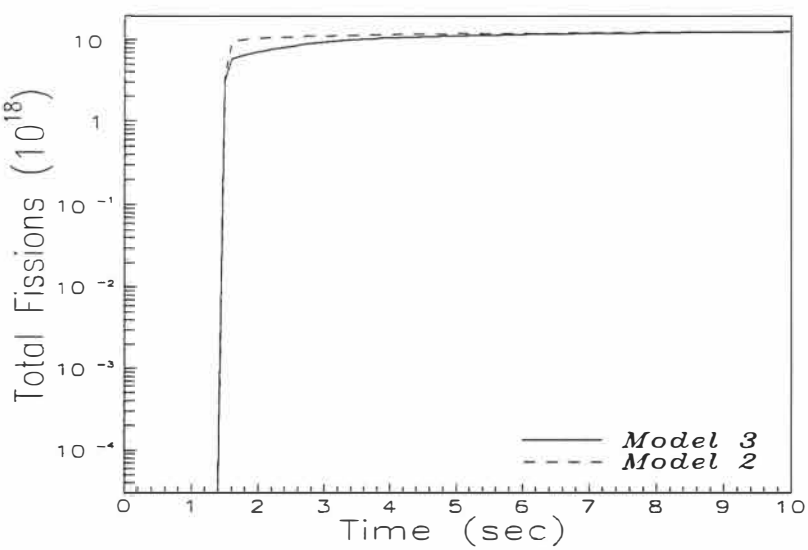

FIGURE 6.23 Comparison of Model 2 (Vented System) and Model 3 (Unvented System) for ~1 $/sec Reactivity Addition Rate.

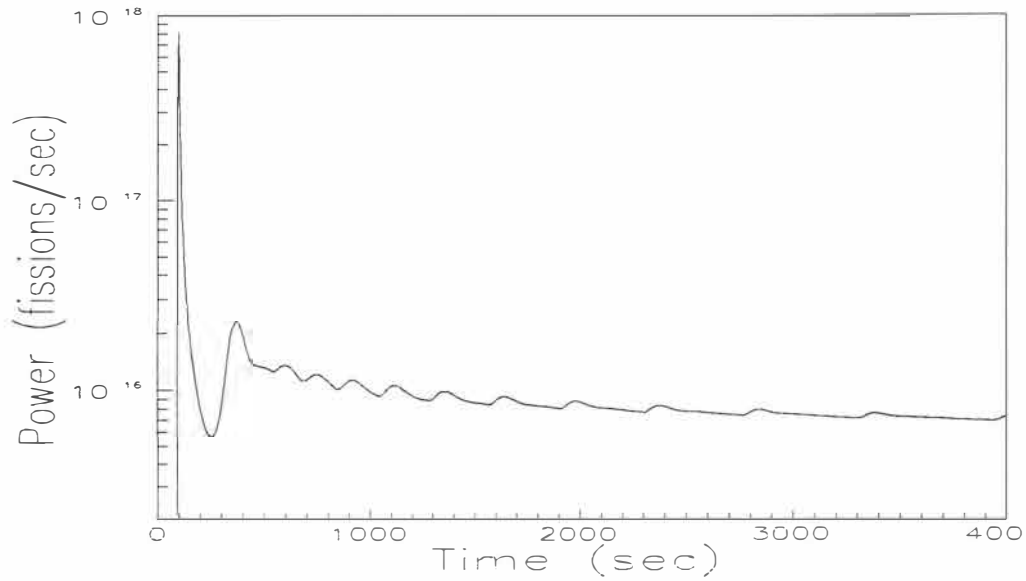

Figure 6.24a Power versus Time for Continuous Water Ingress at ~1 ¢/sec Reactivity Addition Rate.

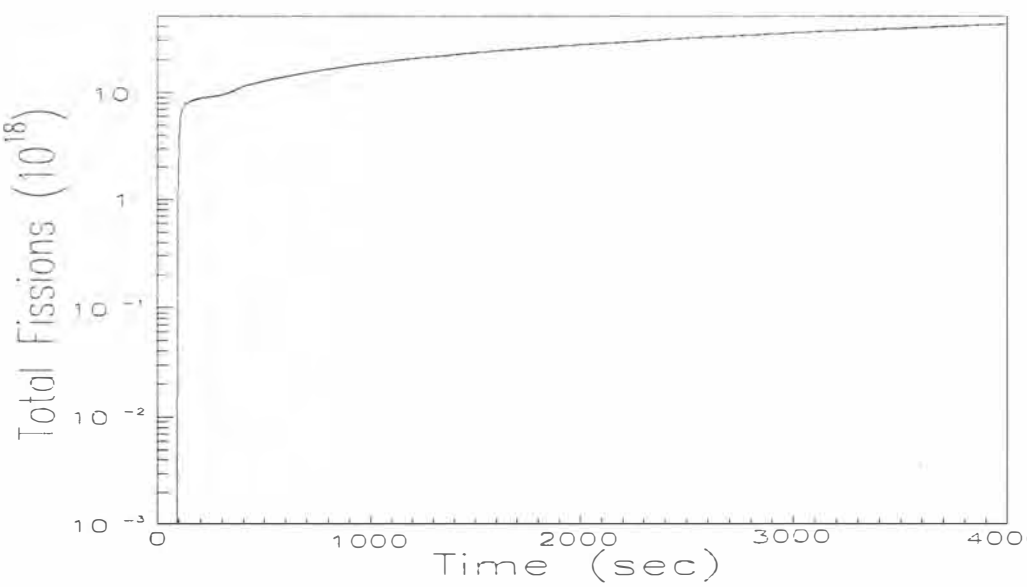

Figure 6.24b Total Fissions versus Time for Continuous Water Ingress at ~1 ¢/sec Reactivity Addition Rate.

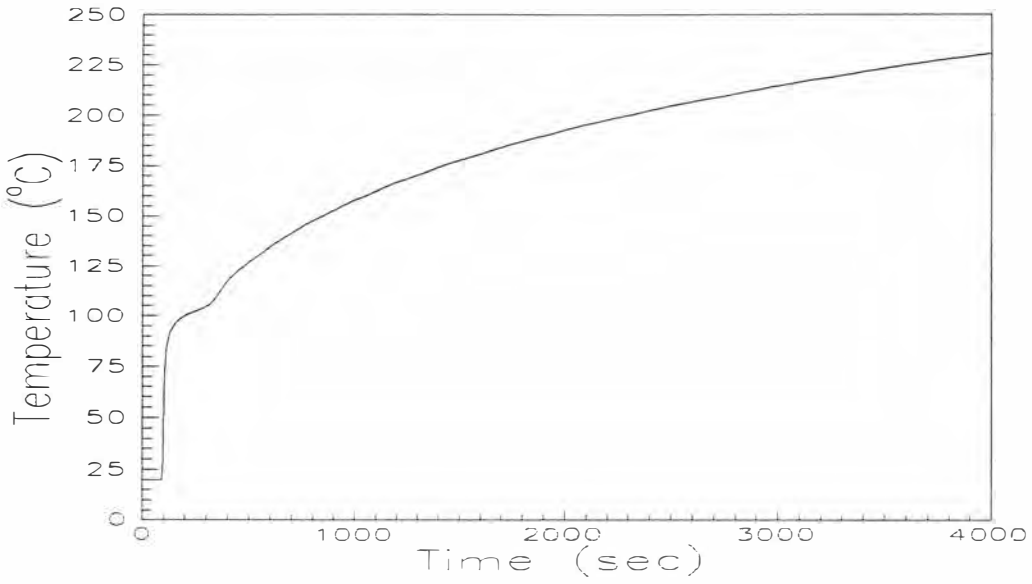

Figure 6.24c Temperature versus Time for Continuous Water Ingress at ~1 ¢/sec Reactivity Addition Rate.

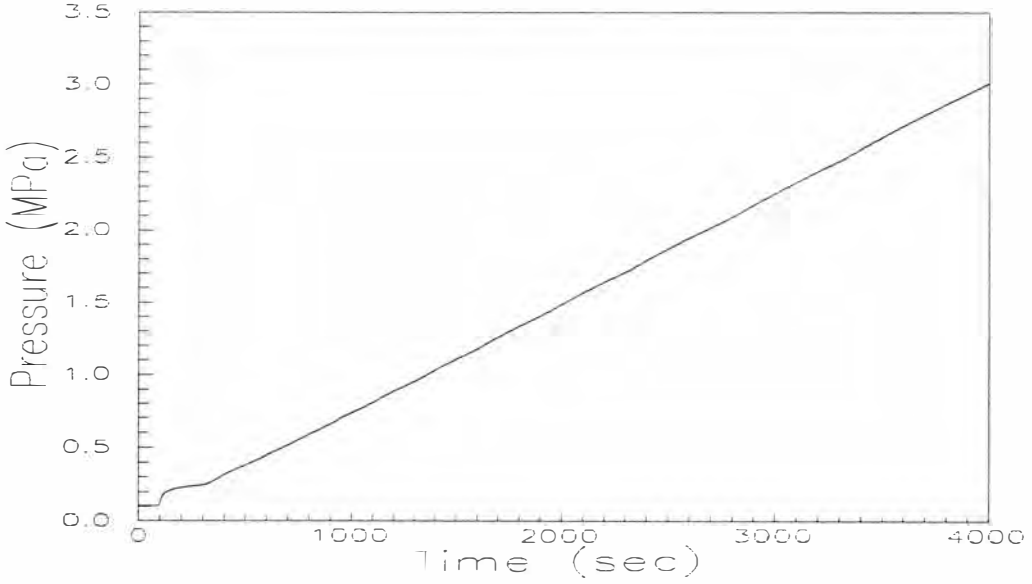

Figure 6.24d Pressure versus Time for Continuous Water Ingress at ~1 ¢/sec Reactivity Addition Rate.

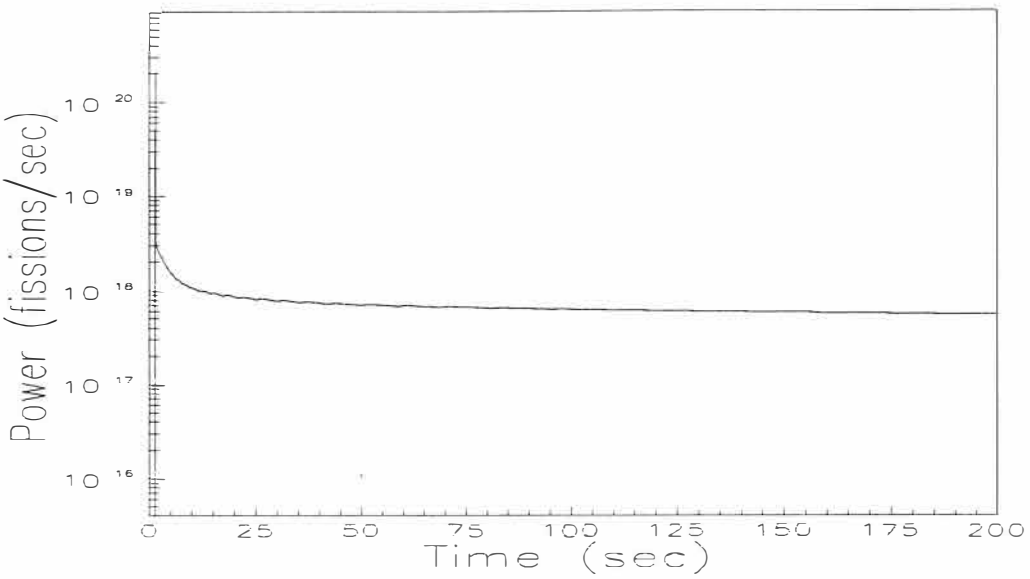

Figure 6.25a Power versus Time for Continuous Water Ingress at ~1 $/sec Reactivity Addition Rate.

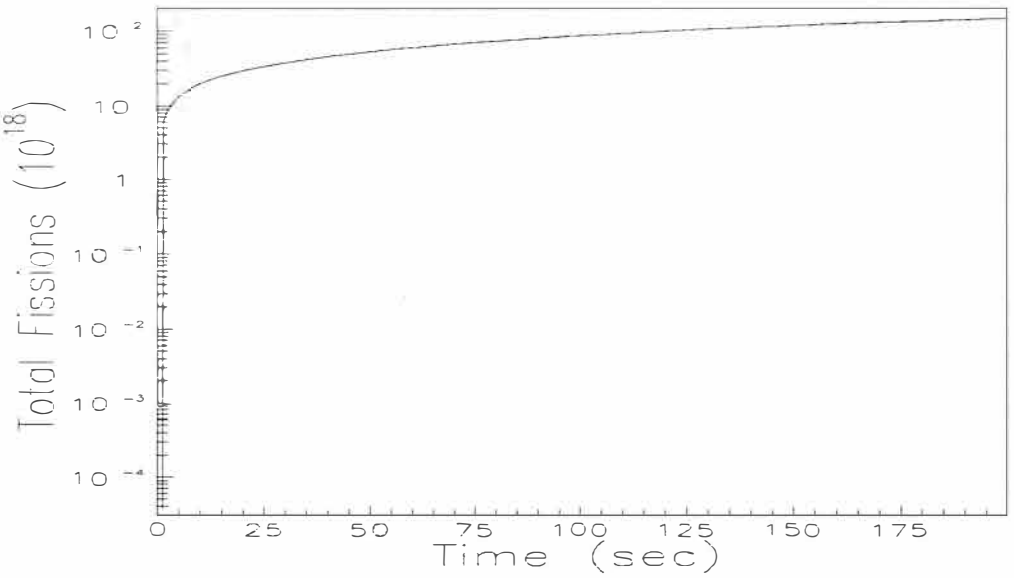

Figure 6.25b Total Fissions versus Time for Continuous Water Ingress at ~1 $/sec Reactivity Addition Rate.

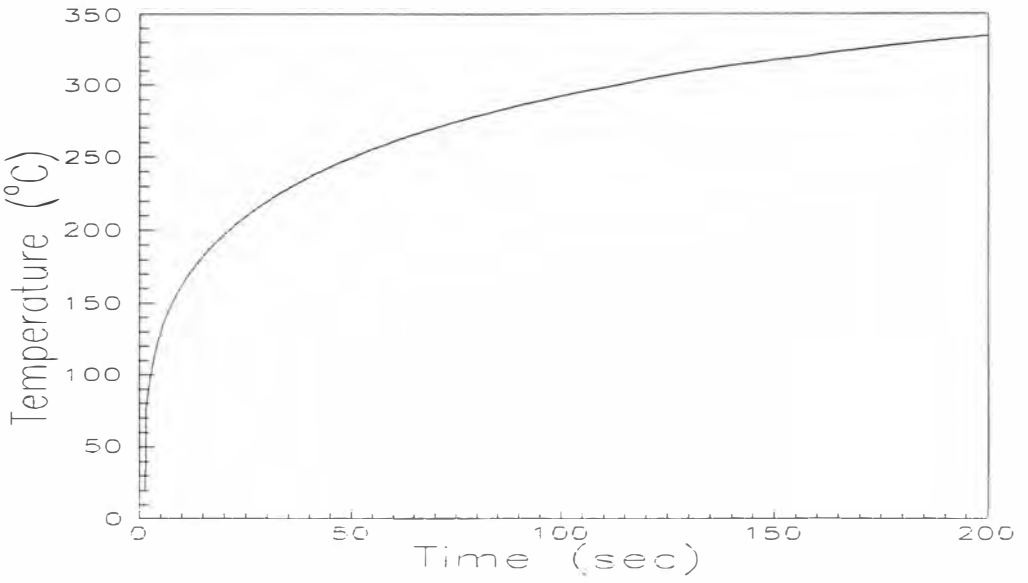

Figure 6.25c Temperature versus Time for Continuous Water Ingress at ~ 1 $/sec Reactivity Addition Rate.

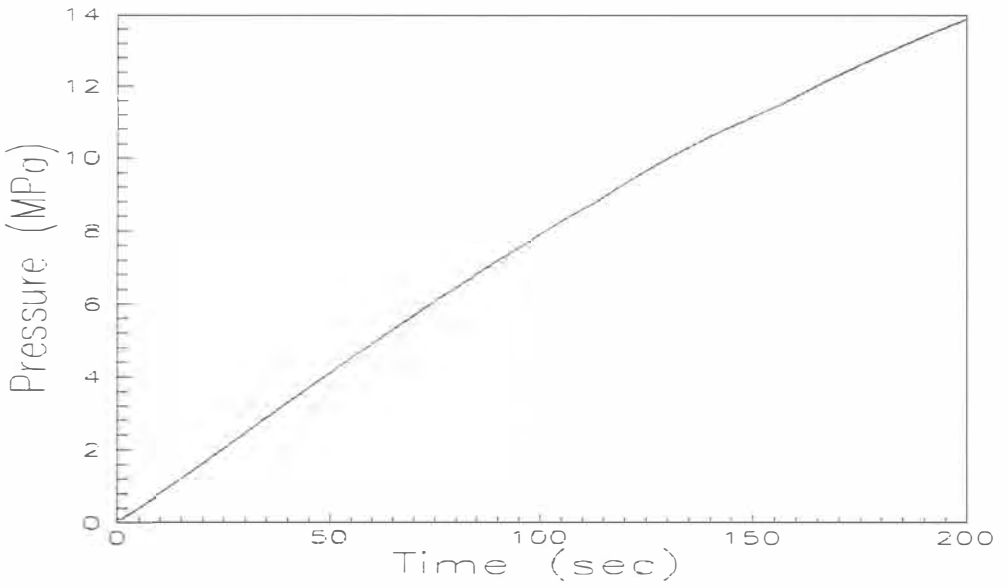

Figure 6.25d Pressure versus Time for Continuous Water Ingress at ~ 1 $/sec Reactivity Addition Rate.

The power pulses occur as a result of sequential domination of the total reactivity by feedback and external reactivity. Feedback mechanisms force the total reactivity to decrease due to temperature increase, however, water addition increases the total reactivity. Thus, the total reactivity may oscillate between positive and negative values as a trade-off between feedback and external reactivity.

The total fissions increase gradually following the first sudden increase accompanying the spike. From figures 6.24a and 6.24b, (also from figures 6.25a and 6.25b), it is obvious that the spike is the main contributor of the total fission yield. The temperature rises rapidly but with a decreasing growth rate. The plateau power is $\sim 10^{16}$ fissions/sec for the first base accident scenario as shown in Figure 6.24a. Similarly, it is approximately $\sim 10^{18}$ fissions/sec for the second base accident scenario. However, the blender system will probably fail due to instantaneous energy release. Such a destructive failure accompanying the spike should be expected primarily for large reactivity addition rates. Also, some feedback mechanisms which are not taken into account in our model may be important, and therefore, the results for the plateau power and the subsequent pulses should not be taken seriously.

Also, the pressure increases almost linearly to extreme values. As seen in figures 6.24d, the pressure attains a value that is 30 times larger than atmospheric in ~ 1.11 hours after delayed criticality for the first base accident scenario. If the reactivity addition rate is large, the results are even more extreme. Figure 6.25d shows that the pressure increases to ~ 14 MPa in ~ 3.33 minutes which is 140 times larger than atmospheric. The blender system should fail long before reaching these pressures.

6.2.8. Free Convection Correlation

The sensitivity of the results to the different free convection correlations discussed in Section 3.5 are shown in Table 6.4 for the first base accident scenario. Table 6.4 shows that the difference between results are insignificant. Cylinder correlations yields negligibly higher total fissions than cone correlations, however, the first fission pulse peak value seems to be higher for the cone correlations. Similar results are obtained for the second base accident scenario. The correlation chosen for the analysis is the one given by Michowycz and Sparrow.

6.2.9. LSODE Integration Method

LSODE uses *Implicit Adams* and *Backward Differentiation* as integration methods for non-stiff and stiff problems, respectively. Stiffness in a system of ordinary differential equations refers to a broad difference in the time scales of the components in the vector solution [60]. In other words, stiffness is more likely to happen when stability in the numerical solution can be achieved only with very small step size. Theoretically speaking, the non-linear system is said to be stiff in any specified interval of the dependent variable if the eigenvalues of its Jacobian satisfy the following two conditions: the real parts of all the eigenvalues are less than zero and the real part of the largest eigenvalue is much larger than the real part of the smallest eigenvalue [61]. Some numerical methods that are quite satisfactory in general will perform very poorly on stiff equations. Attempts to use such methods to solve stiff system of differential equations causes significant difficulties.

TABLE 6.4

Effect of Different Free Convection Correlations on the First Fission Pulse and Total Fissions with 500 kg Water Ingress at a Rate of 0.068 l/sec(~ 1 ¢/sec).

Free Convection Correlation	First Fission Pulse (MW)	Total Fissions
Churchill and Chu (Cylinder)	26.561083	1.047016×10^{19}
Minkowycz and Sparrow (Cylinder)	26.576616	1.047007×10^{19}
LeFevre and Ede (Cylinder)	26.531732	1.046930×10^{19}
Kuiken (Cone)	26.479243	1.045789×10^{19}
Oosthuizen and Donaldson (Cone)	26.468975	1.045900×10^{19}
Rohsenow, Hartnett, and Ganic (Cone)	26.473974	1.045796×10^{19}

In a criticality excursion, stiff problems may arise because transients with the time scales of the order of a microsecond can be imposed on the generally smooth behavior of the system parameters such as power. Since it is not feasible to calculate the Jacobian beforehand, a parametric study was conducted to study the effect of different integration methods. Table 6.5 shows the results of the spike and total fissions with respect to different LSODE integration methods for the first base accident scenario. This table also includes results for various iteration schemes for both methods. The results show that the problem is not stiff for ~ 1 ¢/sec reactivity addition rate. Similar results are obtained for the second base accident scenario which involves a ~ 1 \$/sec reactivity addition rate. Hence, the problem may be viewed as non-stiff in general.

In the analysis, the backward differentiation with chord iteration and an internally generated full Jacobian is used. However, using the non-stiff method may save computational time and cost and is recommended for study in future calculations.

6.3. Summary of Results

Finally, results may be summarized as shown in Figure 6.26. This figure presents a generic flow chart for a hypothetical criticality excursion involving homogeneous damp low-enriched UO_2 powders. Knowledge of the exact path that will be traced by a real-life accident requires experimental work and more computational efforts.

TABLE 6.5

Effect of LSODE Integration Method on the First Fission Pulse and Total Fissions, with 500 kg Water Ingress at a Rate of 0.068 lt/sec(~ 1 ¢/sec).

LSODE Integration Method	**First Fission Pulse (MW)**	**Total Fissions**
Implicit Adams Method with Functional Iteration (No Jacobian is Involved)	26.315487	1.047316×10^{19}
Backward Differentiation with Functional Iteration (No Jacobian is Involved)	26.313325	1.047311×10^{19}
Implicit Adams Method with Chord Iteration and Internally generated Banded Jacobian	26.535329	1.047091×10^{19}
Backward Differentiation with Chord Iteration and Internally generated Banded Jacobian	26.387976	1.047237×10^{19}
Implicit Adams Method with Chord Iteration and Internally generated Full Jacobian	***Divergent***	
Backward Differentiation with Chord Iteration and Internally generated Full Jacobian	26.576616	1.047007×10^{19}
Implicit Adams Method with Chord Iteration and Internally generated Diagonal Jacobian	***Meaningless Results***	
Backward Differentiation with Chord Iteration and Internally generated Diagonal Jacobian	***Meaningless Results***	

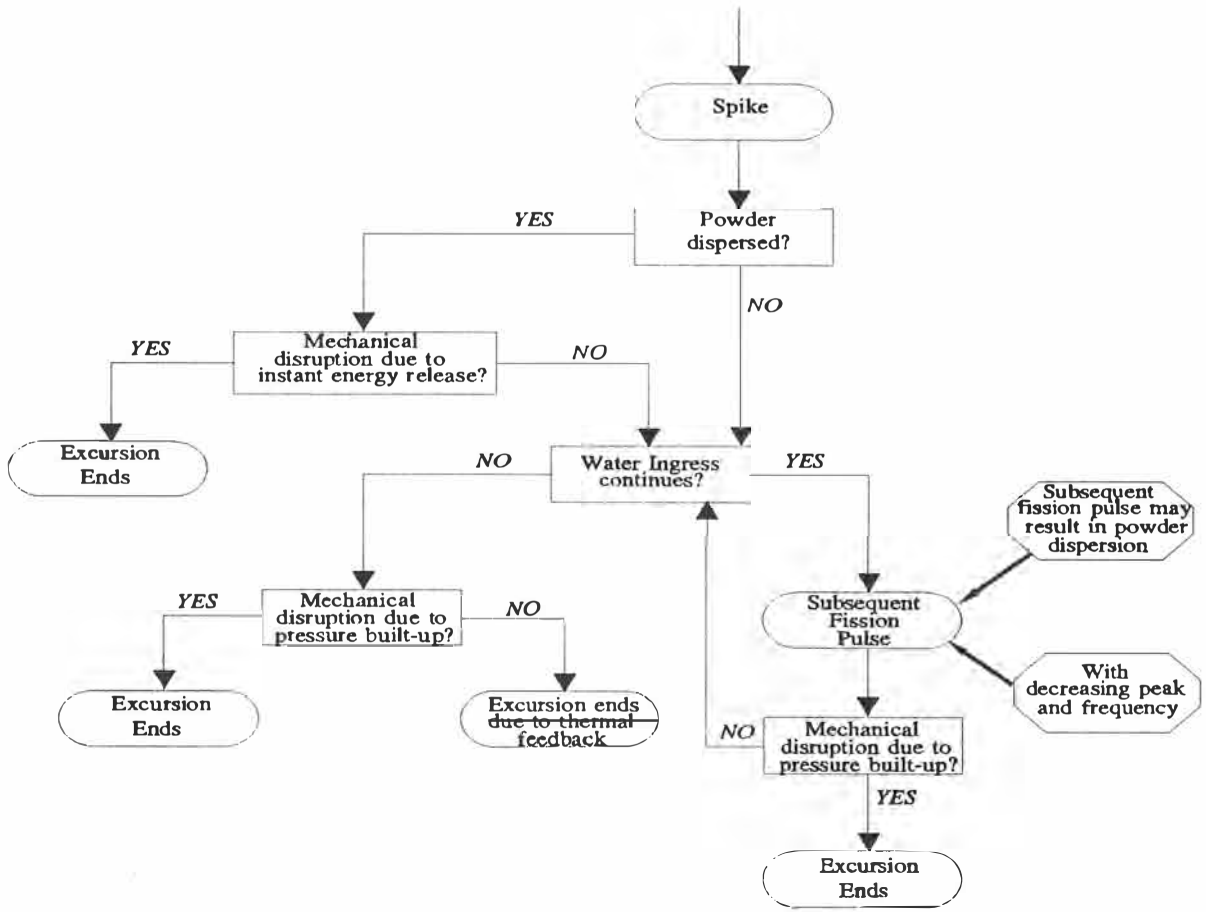

Figure 6.26 Flow Chart for a Hypothetical Criticality Excursion Involving Homogeneous Damp Low-enriched UO_2 Powders.

Chapter 7

CONCLUSIONS

7.1. Introduction

The analysis presented in this thesis estimates the behavior of hypothetical criticality excursions involving homogeneous damp low-enriched UO_2 powders. As presented in the earlier sections, a computer code, SKINATH-WP, has been developed which can predict the spike peak value, the total number of fissions, pressure, etc. as a function of time for a wide range of input conditions. This code should be viewed as one of the first attempts at modelling neutronic and thermal effects of criticality excursions involving dry LEU powders.

The results of this program demonstrate reasonable trends and have been verified against the POWDER code, the only code having the same nature as SKINATH-WP, with results which are reported in the open literature. No validation study has been performed due to lack of experimental results on excursion characteristics of damp UO_2 powder systems.

7.2. Conclusions

The excursion, parametric, and sensitivity studies presented in this work permit several conclusions to be drawn about the consequences of a criticality accident involving 5000 kg of homogeneous low-enriched(5%) damp UO_2 powder in a

cylindrical blender:

a. The maximum expected fission yield of an accident has been shown to be approximately $\sim 10^{19}$ fissions regardless of the reactivity addition rate.

b. The spike increases almost linearly from 2.94×10^{17} fissions/sec to 2.51×10^{21} fissions/sec for reactivity addition rates from ~ 0.1 ¢/sec to ~ 10 \$/sec. For large reactivity addition rates, the energy release occurs in a short time interval which could result in mechanical failure, or disassembly of the blender.

c. The pressure increases to large values in a very short time interval for some accident scenarios(i.e., 140 times larger than the atmospheric in ~ 3.33 minutes for 1 \$/sec reactivity addition rate). Hence, the pressure build-up could also result in mechanical disruption even if the blender survives the spike.

d. If water continues to flow into the blender following the spike, the system may experience several more fission pulses which will further increase the fission yield, pressure, etc.

e. The U.S. NRC has recommended the following criteria for Evaluating the Potential Radiological Consequences of Accidental Nuclear Criticality in Uranium Fuel Fabrication Plants in the Regulatory Guide 3.34 *(Revision 1, July 1979)*:

> The minimum accident to be considered for any unfavorable geometry container should contain an initial pulse of 10^{18} fissions followed by 47 subsequent pulses, 10 min. apart of 1.9×10^{17} fissions. This provides a total yield of 10^{19} fissions over 8 hours.

The above statement is based on experiments for a vented container with a solution of 400 g/l of uranium enriched in U^{235}. The NRC has not recommended criteria for

damp powder systems due to lack of experimental results. However, all scenarios considered in this work indicate at least 10^{19} fissions over a time interval which is dependent on the reactivity addition rate.

f. According to the present theoretical model, a homogeneous powder/water system does not have a well developed plateau like the solution systems. The plateau does not contribute most of energy and fissions relative to the spike.

g. In Reference 32, Woodcock estimated $3x10^{20}$ fissions as the spike yield with no plateau and resulting in considerable mechanical damage and explosion for heterogeneous liquid/powder systems. Our results are one order of magnitude lower than Woodcock's estimate.

7.2. Future Work

Further analysis is desirable with a more detailed evaluation of all of the phenomena since several assumptions are used in the present model. The phenomena listed below should be investigated in more detail:

a. The present model assumes that the transient will not be terminated by powder dispersion or disassembly, however, it is not clear that disassembly will sufficiently disrupt the system completely and, thus, terminate the excursion.

b. If the material is not dispersed out of the blender, the powder may settle back forming a new critical system since the blender is closed at the upper end, thus, resulting in further energy release.

c. Space-dependent effects as well as some other effects such as the speed of

water penetration and powder collapse are neglected in our model due to the mixing mechanism.

d. The fission fragments may decompose the water into its constituent gases which could lead to micro-bubble formation. These bubbles may expand reducing the density of the system and cause a decrease in the reactivity.

e. The reactivity effects of moderator thermal expansion, formation and migration of vapor bubbles are not considered in our model.

f. The conical shaped blender system is approximated as a cylinder for the calculations of reactivity feedback coefficients and the reactivity driving force function.

7.3. Recommendations

The following recommendations are suggested as a result of the analysis presented in this thesis regarding criticality accidents involving damp fissile powders:

a. Experiments should be performed on excursion characteristics as well as the thermal hydraulic behavior of damp powder systems.

b. More detalied computer models should be developed for such excursions.

c. New regulatory guides should be developed using the results of experiments and computer simulations.

REFERENCES

REFERENCES

1. R.A. KNIEF, Nuclear Criticality Safety; Theory and Practice, American Nuclear Society, La Grange Park, Illinois (1991).

2. W.L. GOODWIN, N.A. KENT, R.D. MONTGOMERY, Westinghouse Fuel Fabrication Plant, Columbia, South Carolina, *Personal Communication*, November 2, 1990.

3. Westinghouse Document, No:70-1151, Revision 2, Westinghouse Electric Corporation, Nuclear Fuel Division.

4. R.A. WILLIAMS, "Columbia Fuel Fabrication Facility Application of Nuclear Criticality Control Criteria", Westinghouse Electric Corporation, Columbia, South Carolina, Page 4.1-19 (July 1990).

5. Westinghouse Document, "Additional Criticality Calculations for Kiln and Cone Blenders", No: 78-6, Revision 0, Westinghouse Electric Corporation, Nuclear Fuel Division.

6. Westinghouse Document, "Criticality Calculations for Kiln and Blender", No: 80-1, Revision 1, Westinghouse Electric Corporation, Nuclear Fuel Division.

7. Westinghouse Document, "Criticality Dimensions for $U(5)O_2$ and $U(5)U_2F_2$ Homogeneous Mixtures", No: 82-6, Revision 0, Westinghouse Electric Corporation, Nuclear Fuel Division.

8. J.J. KOELLING, G.E. HANSEN, C.BYERS, "Fission and Explosive Energy Releases of Pu_2, PuO_2-UO_2, UO_2, and UO_3 Assemblies", *Nuclear Technology*, **35**, 611 (1977).

9. G.E. HANSEN, C.C.BYERS, J.J.KOELLING, "Fission and Explosive Energy Releases of PuO_2 and PuO_2-UO_2 Assemblies", *Trans. Am. Nucl. Soc.*, (November 1976).

10. P. LECORCHE, R.A. SEALE, "A Review of the Experiments Performed to Determine the Radiological Consequences of a Criticality Accident", Y-CDC-12, Oak Ridge Y-12 Plant, (November 1973).

11. C.E. NEWTON, A.H. HANSEN, C. FITHIAN, "An Assessment of the Minimum Criticality Accident of Concern", H & R Technical Associates, Inc., H&R 82-2, Oak Ridge, TN (1982).

12. M.S. DUNENFELD, R.K. STITT, "Summary Review of the Kinetics Experiments on Water Boilers", NAA-SR-7087, Atomics International (1963).

13. F. BARBRY, "Fuel Solution Criticality Accident Studies with the Silene Reactor", Proc. Int. Seminar Criticality Studies Program and Needs, Dijon, France (September 19-22, 1983).

14. W.R. STRATTON, "A Review of Criticality Accidents", DOE/NTC-04, Nuclear Criticality Technology, (March 1989).

15. W.E. NYER, G.O. BRIGHT, R.J. MCWHORTER, "Reactor Excursion Behavior", International Conference on the Peaceful Uses of Atomic Energy, paper 283, Geneva (1966).

16. W.T. MEE, D.A. REED, R.G. TAYLOR, "Consequences of a Postulated, Moderated Criticality Accident at the Oak Ridge Y-12 Plant", Y-12 Plant, Y/DD-384, Oak Ridge, TN (1988).

17. G.E. HANSEN, "Assembly of Fissionable Material in the Presence of a Weak Neutron Source", *Nucl. Sci. and Eng.*, **8**, 709, (Dec. 1960).

18. G. TUCK, "Simplified Methods of Estimating the Results of Accidental Solution Excursions", *Nuclear Technology*, **23**, 177 (1974).

19. H.F. LUTZ, "Nuclear Criticality Safety Assessment Calculations: Part I. Calculating Power Histories in Nuclear Excursions", H.J. Kroopnick, Ed., M-164, Lawrence Livermore National Lab., Livermore, Calif. (1985).

20. D.J. MATHER, P.M. SHAW, "CRITEX - A Computer Program to Calculate Criticality Excursions in Fissile Liquid Systems", SRD R 380, UK Atomic Energy Authority (July 1984).

21. D.J. MATHER, P.M.SHAW, "Calculations of Criticality Excursions in Fissile Liquid Systems", SRD R 308, C.6, United Kingdom Atomic Energy Authority, Culchelt, Warrington (1984).

22. W. THOMAS, B. GMAL, "Modelling of Criticality Accidents and Their Environmental Consequences", *Trans. Am. Nucl. Soc.*, **55**, 409 (November 1987).

23. R. KATO, T. NARAMURA, Y. SENDA, "The Code CREST to Simulate Criticality Excursion in Fuel Solution", Mitsubishi Atomic Power Industries, Inc., Tokyo, Japan.

24. H.L. DODDS, R.M. WESTFALL, "SKINATH - A Computer Program for Solving the Reactor Point Kinetics Equations with Sample Thermal Hydraulic Feedback", ORNL/CSD/TM-210, Oak Ridge National Lab. (September 1984).

25. D.M. PETERSON, W.L. STRATTON, T.P. MCLAUGHLIN, "PAD : A One-Dimensional Coupled Neutronic - Thermodynamic Computer Code", LA-6540-MS, Los Alamos National Lab. (December 1976).

26. F. BARBRY, C. BONHOMME, P. HAGUE, D.J. MATHER, P.M. SHAW, "Theoretical Studies of Transient Criticality if Irradiated Fuel Elements", *Trans. Am. Nucl. Soc.*, **55**, 410 (November 1987).

27. W.D. NEWMYER, B.BASOGLU, D.F.HOLLENBACH, H.L.DODDS, "Analysis of a Hypothetical Criticality Accident Involving Dry Highly Enriched Uranium Powder", *Trans. Am. Nucl. Soc.*, **64**, 344 (November 1991).

28. W.D. NEWMYER, "The Analysis of a Hypothetical Criticality Accident Involving Dry Highly-Enriched Uranium Powder", M.S. Thesis, The University of Tennessee, Knoxville (1991).

29. P. ROZAIN, P. FOUILLAUD, F. BARBRY, D.J. MATHER, A.M. BICKLEY, A. PRESCOTT, "Criticality Excursions in Wetted UO_2 Powder", Proceedings of the ICNC '91 - International Conference on Nuclear Criticality Safety, Oxford, United Kingdom, Paper VII:6, pp.40-50, (September 1991).

30. F.Y. BARBRY, "Review of Studies on Criticality Accidents Undertaken at CAE/Valduc", *Trans. Am. Nucl. Soc.*, **63**, 225 (June 1991).

31. J.P. ROZAIN, P. FOUILLAUD, D.J. MATHER, A.M BICKLEY, "Criticality Excursions in Wetted UO_2 Powder", *Trans. Am. Nucl. Soc.*, **63**, 228 (June 1991).

32. E.R. WOODCOCK, "Potential Magnitude of Criticality Accidents", AHSO(RP) R-14, United Kingdom Atomic Energy Authority.

33. M. BECKER, "A Generalized Formulation of Point Nuclear Reactor Kinetics Equations", *Nuclear Science and Engineering*, **31**, 458-464 (1968).

34. E.P. GYFTOPOULOS, The Technology of Nuclear Reactor Safety, **Vol. I**, pp.175-204, T.J. THOMPSON and J.G.BECKERLY, Eds., MIT Press, Cambridge, Mass. (1964).

35. A.F. HENRY, Nuclear-Reactor Analysis, MIT Press, Cambridge, Mass. (1975).

36. J.R. LAMARSH, Introduction to Nuclear Reactor Theory, Addison-Wesley, Reading, Mass. (1966).

37. J.J. DUDERSTADT, L.J. HAMILTON, Nuclear Reactor Analysis, John Wiley and Sons, New York (1976).

38. G.R. KEEPIN, Physics of Nuclear Kinetics, Addison-Wesley, Reading, Mass. (1965).

39. "SCALE: A Modular Code System for Performing Standardized Computer Analysis for Licensing Evaluation", NUREG/CR-0200, **Vols. 1-5**, U.S. Nuclear Regulatory Commission (revisited and reissued January 1990).

40. J.A. BUCHOLZ, "CSAS1: A One-Dimensional Criticality Safety Analysis Module", NUREG/CR-0200, **Vol. 1**, Section C1, ORNL/NUREG/CSD 2/V1/R1 (October 1981).

41. Westinghouse Document, "Criticality Safety Analysis for the Wet Pellet Grinding System Centrifuge", No: 88-1, Revision 0, Westinghouse Electric Corporation, Nuclear Fuel Division.

42. L.M. PETRIE, N.F. LANDERS, "KENO V.a: An Improved Monte Carlo Criticality Program with Supergrouping", NUREG/CR-0200, **Vol. 2**, Section F11, ORNL/NUREG/CSD-2/V1/R1 (December 1984).

43. O.W. HERMAN, R.M. WESTFALL, "ORIGEN-S: Scale System Module to Calculate Fuel Depletion, Actinite Transmutation, Fission Product Buildup and Decay, and Associated Radiation Source Terms", ORNL Computing and Telecommunication Division (February 1989).

44. M.J. SCHUH, K.S. UDEL, Heat Transfer in Porous Media and Particulate Flows, pp.159-165, L.S. YAO et al., Eds., The 23rd National Heat Transfer Conference(Heat Transfer Division, ASME), Denver, Colorado, **HTD-Vol. 46**, New York (1985).

45. P.F. PASQUA, Department of Nuclear Engineering, The University of Tennessee, Knoxville TN, *Personal Communication*, June 19, 1991.

46. J.P. HOLMAN, Thermodynamics, McGraw Hill, Tokyo (1983).

47. N.A. GOKCEN, Thermodynamics, Techscience Incorporated, Hawthorne, California (1975).

48. S. KAKAÇ, W. AUNG, R. VISKANTA, Natural Convection: Fundamentals and Applications, Hemisphere Publishing Corporation, Washington (1985).

49. M. BECKER, Heat Transfer: A Modern Approach, Plenum Press, New York (1986).

50. F. INCROPERA, D. DEWITT, Fundamentals of Heat and Mass Transfer, John Wiley and Sons, New York (1985).

51. J.P. HOLMAN, Heat Transfer, McGraw Hill, New York (1986).

52. S. KAKAÇ, R.K. SHAH, W. AUNG, Handbook of Single-Phase Convective Heat Transfer, John Wiley and Sons, New York (1987).

53. M. FISHERDEN, O.A. SAUNDERS, An Introduction to Heat Transfer, Oxford University Press, United Kingdom (1950).

54. W.H. MCADAMS, Heat Transmission, McGraw-Hill, New York (1954).

55. H.K. KUIKEN, "Axisymmetric Free Convection Boundary-Layer Flow past Slender Bodies," *Int. J. of Heat Mass Transfer*, **11**, 1141-1153 (1968).

56. P.H. OOSTHUIZEN, E. DONALDSON, "Free Convection Heat Transfer from Vertical Cones", *Trans. ASME, ser. C, J. Heat Transfer*, **94**, 330-331 (1972).

57. W.M. ROHSENOW, J.P. HARTNETT, E.N. GANIC, Handbook of Heat Transfer Fundamentals, McGraw-Hill Book Company, New York (1985).

58. H.Y. WONG, Handbook of Essential Formulae and Data on Heat Transfer for Engineers, Longman, London (1977).

59. A.C. HINDMARSH, "LSODE and LSODI - Two New Initial Value Ordinary Differential Equation Solvers", *ACM-Signum Newsletter*, **Vol. 15**, No 4 (1980).

60. D. KINCAID, W. CHENEY, Numerical Analysis; Mathematics of Scientific Computing, Brooks/Cole Publishing Company, Pacific Grove, California (1991).

61. J.D. LAMBERT, Computational Methods in Ordinary Differential Equations, John Wiley and Sons, New York (1986).

62. Nuclear Systems Materials Handbook, **Vol. 1**, Design Data, Part IV - Nuclear Fuels, Hanford Engineering Laboratory, Richland, WA.

63. T.F. IRVINE, P.E. LILEY, Steam and Gas Tables with Computer Equations, Academic Press Inc., Orlando (1984).

64. K. RAZNJEVIC, Handbook of Thermodynamic Tables and Charts, Hemisphere Publishing Corporation, Washington (1976).

65. J.H. KEENAN, F.G.KEYES, P.G. HILL, J.G. MOORE, Steam Tables: Thermodynamic Properties of Water Including. Vapor, Liquid, and Solid Phases, John Wiley and Sons, New York (1936).

66. J. BELLE, Uranium Dioxide: Properties and Nuclear Applications, Naval Reactors, Div. of Reactor Development, USAEC, Washington (1961).

67. L. HARR, J. GALLAGHER, G. KELL, NBS/NRC Steam Tables, Thermodynamic and Transport Properties and Computer Programs for Vapor and Liquid States of Water in SI Units, McGraw-Hill, New York (1984).

APPENDIXES

APPENDIX A

ADDITIONAL RESULTS

The following pages show transient simulation results with reactivity addition rates of ~0.1 ¢/sec, ~0.6776 ¢/sec, ~10 ¢/sec, and ~10 $/sec. Tables A.1 to A.4 are provided as a summary of each hypothetical accident scenario for the approximated cylindrical blender described in Chapter 2. The blender is assumed to contain 5000 kg of initially dry and 5 w/o U^{235} enriched UO_2 powder with a powder density of 2.2 g/cm^3 at 20 °C. The dimensions for the approximated cylindrical blender are given in Figure 2.1.

TABLE A.1 Summary of Accident Scenario #3.

Water Ingress Rate	0.0211 l/sec (0.0056 gal/sec)
Reactivity Addition Rate	~0.1 ¢/sec
Elapsed Time to Delayed Critical	6.30 hr

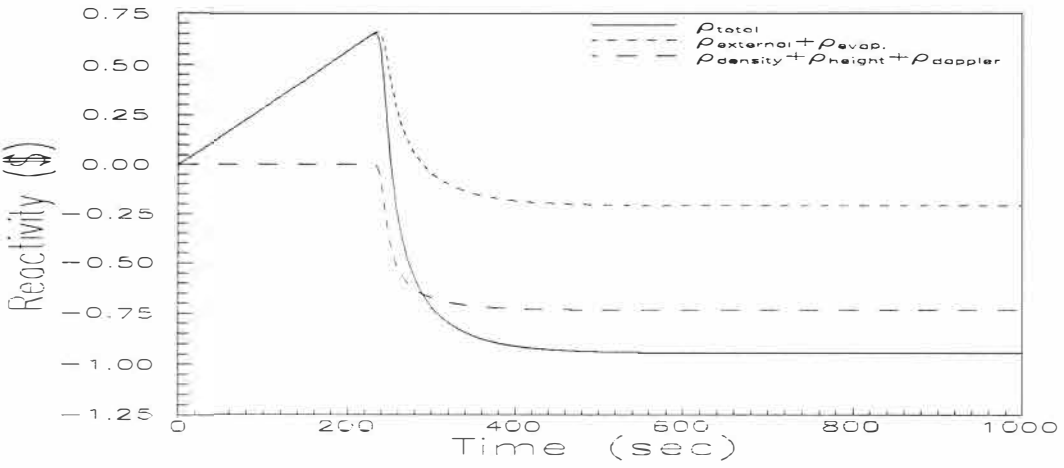

Figure A.1a Reactivity versus Time for ~0.1 ¢/sec Reactivity Addition Rate if Water Ingress is Stopped at the First Power Peak.

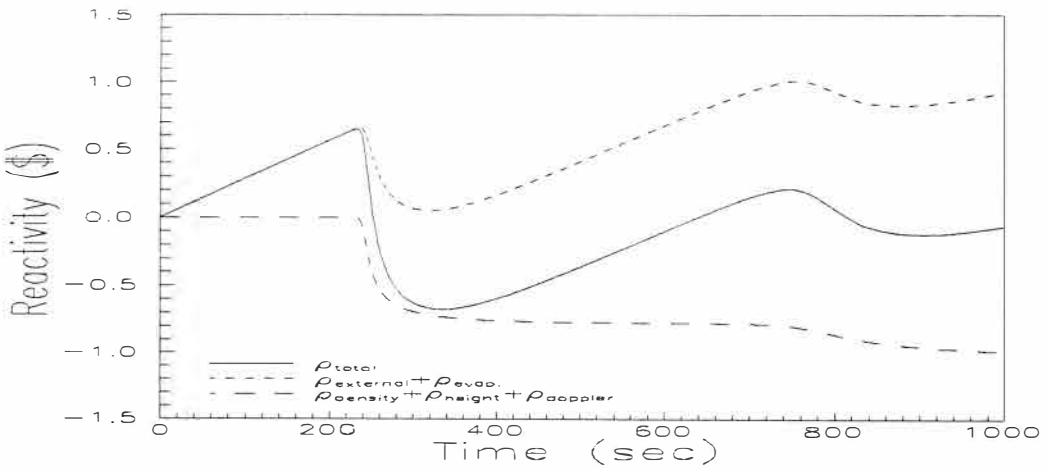

Figure A.1b Reactivity versus Time for ~0.1 ¢/sec Reactivity Addition Rate for Continuous Water Ingress.

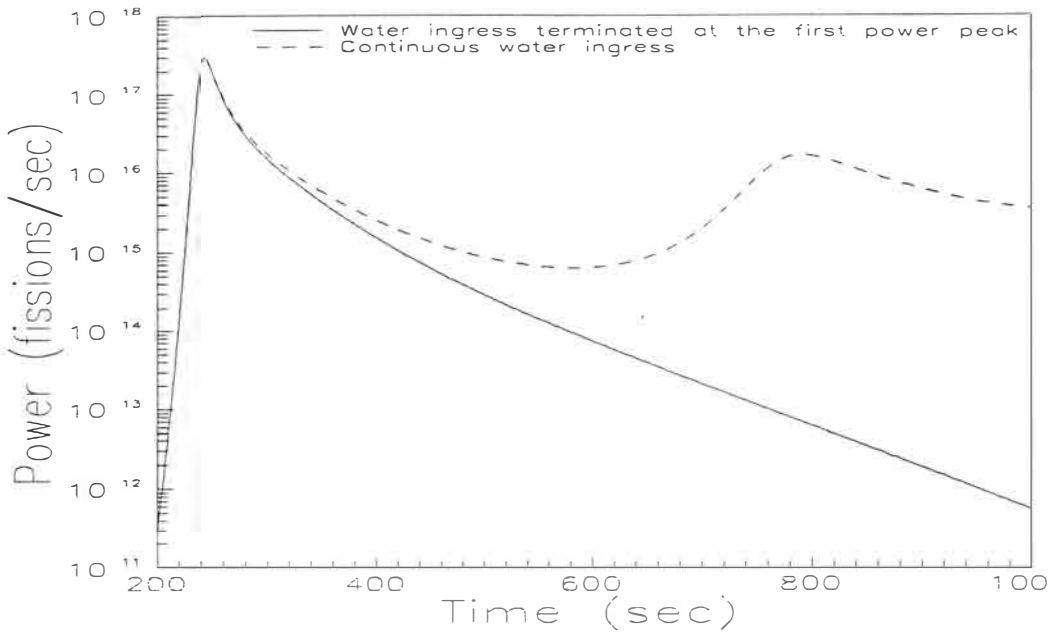

Figure A.1c Power versus Time for ~0.1 ¢/sec Reactivity Addition Rate.

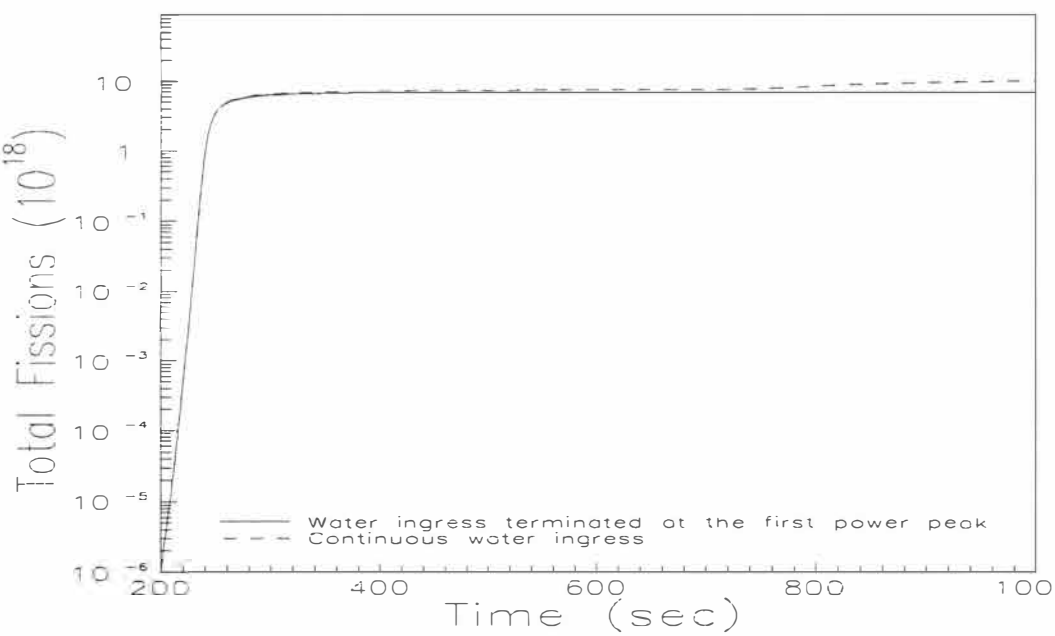

Figure A.1d Total Fissions versus Time for ~0.1 ¢/sec Reactivity Addition Rate.

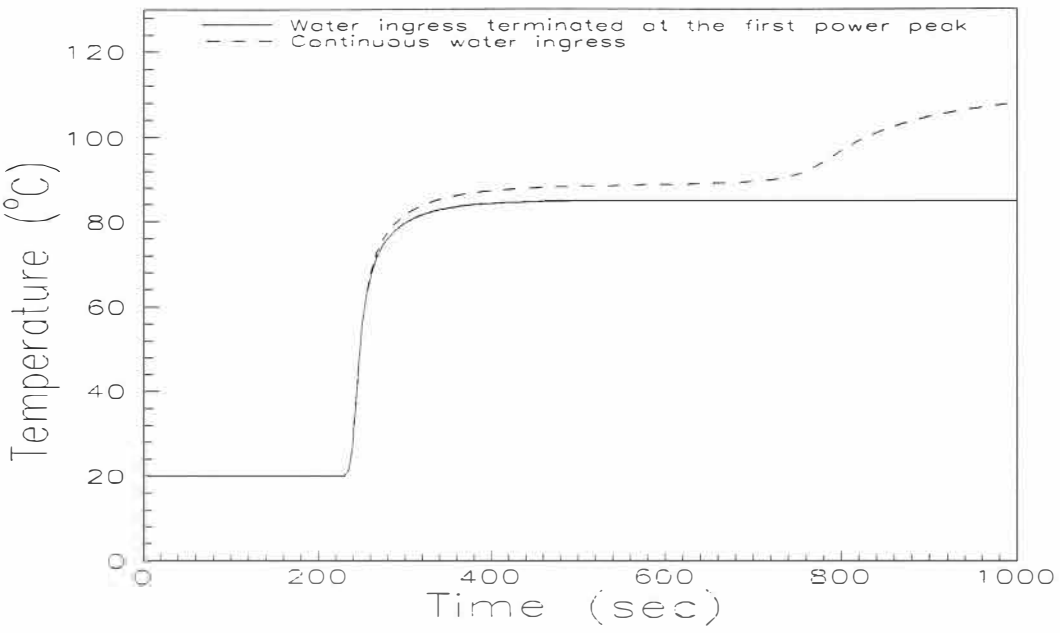

Figure A.1e Temperature versus Time for ~0.1 ¢/sec Reactivity Addition Rate.

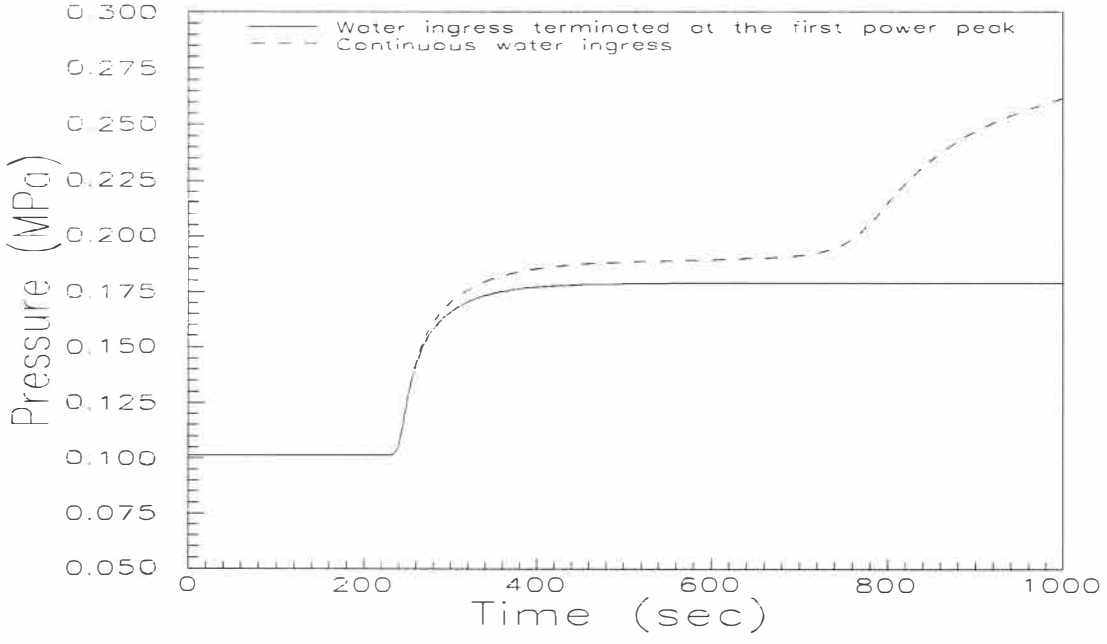

Figure A.1f Pressure versus Time for ~0.1 ¢/sec Reactivity Addition Rate.

TABLE A.2 Summary of Accident Scenario #4.

Water Ingress Rate	0.5 l/sec (0.1321 gal/sec)
Reactivity Addition Rate	~6.776 ¢/sec
Elapsed Time to Delayed Critical	15.99 min

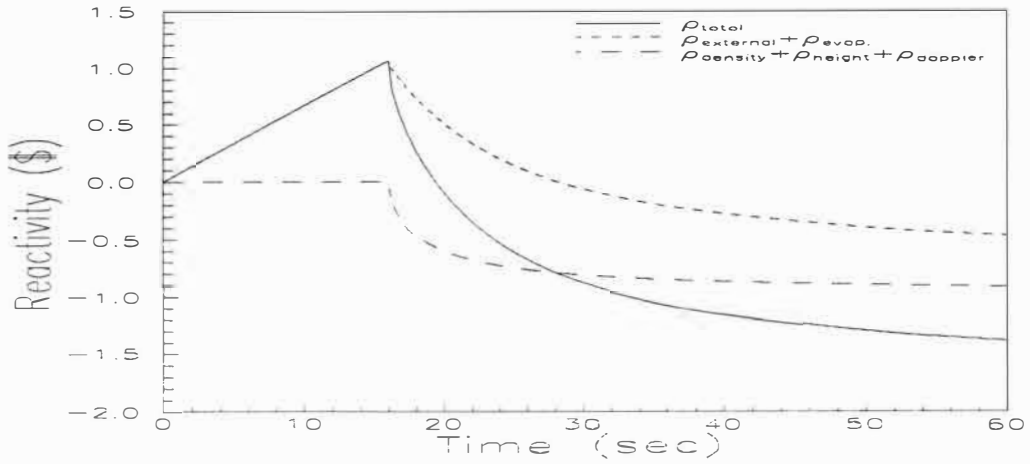

Figure A.2a Reactivity versus Time for ~6.776 ¢/sec Reactivity Addition Rate if Water Ingress is Stopped at the First Power Peak.

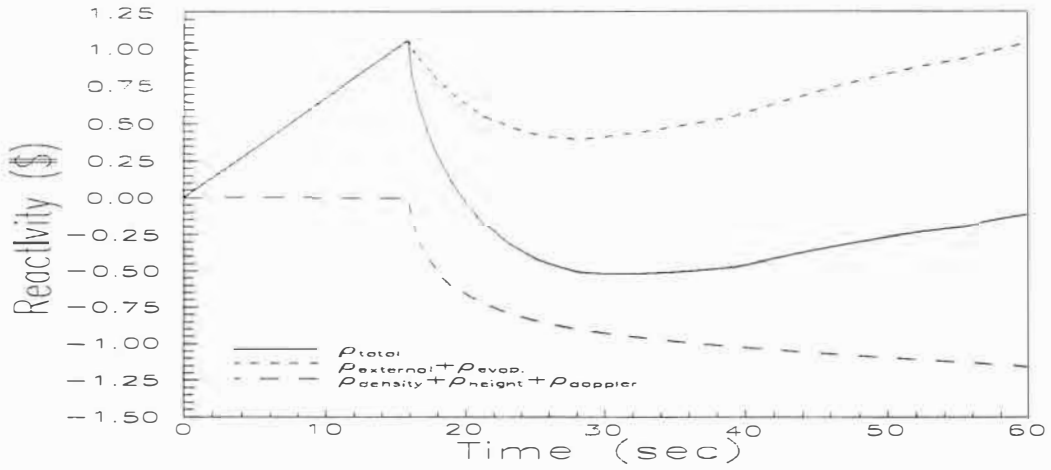

Figure A.2b Reactivity versus Time for ~6.776 ¢/sec Reactivity Addition Rate for Continuous Water Ingress.

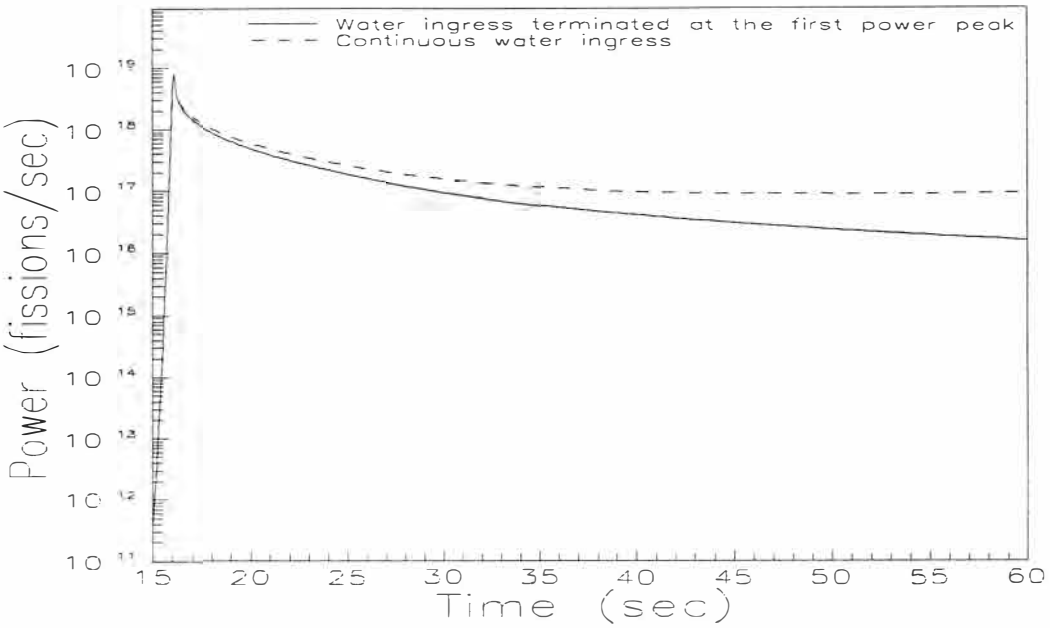

Figure A.2c Power versus Time for ~6.776 ¢/sec Reactivity Addition Rate.

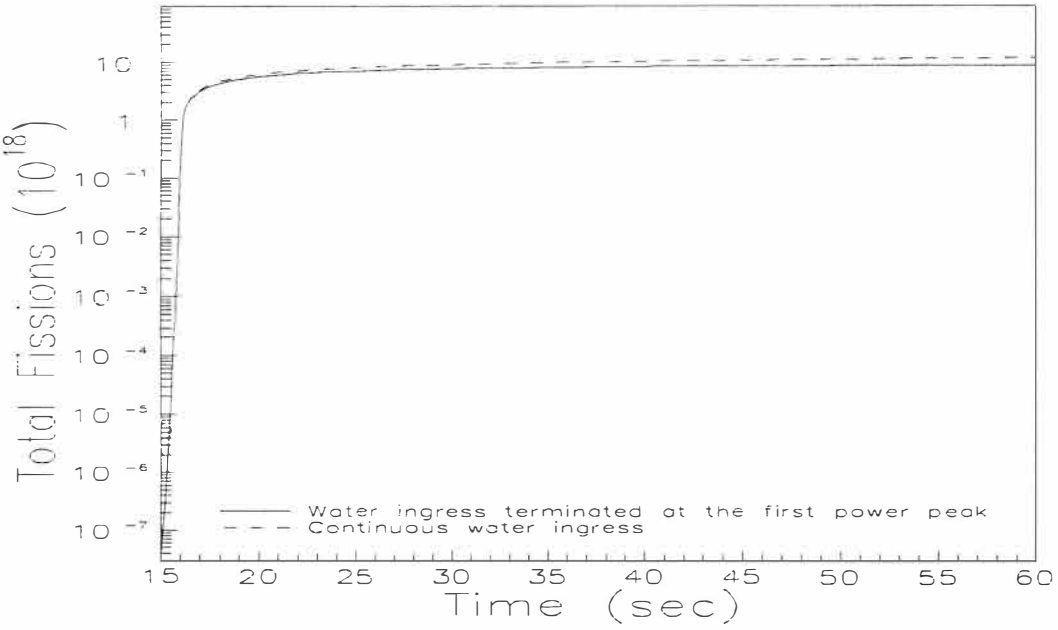

Figure A.2d Total Fissions versus Time for ~6.776 ¢/sec Reactivity Addition Rate.

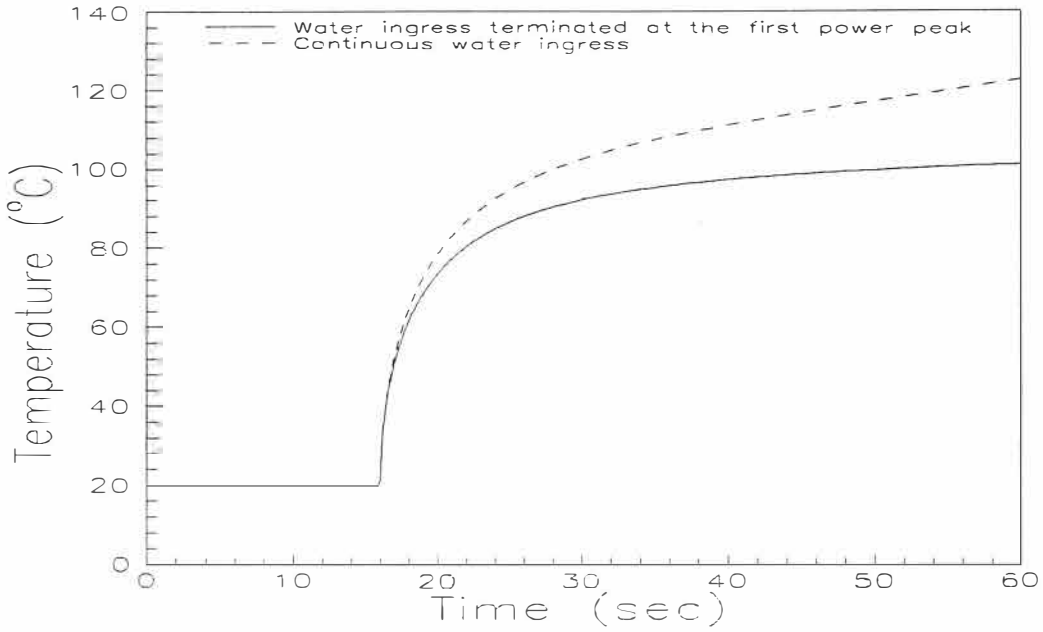

Figure A.2e Temperature versus Time for ~6.776 ¢/sec Reactivity Addition Rate.

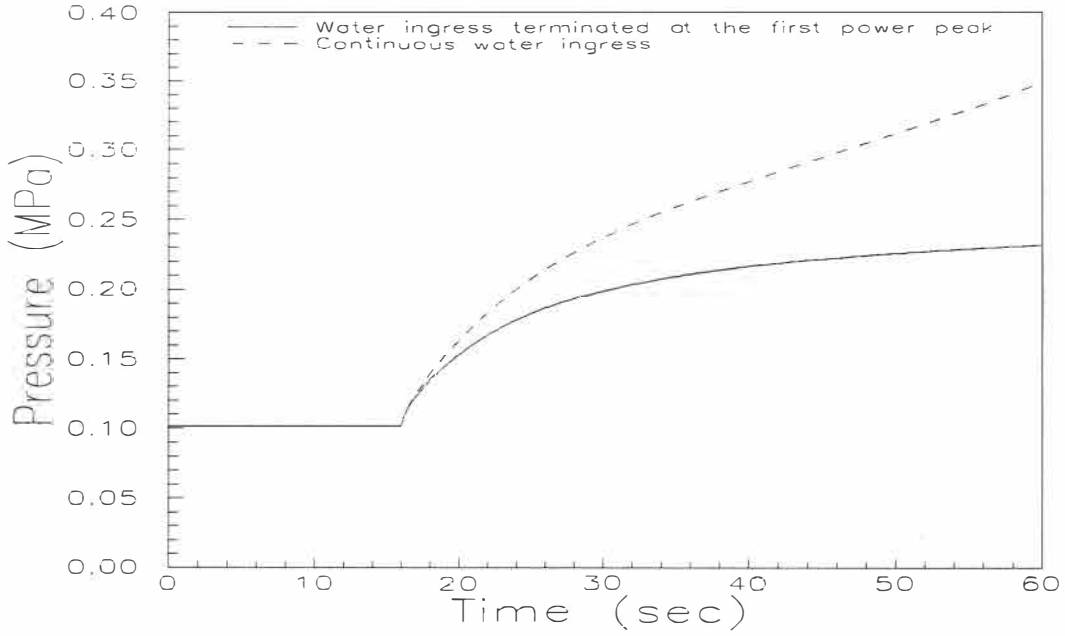

Figure A.2f Pressure versus Time for ~6.776 ¢/sec Reactivity Addition Rate.

TABLE A.3 Summary of Accident Scenario #5.

Water Ingress Rate	0.7494 l/sec (0.1980 gal/sec)
Reactivity Addition Rate	~ 10 ¢/sec
Elapsed Time to Delayed Critical	10.67 min

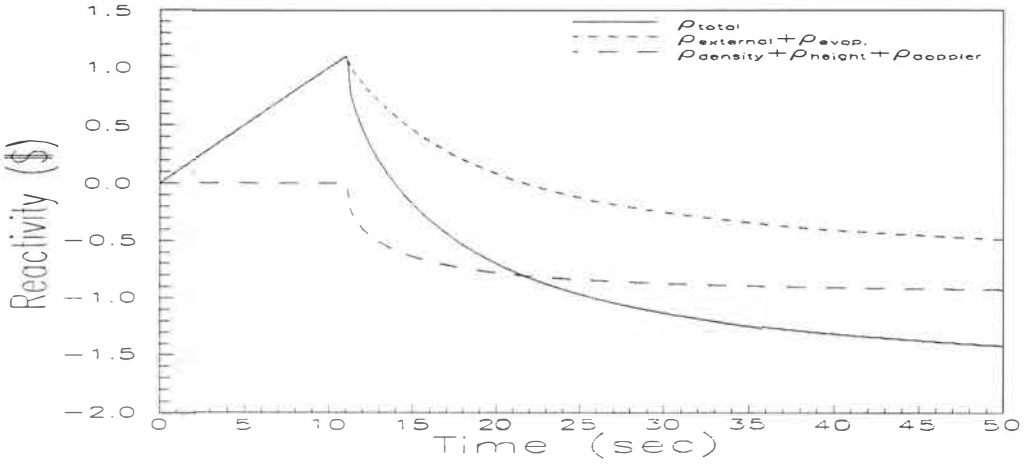

Figure A.3a Reactivity versus Time for ~ 10 ¢/sec Reactivity Addition Rate if Water Ingress is Stopped at the First Power Peak.

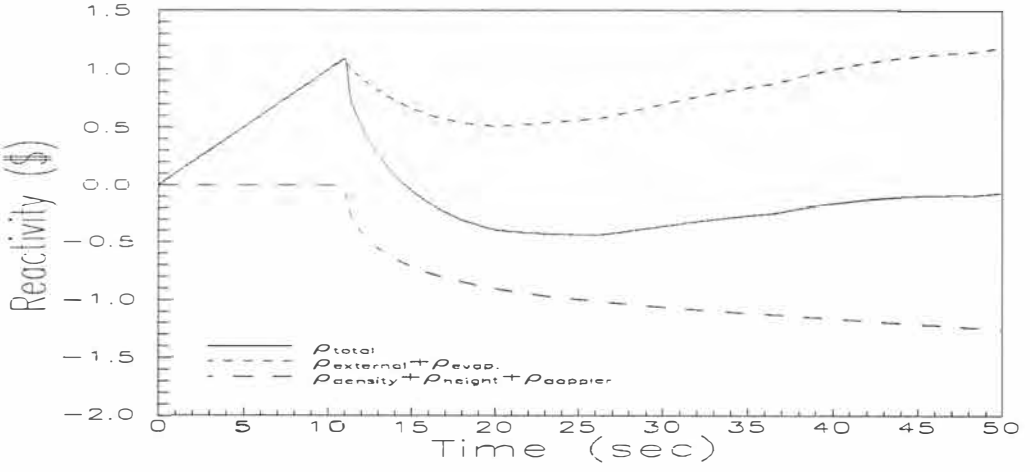

Figure A.3b Reactivity versus Time for ~ 10 ¢/sec Reactivity Addition Rate for Continuous Water Ingress.

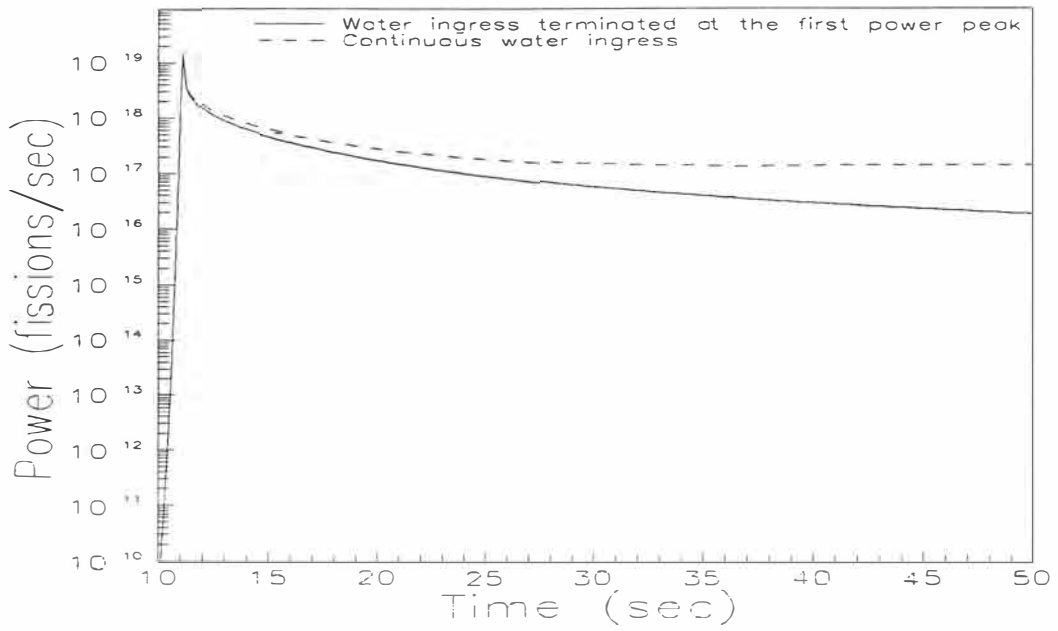

Figure A.3c Power versus Time for ~ 10 ¢/sec Reactivity Addition Rate.

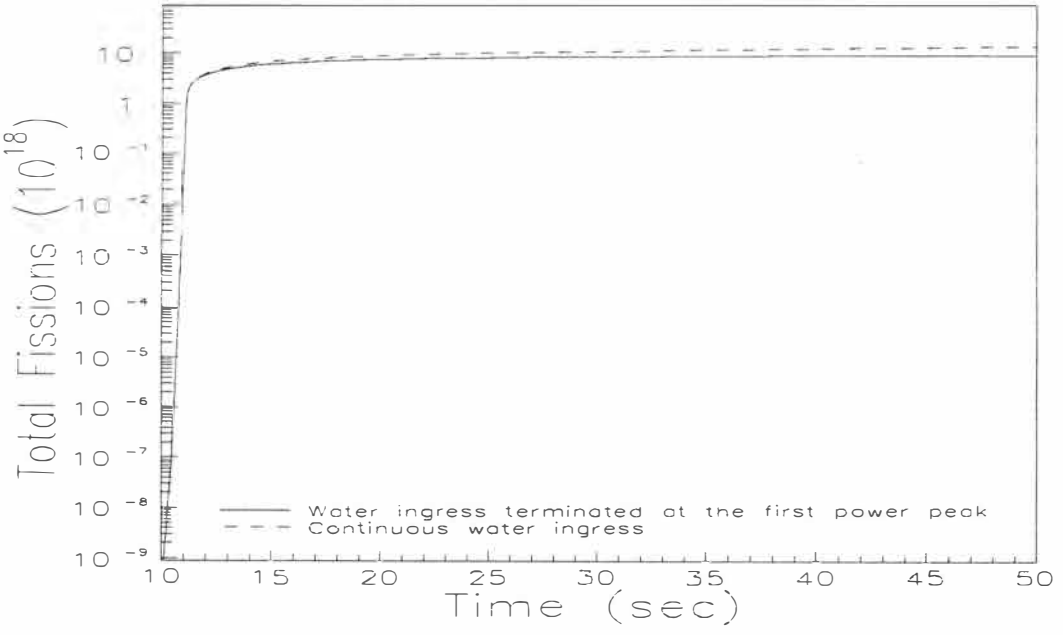

Figure A.3d Total Fissions versus Time for ~ 10 ¢/sec Reactivity Addition Rate.

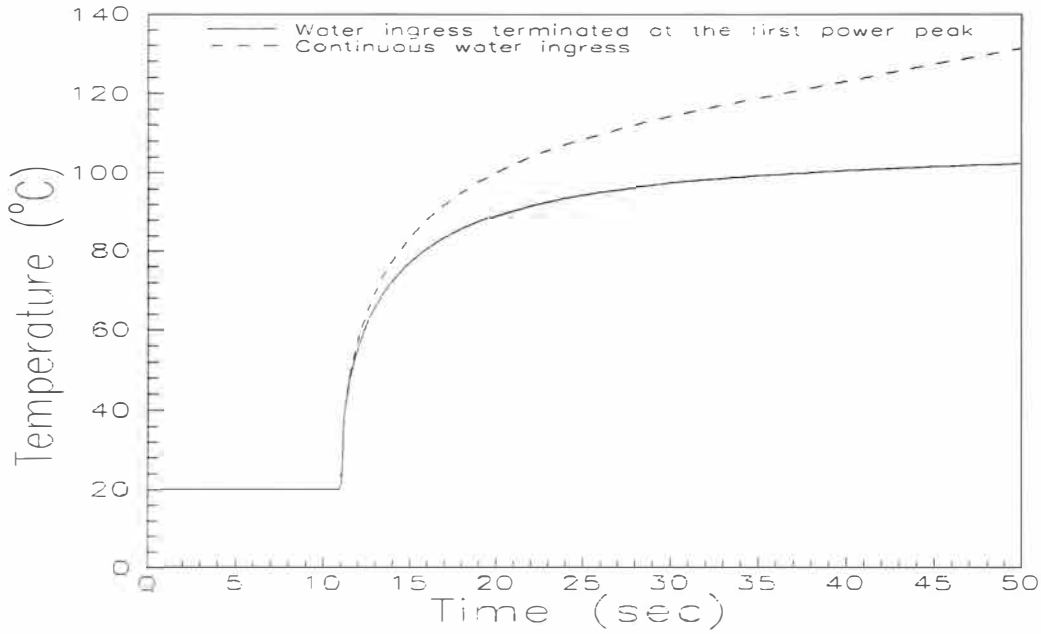

Figure A.3e Temperature versus Time for ~10 ¢/sec Reactivity Addition Rate.

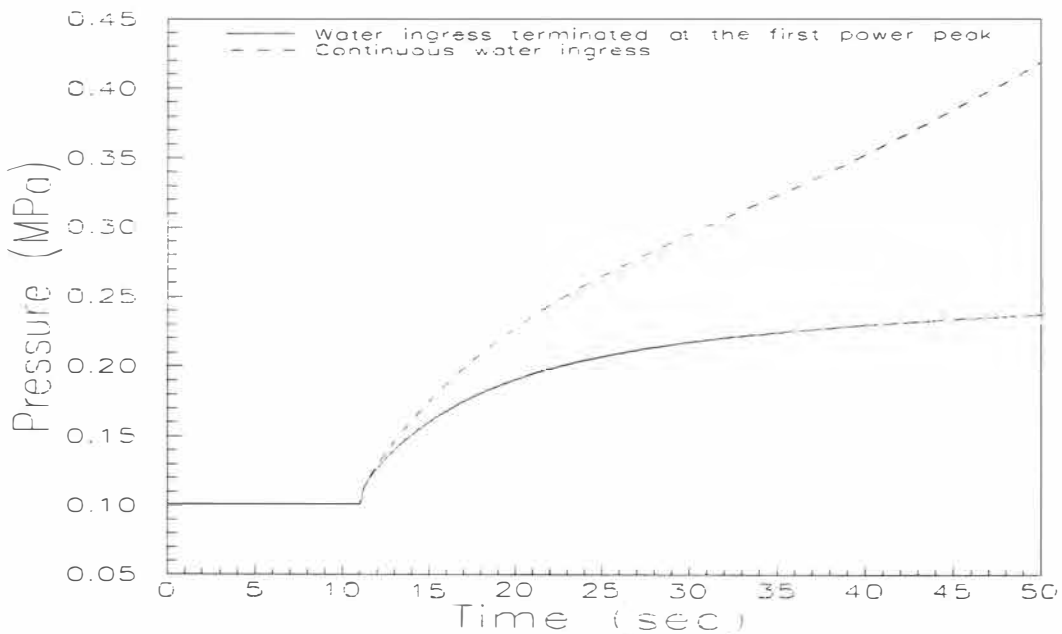

Figure A.3f Pressure versus Time for ~10 ¢/sec Reactivity Addition Rate.

TABLE A.4 Summary of Accident Scenario #6.

Water Ingress Rate	86.6662 l/sec (22.8972 gal/sec)
Reactivity Addition Rate	~ 10 $/sec
Elapsed Time to Delayed Critical	5.54 sec

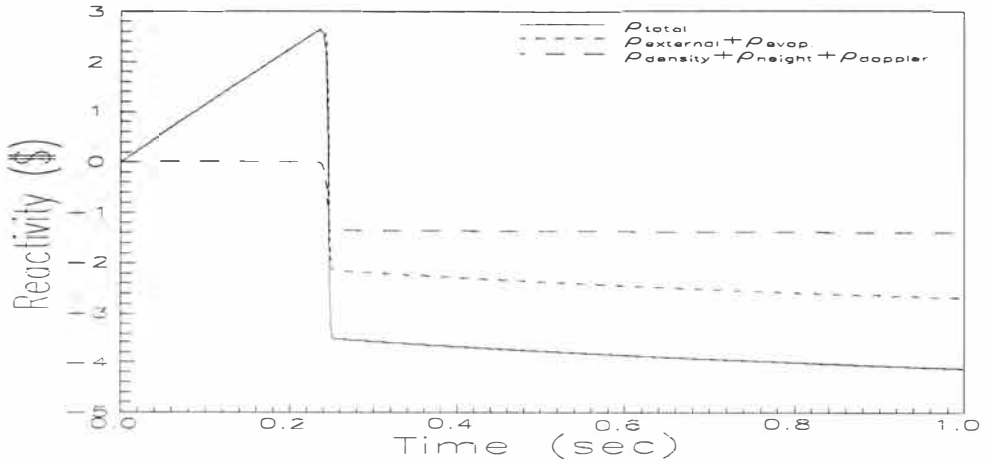

Figure A.4a Reactivity versus Time for 10 $/sec Reactivity Addition Rate if Water Ingress is Stopped at the First Power Peak.

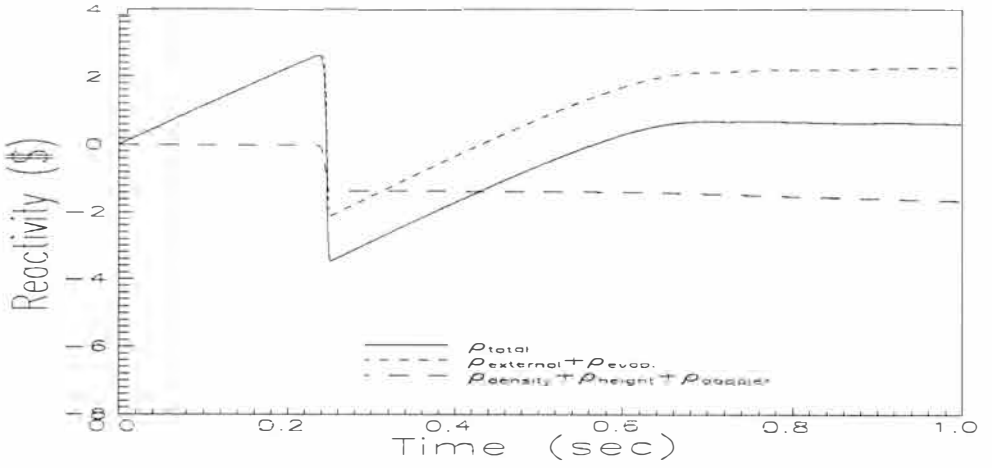

Figure A.4b Reactivity versus Time for 10 $/sec Reactivity Addition Rate for Continuous Water Ingress.

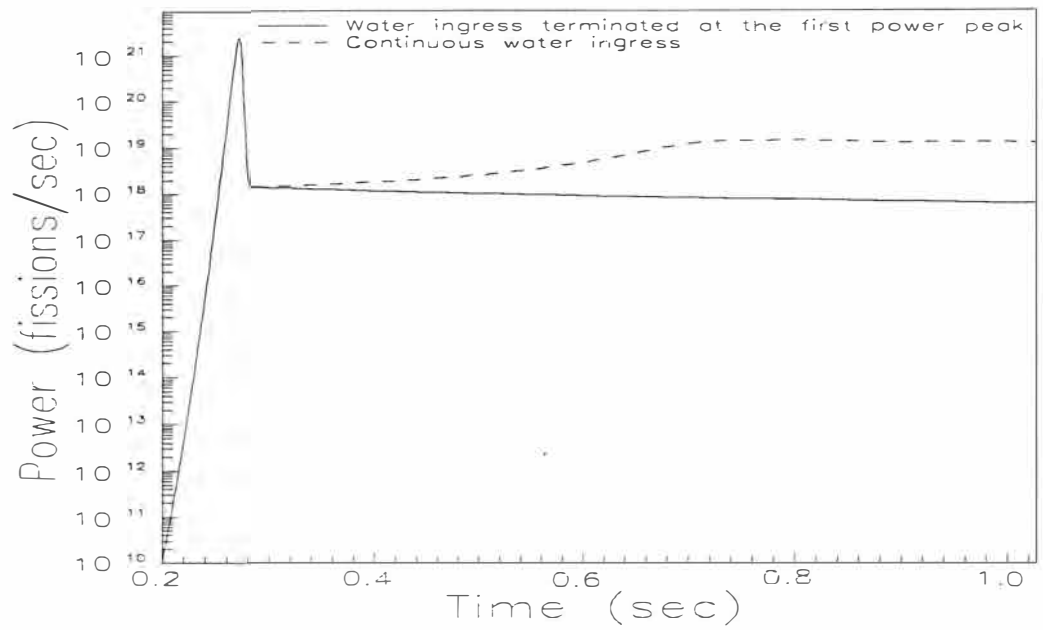

Figure A.4c Power versus Time for 10 $/sec Reactivity Addition Rate.

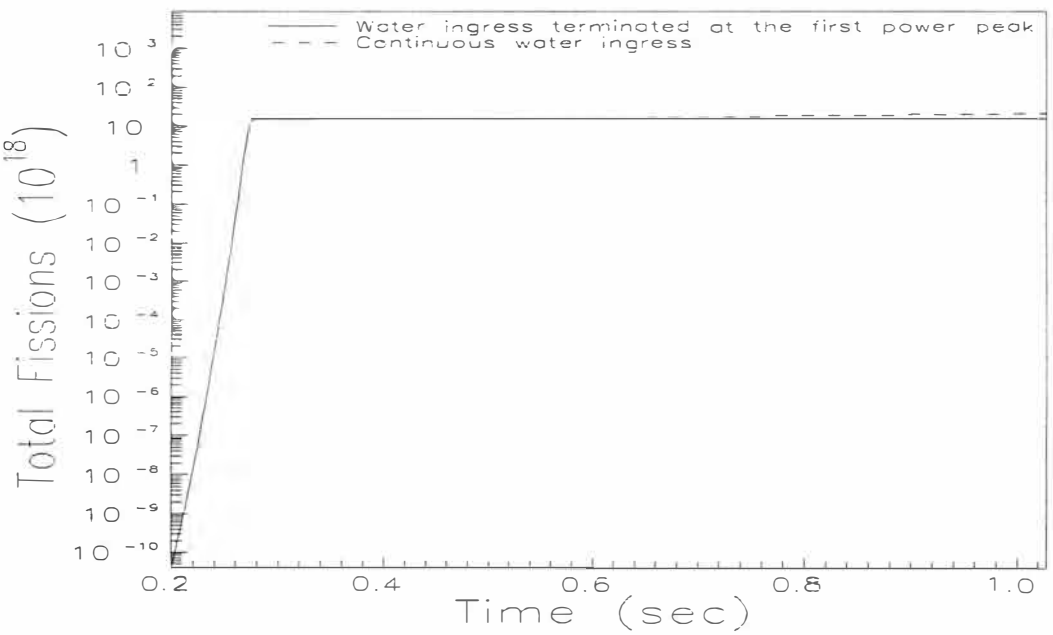

Figure A.4d Total Fissions versus Time for 10 $/sec Reactivity Addition Rate.

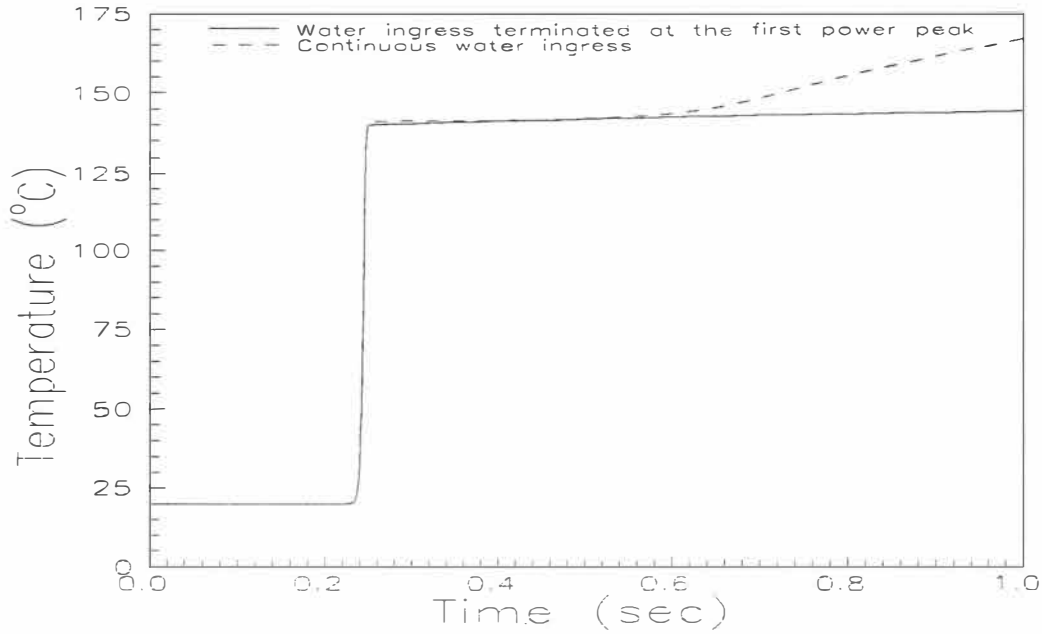

Figure A.4e Temperature versus Time for 10 $/sec Reactivity Addition Rate.

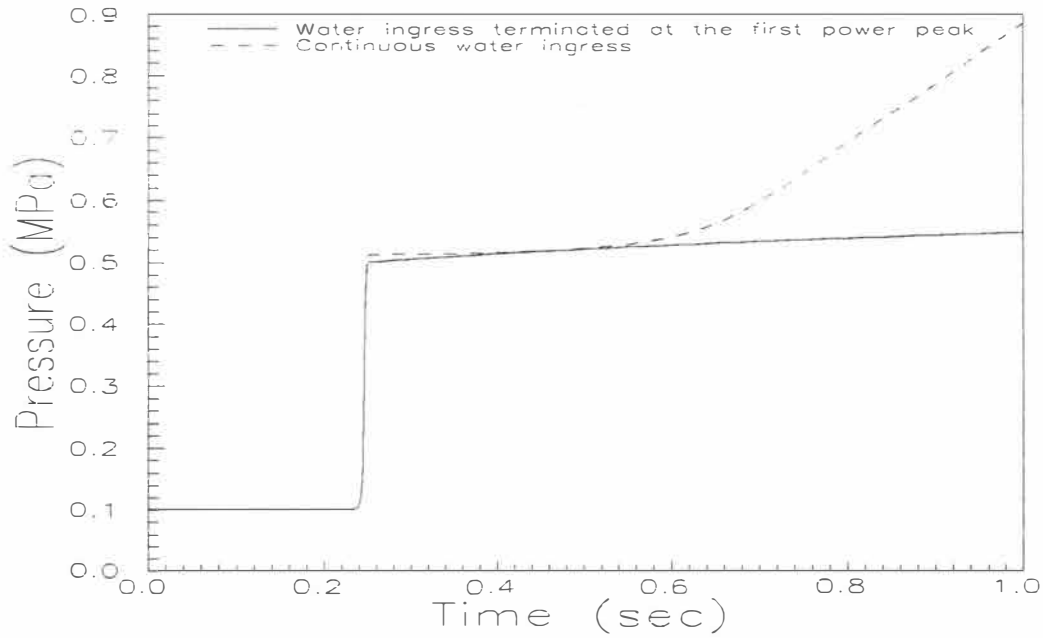

Figure A.4f Pressure versus Time for 10 $/sec Reactivity Addition Rate.

APPENDIX B

SKINATH-WP USER'S MANUAL

B.1. Introduction

SKINAHT-WP uses three input files, namely, SKIWP.INP, SKIST1.DAT, and SKIST2.DAT. SKIWP.INP is the general input file and the other two contain data for steam tables. The calculated output values are written into four different output files that are SKIWP.OU1, SKIWP.OU2, SKIWP.OU3, SKIWP.OU4. Also, output files SKIWP.ERR, SKIWP.WAR, and SKIWP.MAX are employed to facilitate the use of the program. Table B.1 presents the information contained in each output file. SKINATH-WP contains three major computational subprograms, namely, WPINTGEN, WPDYN, and LSODE. Simplified flow charts for these subprograms are given in Figures B.1 to B.3. Also, Figures B.4, B.5, and B.6 show a sample input file, a sample screen output, and the code listing of SKINATH-WP, respectively. Description of the subroutines and the input are given in the following sections.

B.2. Description of Subroutines

SKINATH-WP consists of 1 main and 38 subprograms. Equations and polynomial fits of property data are utilized in several subprograms associated with thermodynamic properties of system components (i.e., powder, air, and SS304 container wall). These equations and property data come from References 46, 62,

63, 64, 65, 66, and 67. The subprograms for steam tables utilize functions developed by W.J. Garland of McMaster University, Hamilton, Canada. These functions are low-order fits that are fast running and reasonably accurate (usually less that 0.1% error). We also modified some of these functions to extend their validity range. The purpose of each subprogram is briefly described in the following list.

WPOUT - This subroutine outputs results in each communication interval.

WPRDGEN - This subroutine opens I/O files and reads input data.

F - This subroutine is required by LSODE. It calls FWP to initialize LSODE calculations.

WPM1DYN - This subroutine contains the statements executed periodically on every communication interval for Model 1.

WPM2DYN - This subroutine contains the statements executed periodically on every communication interval for Model 2.

WPM3DYN - This subroutine contains the statements executed periodically on every communication interval for Model 3.

FWP - This driver routine calls the subroutine WPM**x**DYN (**x**=1,2, or 3) according to the model selection.

PRDCL - This subroutine contains the statements executed periodically on every integration interval.

HPAUP - This function calculates the free convection heat transfer coefficient of a heated horizontal surface facing upward and immersed in air.

HPADW - This function calculates the free convection heat transfer coefficient of a heated horizontal surface facing downward and immersed in air.

VCYMB - This function calculates the free convection heat transfer coefficient of a vertical cylinder immersed in air, provided the diameter of the cylinder is large enough to ignore curvature effects.

VCYSK - This function calculates the laminar natural convection heat transfer coefficient over vertical cylinders immersed in air where curvature effects are important.

VCNWR - This function calculates the natural convection heat transfer coefficient from the sides of a cone.

WPINTGEN - This subroutine conducts the initial calculations.

TCCNT - This function calculates the thermal conductivity of the blender wall (Annealed-SS304) for a given temperature.

SPCNT - This function calculates the specific heat of the blender wall (Annealed-SS304) for a given temperature.

DNSCNT - This function calculates the density of the blender wall (Annealed-SS304) for a given temperature.

PRPA - This subroutine calculates the density, specific heat, thermal conductivity, viscosity and coeffcient of thermal expansion for air at atmospheric pressure, for a given temperature.

DFSUB - This function calculates the density of light water in the subcooled liquid phase.

CPF - This function calculates the specific heat of light water for a given pressure.

CPFSUB - This function calculates the heat capacity of light water in the subcooled liquid phase, given its temperature and pressure.

CVAIR - This function calculates the heat capacity of air at constant volume given its temperature using the computer equations given by T.F. Irvine,Jr. and P.E. Liley.

CPFP - This function calculates the heat capacity of UO_2 powder given its temperature.

PDNS - This function calculates the density of stoichiometric UO_2 given its temperature and density at 0 °C.

VF - This function calculates the specific volume of light water in the liquid phase at saturation for a given pressure.

VG - This function calculates the specific volume of light water in the gas phase at saturation for a given pressure.

PSAT - This function calculates the saturation pressure of light water for a given temperature.

TSAT - This function calculates the saturation temperature of light water for a given pressure.

DF - This function calculates the density of light water in the liquid phase at saturation for a given pressure.

INTRPLT1 - This subroutine interpolates the thermophysical properties of saturated water such as saturation temperature and pressure, vapor and liquid densities, heat of vaporization, liquid specific heat, viscosity, thermal conductivity, Prandtl number, surface tension and thermal expansion coefficient, for a given temperature.

INTRPLT2 - This subroutine interpolates the thermophysical properties of saturated water such as saturation pressure, vapor and liquid specific volumes, vapor and liquid internal energies, for a given temperature.

REWPC - This function calculates reactivity for a given water content.

RECIT - This function calculates the constant water ingress rate corresponding to an initial reactivity addition rate.

GSTBS - This function calculates the rate of radiant heat exchange between diffuse-grey surface and blackbody surrounding.

EMMC - This function calculates the emissivity of the container wall for a given temperature.

FHCYL - This subroutine updates the geometric information for a cylindrical shaped system.

FHCONE - This subroutine updates the geometric information for a conical shaped system.

SCRNMKR - This subroutine resets the computer screen.

B.3. Input Description

Namelist input format is used for the general input where each input parameter can be described as follows:

NEQ - Number of first order differential equations.

ITOL - An indicator for the type of error control. 1 or 2 according as ATOL and RTOL (below) is a scalar or array.

RTOL - A relative error tolerance parameter(either scalar of an array of length NEQ).

ATOL - An absolute error tolerance parameter(either scalar or array of length NEQ).

ITASK - An index specifying the task to be performed:
=1 : For normal computation.

ISTATE - An index used for input and output to specify the state of the calculations.

IOPT - An integer flag to specify whether or not any optional inputs are being used on each LSODE call:
=0 : To indicate no optional input used.

MF - Method flag:
=22 : For stiff method, internally generated full jacobian (Recommended).

LRW - User-declared length of real work array:
$=20 + (NEQ)$: For MF = 22.

LIW - User-declared length of IWORK:
$=22 + 9 \times (NEQ) + (NEQ)^2$: For MF = 22.

M - Number of delayed neutron precursor groups.

XT - Initial value of the independent variable, time.

TOUT - First point where output is desired.

DT - Length of each communication interval following the first interval.

TSTOP - Final point where the output is desired.

TQT - Time at which the water ingress is terminated.

ALF - Factor for Model 3 steam table search (=10 is recommended).

CCRT - Convergence criteria for Model 3 steam table search ($=10^{-4}$ is recommended).

XY(i) **i=1,...,NEQ** - Array of initial values of dependent variables.

XYDOT(i) **i=1,...,NEQ** - Array of initial values of $dy(i)/dt$.

AMDA(i) **i=1,...,M** - Array of decay constant for delayed neutron precursors.

B(i) **i=1,...M** - Array of fractions for delayed neutron precursors.

IFLGC - Free convection correlation flag:
=1 : Churchill and Chu (Cylinder).
=2 : Minkowycz and Sparrow (Cylinder).
=3 : LeFevre and Ede (Cylinder).
=4 : Kuiken (Cone).
=5 : Oosthuizen and Donaldson (Cone).
=6 : Rohsenow, Hartnett and Ganic (Cone).

IFLGM - Model flag:
=1 : Model 1.
=2 : Model 2.
=3 : Model 3.

IFLGU - Flag for reactivity driving force function:
=0 : Cylindrical blender,
Inner diameter= 1.0692 m, Powder level= 2.4496 m,
Enrichment= 5 w/o U^{235} enriched,
UO_2 Powder density= 2.2 g/cm^3.
=1 : Cylindrical blender,
Inner diameter= 0.8 m, Powder level= 1 m,
Enrichment= 5 w/o U^{235} enriched,
UO_2 Powder density= 2.2 g/cm^3.
=2 : Cylindrical blender,
Inner diameter= 0.8 m, Powder level= 1 m,
Enrichment= 5 w/o U^{235} enriched,
UO_2 Powder density= 1 g/cm^3.

EPSIL - Fraction of the energy from fission deposited in the system.

GEN - Neutron mean generation time (s).

SOURCE - Extraneous source neutron generation rate (#/s).

ENRIC - Fuel enrichment.

ZNU - Average number of neutrons per fission (#).

PRSFN - Initial neutron source per 100 g of powder-water mixture (#/s).

SUBMUL - Subcritical multiplication factor to calculate the initial neutron source.

DIUP - Blender upper surface inner diameter (m).

DIDW - Blender bottom surface inner diameter (m).

THCNT - Container wall thickness (m).

RHODENS - Reactivity feedback coefficient due to powder density ($).

RHOHEIG - Reactivity feedback coefficient due to height ($).

RHODOPP - Reactivity feedback coefficient due to doppler effect of the powder/water mixture ($).

PL - Initial powder level (m).

BL - Blender height (m).

PRESS0 - Initial pressure (Mpa).

WW0 - Initial water content (kg/m^3).

WLR - Water ingress rate (kg/s).

WMQT - Maximum ingress water mass (kg).

SOR - Steam removal rate (kg/s).

TCA - Ambient air temperature ouside blender (°C).

TMP0 - Initial temperature of the blender and its contents (°C).

PDNS0 - Powder density at 0 °C (kg/m^3).

DNS0 - Initial powder density (kg/m^3).

The reader is referred to LSODE documentation for a detailed description of LSODE options and LSODE parameters such as ITOL, RTOL, ATOL, ITASK, ISTATE, IOPT, LWR, LIW, and MF.

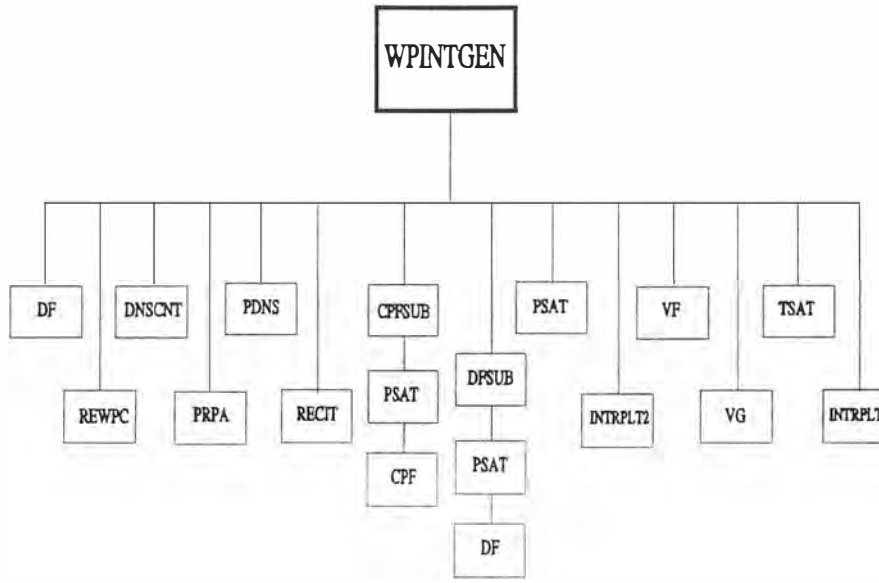

FIGURE B.1 Flow Chart of Initial Calculations.

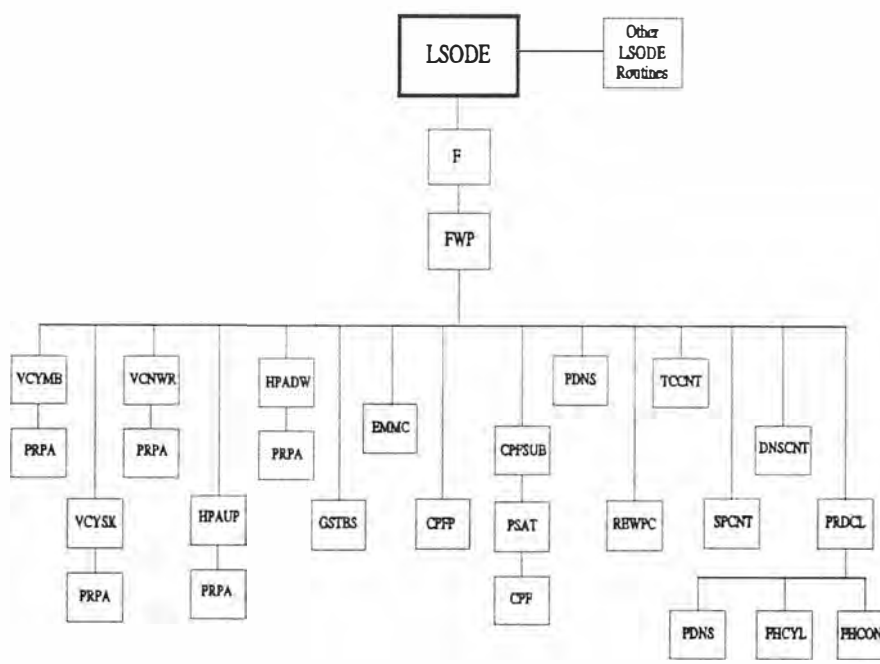

FIGURE B.2 Flow Chart of LSODE Calculations.

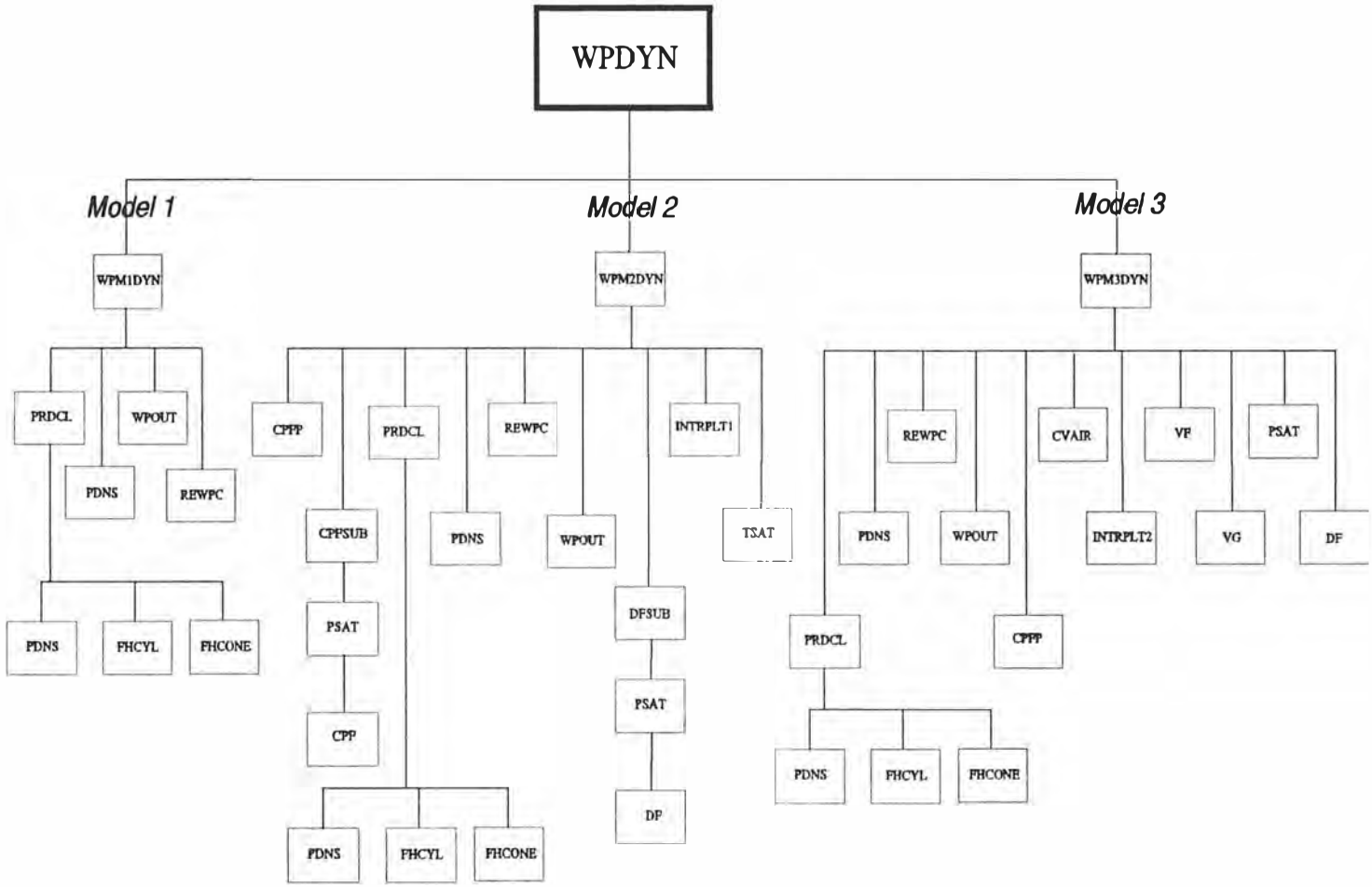

Figure B.3 Flow Chart for Communication Interval Calculations.

TABLE B.1 Contents of Output Files

FILE NAME	CONTENTS
SKIWP.OU1	Total, external, and feedback reactivities with respect to time.
SKIWP.OU2	Bulk temperature, container outer surface temperature, partial water pressure, partial air pressure, and total pressure with respect to time.
SKIWP.OU3	Power, total fissions, and bulk temperature/net energy generated with respect to time.
SKIWP.OU4	Water mass, steam mass, and quality with respect to time.
SKIWP.ERR	Error message, if program is terminated due to an error.
SKIWP.WAR	Warning message(s).
SKIWP.MAX	Maximum values of power, bulk temperature, number of fissions, pressure, water mass, steam mass, and quality.

```
$INP1
NEQ=10,    ITOL=1,    RTOL=1.D-6,     ATOL=1.D-6,  ITASK=1,
ISTATE=1,    IOPT=1,    LRW=242,    LIW=30,    MF=22,    M=6,
XT=0.D+0, TOUT=1.D-2, DT=1.D-2, TSTOP=1.D+3,  TQT=1.D+3,
ALF=1.D+1,    CCRT=1.D-8,   XY=1.D-2,   7*0.D+0,    2*2.D+1,
XYDOT=10*0.D+0,     AMDA=1.27D-2,     3.17D-2,     1.15D-1,
3.11D-1,    1.4D+0,    3.87D+0,     B= 2.47D-4,   1.3845D-3,
1.222D-3,    2.6455D-3,     8.32D-4,    1.69D-4,    IFLGC=2,
IFLGM=1,    IFLGU=0,     PI=3.14159D+0,     G= 9.80665D+0,
M=6,     EPSIL=1.D+0,     GEN=2.4121D-5,      SOURCE=0.D+0,
ENRIC=5.D-2,  ZNU=2.43D+0, PRSFN=9.39D-1, SUBMUL= 1.D+0,
DIN1=1.0692D+0,      DIN2=1.0692D+0,       THCNT=9.525D-3,
DIUP=1.0882D+0,    DIDW=1.0882D+0,     RHODENS=5.49936D-3,
RHOHEIG=0.84543D+0,  RHODOPP=-0.01109D+0,  PL=2.4496D+0,
BL=20.9169D+0,PRESS0=1.0133D-1,WW0=0.21786D+3,WLR=1.D-2,
WMQT=2.11496D+1,    SOR=0.D+0,    TCA=2.D+1,    TMP0=2.D+1,
HGT0=2.4496D+0, PDNS0=2.2D+3, DNS0=2.2D+3
$END
```

Figure B.4 Sample Input File for SKINATH-WP

```
================================================================================
  SSSSS    KK    KK  IIIIII  NN      NN   AAAAAA   TTTTTTTT  HH     HH
 SSSSSSS   KK   KK     II    NNN     NN  AAAAAAAA     TT     HH     HH
 SS   SS   KK  KK      II    NNNN    NN  AA    AA     TT     HH     HH
 SS        KK KK       II    NN NN   NN  AA    AA     TT     HH     HH
  SSSSS    KKKK        II    NN  NN  NN  AAAAAAAA     TT     HHHHHHHHH
   SSSSS   KKKK        II    NN   NN NN  AAAAAAAA     TT     HHHHHHHHH
      SS   KK KK       II    NN    NNNN  AA    AA     TT     HH     HH
 SS   SS   KK  KK      II    NN     NNN  AA    AA     TT     HH     HH
 SSSSSSS   KK   KK     II    NN      NN  AA    AA     TT     HH     HH
  SSSSS    KK    KK  IIIIII  NN      NN  AA    AA     TT     HH     HH
================================================================================
                  <<< By Benan BASOGLU - October 1991 >>>

                    $$$  WET POWDER : MODEL  III  $$$

   WIR: 0.068          PIT: 117.4406        IEDIT : 10          ICHMS: 0
   TWI: 21.1496        TIT: 122.6277        IFTRAP: 1             TQT: 1000
   IWM: 478.8504       TWM: 500.            IFLGC : 2           TSTOP: 1000

TIME=   5.00 # REAC=   0.050 # TEMP=   20.000   +++ PROGRAM RUNNING +++
```

Figure B.5 Sample Screen Output for SKINATH-WP

Figure B.6

Code Listing of SKINATH-WP

Main Program

```
      PROGRAM SKIWP
C Main Program
      IMPLICIT REAL*8(A-H,O-Z)
      CHARACTER*4 CFLGO
      CHARACTER*24 CMESS(4)
      DIMENSION RWORK(212),IWORK(30),Y(10),YDOT(10)
      DIMENSION AMDA(6),B(6)
      DIMENSION TPSW1(35,10),TPSW2(45,6)
      EXTERNAL F
      COMMON /TTPSW/ TPSW1,TPSW2
      COMMON /LSODE1/ NEQ,ITOL,RTOL,ATOL,ITASK
      COMMON /LSODE2/ ISTATE,IOPT,LRW,LIW,MF
      COMMON /WPGEN/AMDA,B,CFLGO, IFLGC,IFLGS, PI,G, M, EPSIL,GEN,
     >SOURCE, ENRIC, DIN1, DIN2,THCNT, DIUP,DIDW, PL,BL, WW0, WLR,
     >TMP0, HGT0, PDNS0, REF0, DNS0, REACTOT,REACEX, REACFB,PRESS,
     >WMSS, DT,TMST,ZMUO2, HFTCA,BT,TCON,RHODENS,RHOHEIG, RHODOPP,
     >RHOREFL,WCON,REFHGT, PMSS,VOL,THETA,X, DOUT1, DOUT2,SPL,SPS,
     >S, S1, S2, TSTOP, TERA ,POWA,STEA,TOPA, BOTA,TCA,PRESS0,EF0,
     >TQT,WMSN,TWMSS,TOUT,IFLGM,IEDIT, IFLGE, IFLGW, ICNTF,IFTRAP,
     >ICHMS,WMQT,DTMS,VOLST,FRVOL,IFLGD, DELTA,R1,R2,R3,DSW,TMPW ,
     >CREAC,CPW,HFG,IFLGX,YOLD,WMSS0,IFLGB,IFLGA,IFLGU, ZNU,PRSFN,
     >SUBMUL,IDCP,EF20,CMSS
      COMMON /WPM3/AVAEN,AVAENW,EXEN
      COMMON /WPM1/SOR, CPS, SMSS, COEP, VOLI,ALF,U1,U2,QUAL,AIRM,
     >PAIR,PH2O,TAIR1,PAIR1,VV,CCRT
      COMMON /MXM/  ZPWMX,ZTMMX,ZNFMX,ZPRMX,ZWMMX,ZQLMX,ZSMMX,
     >              TPWMX,TTMMX,TNFMX,TPRMX,TWMMX,TQLMX,TSMMX
      CMESS(1)=' PLEASE DO NOT DISTURB !'
      CMESS(2)=' +++ PROGRAM RUNNING +++'
      CMESS(3)=' >>>>>  THANK YOU  <<<<<'
      CMESS(4)=' BENAN BASOGLU(974-0667)'
      IMESS=1
      IWORK(6)=10000
C
C Open I/O files and read general input
      CALL WPRDGEN(T,Y,YDOT)
C
C Initialize
      CALL WPINTGEN(NEQ,Y)
C
C Call screen maker
      CALL SCRNMKR(IFLGM,WMSS,WLR,IEDIT,WMQT,IFTRAP,TQT,
     >TSTOP,ICHMS,IFLGC)
C
C Solve DEs for each communication time step using LSODE and keep
C track of the maxima of some important parameters.
 10   CONTINUE
      IF (IFLGE.EQ.1) THEN
      WRITE(*,'(A7,F7.2,A8,F8.3,A8,F9.3,2X,A24)') '+ TIME=',
     >(TOUT-DT),' # REAC=',REACTOT,' # TEMP=',TMPW,CMESS(IMESS)
      END IF
      IMESS=IMESS+1
      IF (IMESS.GT.4) IMESS=1
      IF (IFLGM.EQ.1) CALL WPM1DYN(NEQ,Y)
      IF (IFLGM.EQ.2) CALL WPM2DYN(NEQ,Y)
      IF (IFLGM.EQ.3) CALL WPM3DYN(NEQ,Y)
      CALL LSODE(F,NEQ,Y,T,TOUT,ITOL,RTOL,ATOL,ITASK,ISTATE,IOPT,
```

Main Program (cont.)

```
     >RWORK,LRW,IWORK,LIW,JEX,MF)
      TMSS=WMSS+SMSS
      IF (TMSS.EQ.0) THEN
      QUAL=0.D+0
      ELSE
      QUAL=SMSS/TMSS
      END IF
      FISSN=Y(2)/(2.02D+2*1.602D-13)
      IF (Y(1).GT.ZPWMX) THEN
      ZPWMX=Y(1)
      TPWMX=TOUT
      END IF
      IF (TMPW.GT.ZTMMX) THEN
      ZTMMX=TMPW
      TTMMX=TOUT
      END IF
      IF (FISSN.GT.ZNFMX) THEN
      ZNFMX=FISSN
      TNFMX=TOUT
      END IF
      IF (PRESS.GT.ZPRMX) THEN
      ZPRMX=PRESS
      TPRMX=TOUT
      END IF
      IF (WMSS.GT.ZWMMX) THEN
      ZWMMX=WMSS
      TWMMX=TOUT
      END IF
      IF (QUAL.GT.ZQLMX) THEN
      ZQLMX=QUAL
      TQLMX=TOUT
      END IF
      IF (SMSS.GT.ZSMMX) THEN
      ZSMMX=SMSS
      TSMMX=TOUT
      END IF
      IF(ISTATE.LT.0) GO TO 20
      IF(T.GE.TSTOP) GO TO 30
      TOUT=TOUT+DT
      ICOUNT=ICOUNT+1
      III=MOD(ICOUNT,IEDIT)
      IF (III.EQ.0) THEN
      IFLGE=1
      ELSE
      IFLGE=0
      END IF
      IIJJ=MOD(ICOUNT,IEDIT*IDCP)
      IF (IIJJ.EQ.0) THEN
      CALL SCRNMKR(IFLGM,WMSS0,WLR,IEDIT,WMQT,IFTRAP,TQT,
     >TSTOP,ICHMS,IFLGC)
      END IF
      GO TO 10
C
C Error in LSODE
 20   WRITE(25,21) ISTATE
 21   FORMAT(' ERROR(MAIN)....ISTATE =',I3)
      STOP
```

Main Program (cont.)

```
C
C Output maximas
 30    WRITE(22,*) ' POWER : ',TPWMX,ZPWMX
       WRITE(22,*) ' # FIS : ',TNFMX,ZNFMX
       WRITE(22,*) ' TEMP  : ',TTMMX,ZTMMX
       WRITE(22,*) ' PRESS : ',TPRMX,ZPRMX
       WRITE(22,*) ' W.MSS : ',TWMMX,ZWMMX
       WRITE(22,*) ' QUAL  : ',TQLMX,ZQLMX
       WRITE(22,*) ' S.MSS : ',TSMMX,ZSMMX
C
C End of program
       PRINT*,'PROGRAM RUN HAS BEEN SUCCESFULLY COMPLETED.....'
       END
```

Subroutine WPOUT

```
      SUBROUTINE WPOUT(NEQ,TMN,IFLGW,Y,REACTOT,REACEX,REACFB,PRESS,
     >PH2O,PAIR,WMSS,SMSS,TCON,TMPW,CREAC,WMSN,VOLI,CFLGO)
C This subroutine outputs results in each communication interval.
      IMPLICIT REAL*8 (A-H,O-Z)
      DIMENSION Y(NEQ)
      CHARACTER*4 CFLGO
      COMMON /MXM/ ZPWMX,ZTMMX,ZNFMX,ZPRMX,ZWMMX,ZQLMX,ZSMMX,
     >             TPWMX,TTMMX,TNFMX,TPRMX,TWMMX,TQLMX,TSMMX
C
      TMSS=WMSS+SMSS
      IF (TMSS.EQ.0) THEN
      QUAL=0.D+0
      ELSE
      QUAL=SMSS/TMSS
      END IF
      IF (IFLGW.EQ.1) THEN
      SSS=CREAC
      UUU=REACFB+(REACEX-CREAC)
      ELSE
      SSS=REACEX
      UUU=REACFB
      END IF
      FISSN=Y(2)/(2.02D+2*1.602D-13)
      ZBPWR=Y(1)/(2.02D+2*1.602D-13)
C
C Output results
      IF (CFLGO(1:1).EQ.'1') WRITE(27,10) TMN,REACTOT,SSS,UUU
      IF (CFLGO(2:2).EQ.'2') WRITE(28,20) TMN,TMPW,TCON,PH2O,
     >PAIR,PRESS
      IF (CFLGO(3:3).EQ.'3') WRITE(29,30) TMN,ZBPWR,
     >(FISSN/1.D+18),Y(9)
      IF (CFLGO(4:4).EQ.'4') WRITE(30,40) TMN,WMSS,SMSS,QUAL
 10   FORMAT(F11.4,2X,3(F10.3,2X))
 20   FORMAT(F11.4,2X,5(2X,F11.6))
 30   FORMAT(F11.4,1X,3(G16.5,1X))
 40   FORMAT(F11.4,1X,3(F16.6,2X))
      RETURN
      END
```

Subroutine WPRDGEN

```
      SUBROUTINE WPRDGEN(T,Y,YDOT)
C This subroutine opens I/O files and read input data.
      IMPLICIT REAL*8 (A-H,O-Z)
      CHARACTER CFLGO*4
      DIMENSION AMDA(6),B(6),Y(10),YDOT(10)
      DIMENSION TPSW1(35,10),TPSW2(45,6)
      DIMENSION XY(10),XYDOT(10)
      COMMON /TTPSW/ TPSW1,TPSW2
      COMMON /LSODE1/ NEQ,ITOL,RTOL,ATOL,ITASK
      COMMON /LSODE2/ ISTATE,IOPT,LRW,LIW,MF
      COMMON /WPGEN/AMDA,B,CFLGO, IFLGC,IFLGS, PI,G, M, EPSIL,GEN,
     >SOURCE, ENRIC, DIN1, DIN2,THCNT, DIUP,DIDW, PL,BL, WW0, WLR,
     >TMP0, HGT0, PDNS0, REF0, DNS0, REACTOT,REACEX, REACFB,PRESS,
     >WMSS, DT,TMST,ZMUO2, HFTCA,BT,TCON,RHODENS,RHOHEIG, RHODOPP,
     >RHOREFL,WCON,REFHGT, PMSS,VOL,THETA,X, DOUT1, DOUT2,SPL,SPS,
     >S, S1, S2, TSTOP, TERA ,POWA,STEA,TOPA, BOTA,TCA,PRESS0,EF0,
     >TQT,WMSN,TWMSS,TOUT,IFLGM,IEDIT, IFLGE, IFLGW, ICNTF,IFTRAP,
     >ICHMS,WMQT,DTMS,VOLST,FRVOL,IFLGD, DELTA,R1,R2,R3,DSW,TMPW ,
     >CREAC,CPW,HFG,IFLGX,YOLD,WMSS0,IFLGB,IFLGA,IFLGU, ZNU,PRSFN,
     >SUBMUL,IDCP,EF20,CMSS
      COMMON /WPM3/AVAEN,AVAENW,EXEN
      COMMON /WPM1/SOR, CPS, SMSS, COEP, VOLI,ALF,U1,U2,QUAL,AIRM,
     >PAIR,PH2O,TAIR1,PAIR1,VV,CCRT
      NAMELIST /INP1/NEQ, ITOL, RTOL, ATOL, ITASK,ISTATE,IOPT,LRW,
     >LIW,MF, M, XT, TOUT, DT, TSTOP,TQT,ALF,CCRT,XY,XYDOT,AMDA,B,
     >IFLGC, IFLGM, IFLGU,PI, G, EPSIL,GEN,SOURCE,ENRIC,ZNU,PRSFN,
     >SUBMUL,DIN1,DIN2,THCNT,DIUP, DIDW, RHODENS, RHOHEIG,RHODOPP,
     >PL, BL, PRESS0, WW0, WLR,WMQT,SOR, TCA,TMP0,HGT0,PDNS0,DNS0
C
C Open I/O files and read general input
      OPEN(22,FILE='SKIWP.MAX',STATUS='UNKNOWN',ERR=20)
      OPEN(24,FILE='SKIWP.INP',STATUS='OLD',ERR=40)
      OPEN(25,FILE='SKIWP.ERR',STATUS='UNKNOWN',ERR=50)
      OPEN(26,FILE='SKIWP.WAR',STATUS='UNKNOWN',ERR=60)
C ---#Read steam tables for saturated water
      OPEN(23,FILE='SKIST1.DAT',STATUS='OLD',ERR=30)
      DO J=1,10
      DO I=1,35
      READ(23,*) TPSW1(I,J)
      END DO
      END DO
      CLOSE(23)
      OPEN(23,FILE='SKIST2.DAT',STATUS='OLD',ERR=30)
      DO I=1,45
      DO J=1,6
      READ(23,*) TPSW2(I,J)
      END DO
      END DO
      CLOSE(23)
C ---#Read general input
      READ(24,INP1)
      T=XT
      DO I=1,10
      Y(I)=XY(I)
      YDOT(I)=XYDOT(I)
      END DO
      IEDIT=100
```

Subroutine WPRDGEN (cont.)

```
      DTMS=1.D+1
      IDCP=100
      CFLGO='1234'
      IFLGS=1
      IFTRAP=1
      ICHMS=0
      IFLGT=1
      IFLGD=0
      IFLGB=0
      IFLGA=0
      RHOREFL=0.D+0
      EF0=418.94D+3
      REF0=0
      EF20=83.83D+3
      HFTCA=83.7693D+3
      HGT0=PL
      DO I=1,4
C ---#Open output files
      READ(CFLGO(I:I),'(I1)') ICMPR
      IF (ICMPR.EQ.I) THEN
      OPEN((26+I),FILE='SKIWP.OU'//CFLGO(I:I),
     >STATUS='UNKNOWN',ERR=70)
      END IF
      END DO
      GO TO 80
C ---#Error messages
 20   WRITE(25,21)
 21   FORMAT(' ERROR(READGEN)....File not found /SKIWP.MAX/')
      STOP
 30   WRITE(25,31)
 31   FORMAT(' ERROR(READGEN)....File not found /SKISTx.DAT/')
      STOP
 40   WRITE(25,41)
 41   FORMAT(' ERROR(READGEN)....File not found /SKIWP.INP/')
      STOP
 50   WRITE(25,51)
 51   FORMAT(' ERROR(READGEN)....File create error /SKIWP.ERR/')
      STOP
 60   WRITE(25,61)
 61   FORMAT(' ERROR(READGEN)....File create error /SKIWP.WAR/')
      STOP
 70   WRITE(25,71)
 71   FORMAT(' ERROR(READGEN)....File create error /SKIWP.OUx/')
      STOP
 80   RETURN
      END
```

Subroutine F

```
      SUBROUTINE F(NEQ,T,Y,YDOT)
C This routine is required by LSODE.  See LSODE documentation.
      IMPLICIT REAL*8 (A-H,O-Z)
      CHARACTER CFLGO*4
      DIMENSION Y(NEQ),YDOT(NEQ)
      DIMENSION AMDA(6),B(6)
      DIMENSION TPSW1(35,10),TPSW2(45,6)
      COMMON /TTPSW/ TPSW1,TPSW2
      COMMON /WPGEN/AMDA,B,CFLGO, IFLGC,IFLGS, PI,G, M, EPSIL,GEN,
     >SOURCE, ENRIC, DIN1, DIN2,THCNT, DIUP,DIDW, PL,BL, WW0, WLR,
     >TMP0, HGT0, PDNS0, REF0, DNS0, REACTOT,REACEX, REACFB,PRESS,
     >WMSS, DT,TMST,ZMUO2, HFTCA,BT,TCON,RHODENS,RHOHEIG, RHODOPP,
     >RHOREFL,WCON,REFHGT, PMSS,VOL,THETA,X, DOUT1, DOUT2,SPL,SPS,
     >S, S1, S2, TSTOP, TERA ,POWA,STEA,TOPA, BOTA,TCA,PRESS0,EF0,
     >TQT,WMSN,TWMSS,TOUT,IFLGM,IEDIT, IFLGE, IFLGW, ICNTF,IFTRAP,
     >ICHMS,WMQT,DTMS,VOLST,FRVOL,IFLGD, DELTA,R1,R2,R3,DSW,TMPW ,
     >CREAC,CPW,HFG,IFLGX,YOLD,WMSS0,IFLGB,IFLGA,IFLGU, ZNU,PRSFN,
     >SUBMUL,IDCP,EF20,CMSS
      COMMON /WPM3/AVAEN,AVAENW,EXEN
      COMMON /WPM1/SOR, CPS, SMSS, COEP, VOLI,ALF,U1,U2,QUAL,AIRM,
     >PAIR,PH2O,TAIR1,PAIR1,VV,CCRT
      CALL FWP(NEQ,T,Y,YDOT)
      ICNTF=ICNTF+1
      RETURN
      END
```

Subroutine WPM2DYN

```
      SUBROUTINE WPM2DYN(NEQ,Y)
C This subroutine contains statements executed periodically on
C every communication interval for Model 2.
      IMPLICIT REAL*8 (A-H,O-Z)
      CHARACTER CFLGO*4
      DIMENSION AMDA(6),B(6),Y(NEQ)
      DIMENSION TPSW(35,10)
      COMMON /TTPSW/ TPSW
      COMMON /WPGEN/AMDA,B,CFLGO, IFLGC,IFLGS, PI,G, M, EPSIL,GEN,
     >SOURCE, ENRIC, DIN1, DIN2,THCNT, DIUP,DIDW, PL,BL, WWO, WLR,
     >TMPO, HGTO, PDNSO, REFO, DNSO, REACTOT,REACEX, REACFB,PRESS,
     >WMSS, DT,TMST,ZMUO2, HFTCA,BT,TCON,RHODENS,RHOHEIG, RHODOPP,
     >RHOREFL,WCON,REFHGT, PMSS,VOL,THETA,X, DOUT1, DOUT2,SPL,SPS,
     >S, S1, S2, TSTOP, TERA ,POWA,STEA,TOPA, BOTA,TCA,PRESSO,EFO,
     >TQT,WMSN,TWMSS,TOUT,IFLGM,IEDIT, IFLGE, IFLGW, ICNTF,IFTRAP,
     >ICHMS,WMQT,DTMS,VOLST,FRVOL,IFLGD, DELTA,R1,R2,R3,DSW,TMPW ,
     >CREAC,CPW,HFG,IFLGX,YOLD,WMSSO,IFLGB,IFLGA,IFLGU, ZNU,PRSFN,
     >SUBMUL,IDCP,EF20,CMSS
      COMMON /WPM3/AVAEN,AVAENW,EXEN
      COMMON /MXM/ ZPWMX,ZTMMX,ZNFMX,ZPRMX,ZWMMX,ZQLMX,ZSMMX,
     >            TPWMX,TTMMX,TNFMX,TPRMX,TWMMX,TQLMX,TSMMX
      IICOUNT=0
      DFFO=0.D+0
C Calculate powder temperature using internal energy increase
      IF (IFLGB.EQ.1.AND.IFLGX.NE.2) THEN
      TMPW=(Y(9)/((CPFP(TMPW,ZMUO2)*PMSS)+(((CPFSUB(PRESS,TMPW))
     >*1.D+3)*WMSS)))+TMPO
      TMPW=DMIN1(TMPW,TMST)
      END IF
C
C Output results
C ---#Check if "SUBROUTINE F" is skipped by LSODE;
C     If answer is "YES" then update geometrical and reactivity
C     information.
      IF (IFTRAP.EQ.1) THEN
      IF (ICNTF.EQ.0.AND.TOUT.NE.DT) THEN
      CALL PRDCL(NEQ,Y)
      FRDNS=(RHODENS*((PDNS(TMPW,PDNSO))-DNSO))*BT
      FRHGT=(RHOHEIG*(PL-HGTO))*BT
      FRDPP=(RHODOPP*(TMPW-TMPO))*BT
      FRREF=(RHOREFL*(REFHGT-REFO))*BT
      RHOEX = REWPC(WCON,IFLGU)*BT
      REACEX=RHOEX/BT
      REACFB=(FRDNS+FRHGT+FRDPP+FRREF)/BT
      REACTOT=REACEX+REACFB
      ELSE
      ICNTF=0
      END IF
      END IF
C
C ---#Output results
      IF (IFLGE.EQ.1) THEN
      IF (TOUT.EQ.DT) THEN
      CALL WPOUT(NEQ, 0.D+0,IFLGW, Y, REACTOT, REACEX,REACFB,PRESS,
     >PH2O,PAIR,WMSS,SMSS,TCON,TMPW, CREAC,WMSN,VOLI,CFLGO)
      ELSE
      CALL WPOUT(NEQ,(TOUT-DT),IFLGW,Y,REACTOT,REACEX,REACFB,PRESS,
```

Subroutine WPM2DYN (cont.)

```
     >PH2O,PAIR,WMSS, SMSS,TCON,TMPW ,CREAC,WMSN,VOLI,CFLGO)
      END IF
      ENF IF
C
C Stop water ingress if time is greater that TQT
      IF (TOUT.GT.TQT.AND.IFLGW.EQ.0) THEN
      IFLGW=1
      WLR=0.D+0
      CREAC=REACEX
C ---#Change communication time interval lenght if desired
      IF (ICHMS.GE.1) DT=DT*DTMS
      END IF
C ---#Mass of ingress water
      WNAD=WLR*DT
C ---#Total water mass(including the ingress water)
      WMSN=WNAD+TWMSS
C
C If WNAD>=WMQT, stop water ingress
C               else   , continue adding water if IFLGW=0
      IF (IFLGW.EQ.1) THEN
      TTT=TQT
      ELSE
      TTT=TOUT
      END IF
      IF ((WLR*TTT).GE.WMQT.AND.IFLGW.EQ.0) THEN
      IFLGW=1
      WLR=0.D+0
      TQT=TOUT
      CREAC=REACEX
C ---#Change communication time interval lenght if desired
      IF (ICHMS.GE.1) DT=DT*DTMS
      END IF
C
C If  TMPW < Saturation  temp.  then   use   subcooled  model.
C Subcooled  model  assumes, the  system is under  atmospheric
C pressure and water exists at  a temperature lower  than  its
C saturation temperature.
      UWAT=(Y(9)-(CPFP(TMPW,ZMUO2)*PMSS*(TMPW-TCA)))+EF20
      IF (UWAT.LT.(EF0*WMSN).AND.IFLGX.EQ.0) THEN
      WMSS=WMSN
      CPW = ((CPFSUB(PRESS,TMPW))*1.D+3)
      DSW = DFSUB(PRESS,TMPW)
      TWMSS=WMSS
      RETURN
      ELSEIF (UWAT.GE.(EF0*WMSN).AND.IFLGX.EQ.0) THEN
      IFLGX=1
      CALL INTRPLT1(PRESS,DSLS,DSVS,HFGS,CPLS,VSLS,ZKLS,PRLS,
     >STS,CTES)
      CPW=CPLS
      DSW=DSLS
      YOLD=(EF0*WMSN)+(CPFP(TMPW,ZMUO2)*PMSS*
     >(TSAT(PRESS)-TCA))
      END IF
C (U2-U1)powder+water
      AVAEN=(Y(9)-YOLD)
      IF(AVAEN.LT.0.D+0.AND.IFLGX.LT.2) THEN
      TMPW=(Y(9)/((CPFP(TMPW,ZMUO2)*PMSS)+(((CPFSUB(PRESS,TMPW))
```

Subroutine WPM2DYN (cont.)

```
     >*1.D+3)*WMSS)))+TMPO
      TMPW=DMIN1(TMPW,TMST)
      GO TO 2
      END IF
C ---#
      IF (IFLGX.EQ.1) THEN
C
C Start TH calculations
C ---#(U2-U1)water
      EXEN=AVAEN/HFG
      WMSS=WMSN-EXEN
      IF (WMSS.LT.0.D+0) THEN
      IFLGX=2
      WMSS=WMSN
      TMPW=TMST
      END IF
      END IF
C ---#
      IF (IFLGX.EQ.2) THEN
      ENP=WMSN*HFG
      IF(AVAEN.GE.ENP) THEN
      AVAENW=AVAEN-ENP
      TMPINC=AVAENW/(CPFP(TMPW,ZMUO2)*PMSS)
      TMPW=TMPW+TMPINC
      WMSS=0.D+0
      ELSEIF(AVAEN.LT.ENP) THEN
      WRITE(25,1)
 1    FORMAT(' ERROR(WPM2DYN)....More complex algms. required!')
      STOP
      END IF
      END IF
 2    YOLD=Y(9)
      TWMSS=WMSS
      RETURN
      END
```

Subroutine WPM3DYN

```
      SUBROUTINE WPM3DYN(NEQ,Y)
C This subroutine contains statements executed periodically on
C every communication interval for Model 3.
      IMPLICIT REAL*8 (A-H,O-Z)
      CHARACTER CFLGO*4
      DIMENSION AMDA(6),B(6),Y(NEQ)
      DIMENSION TPSW1(35,10),TPSW2(45,6)
      COMMON /TTPSW/ TPSW1,TPSW2
      COMMON /WPGEN/AMDA,B,CFLGO, IFLGC,IFLGS, PI,G, M, EPSIL,GEN,
     >SOURCE, ENRIC, DIN1, DIN2,THCNT, DIUP,DIDW, PL,BL, WW0, WLR,
     >TMP0, HGT0, PDNS0, REF0, DNS0, REACTOT,REACEX, REACFB,PRESS,
     >WMSS, DT,TMST,ZMUO2, HFTCA,BT,TCON,RHODENS,RHOHEIG, RHODOPP,
     >RHOREFL,WCON,REFHGT, PMSS,VOL,THETA,X, DOUT1, DOUT2,SPL,SPS,
     >S, S1, S2, TSTOP, TERA ,POWA,STEA,TOPA, BOTA,TCA,PRESS0,EF0,
     >TQT,WMSN,TWMSS,TOUT,IFLGM,IEDIT, IFLGE, IFLGW, ICNTF,IFTRAP,
     >ICHMS,WMQT,DTMS,VOLST,FRVOL,IFLGD, DELTA,R1,R2,R3,DSW,TMPW ,
     >CREAC,CPW,HFG,IFLGX,YOLD,WMSS0,IFLGB,IFLGA,IFLGU, ZNU,PRSFN,
     >SUBMUL,IDCP,EF20,CMSS
      COMMON /WPM1/SOR, CPS, SMSS, COEP, VOLI,ALF,U1,U2,QUAL,AIRM,
     >PAIR,PH2O,TAIR1,PAIR1,VV,CCRT
      COMMON /MXM/ ZPWMX,ZTMMX,ZNFMX,ZPRMX,ZWMMX,ZQLMX,ZSMMX,
     >             TPWMX,TTMMX,TNFMX,TPRMX,TWMMX,TQLMX,TSMMX
      IICOUNT=0
      DFF0=0.D+0
C
C Output results
C ---#Check if "SUBROUTINE F" is skipped by LSODE;
C     If answer is "YES" then update geometrical and reactivity
C     information.
      IF (IFTRAP.EQ.1) THEN
      IF (ICNTF.EQ.0.AND.TOUT.NE.DT) THEN
      CALL PRDCL(NEQ,Y)
      FRDNS=(RHODENS*((PDNS(TMPW,PDNS0))-DNS0))*BT
      FRHGT=(RHOHEIG*(PL-HGT0))*BT
      FRDPP=(RHODOPP*(TMPW-TMP0))*BT
      FRREF=(RHOREFL*(REFHGT-REF0))*BT
      RHOEX = REWPC(WCON,IFLGU)*BT
      REACEX=RHOEX/BT
      REACFB=(FRDNS+FRHGT+FRDPP+FRREF)/BT
      REACTOT=REACEX+REACFB
      ELSE
      ICNTF=0
      END IF
      END IF
C
C ---#Output results
      IF (IFLGE.EQ.1) THEN
      IF (TOUT.EQ.DT) THEN
      CALL WPOUT(NEQ, 0.D+0,IFLGW, Y, REACTOT, REACEX,REACFB,PRESS,
     >PH2O,PAIR,WMSS,SMSS,TCON,TMPW, CREAC,WMSN,VOLI,CFLGO)
      ELSE
      CALL WPOUT(NEQ,(TOUT-DT),IFLGW,Y,REACTOT,REACEX,REACFB,PRESS,
     >PH2O,PAIR,WMSS, SMSS,TCON,TMPW ,CREAC,WMSN,VOLI,CFLGO)
      END IF
      END IF
C
C Stop water ingress if time is greater that TQT
```

Subroutine WPM3DYN (cont.)

```
      IF (TOUT.GT.TQT.AND.IFLGW.EQ.0) THEN
      IFLGW=1
      VOLI=VOL
      CREAC=REACEX
C ---#Change communication time interval lenght if desired
      IF (ICHMS.GE.1) DT=DT*DTMS
      END IF
C
C If IFLGW=1, stop water ingress at T = TQT
C         =0, continue adding water
      IF (IFLGW.EQ.1) THEN
      TTT=TQT
      ELSE
      TTT=TOUT
      VOLI=VOL
      END IF
C
C Mass of ingress water
      WNAD=WLR*TTT
C
C If WNAD>=WMQT, stop water ingress
C       else   , continue adding water if IFLGW=0
      IF (WNAD.GE.WMQT.AND.IFLGW.EQ.0) THEN
      IFLGW=1
      TQT=TOUT
      VOLI=VOL
      CREAC=REACEX
C ---#Change communication time interval lenght if desired
      IF (ICHMS.GE.1) DT=DT*DTMS
      END IF
C
C Total water mass(including the ingress water)
      WMSN=WNAD+TWMSS
C
C New specific volume of water
      VV=FRVOL/WMSN
C Start TH calculations
C ---#(U2-U1)powder+air+water
      EINC=(Y(9)-YOLD)
      TOLD=TMST
      TNEW=TMST
      GO TO 89
 88   TNEW=TNEW+(ALF*ABS(X2X-X2Y))
 89   CONTINUE
C
C ---#Energy for powder
      EPOW=PMSS*CPFP(TOLD,ZMUO2)*(TNEW-TOLD)
C ---#Energy for air
      EAIR=AIRM*CVAIR(TOLD)*(TNEW-TOLD)
C ---#Energy for water
      EWAT=EINC-EPOW-EAIR
C ---#U2=EWAT+U1
      U2=U1+EWAT
      UU=U2/WMSN
C ---#Specific internal energy and specific volume of
C     saturated water at TNEW
      CALL INTRPLT2(TNEW,PRSS,SVF,SVG,EIF,EIG)
```

Subroutine WPM3DYN (cont.)

```
      IF (IFLGA.EQ.1) THEN
      SVF=VF(PSAT(TNEW))
      SVG=VG(PSAT(TNEW))
      END IF
      X2X=(UU-EIF)/(EIG-EIF)
      X2Y=(VV-SVF)/(SVG-SVF)
      DFF=ABS(X2X-X2Y)
      IF (DFF.GT.CCRT) THEN
      IICOUNT=IICOUNT+1
      IF (DFF.GE.DFFO) THEN
      ALF=-ALF
      END IF
      DFFO=DFF
      GO TO 88
      END IF
C Finalize the TH calculations for comm. time int.
 90   IF (TNEW.LT.20.D+0) TNEW=20.D+0
      YOLD=Y(9)
C ---#New temperature
      TMST=TNEW
C ---#Partial vapor pressure
      PH2O=PSAT(TMST)
C ---#Density of liquid water
      DSW = DF(PH2O)
C ---#Quality
      QUAL=X2X
C ---#New internal energy
      U1=((((1.D+0)-QUAL)*EIF)+(QUAL*EIG))*WMSN
C ---#Mass of water in vapor phase
      SMSS=QUAL*WMSN
C ---#Mass of water in liquid phase
      WMSS=WMSN-SMSS
C ---#Calculate  new  partial  pressure  of air using
C     ideal gas approximation for air (P2/P1)=(T2/T1)
      PAIR=PAIR1*((TMST+273.15D+0)/TAIR1)
C ---#Total pressure
      PRESS=PH2O+PAIR
      RETURN
      END
```

Subroutine FWP

```
      SUBROUTINE FWP(NEQ,T,Y,YDOT)
C This subroutine  is  the driver routine to analyze the excursion
C characteristics of the  homogeneous damp uranium dioxide powders
C using 0-htc(Model I), inf-htc model(Model II)[vented system]  or
C inf-htc model(Model III)[unvented system] models.
C!!!!!!!!!!!!!!!!!!!!!!!!!!!!!!!!!!!!!!!!!!!!!!!!!!!!!!!!!!!!!!!!!
C!!                                                             !!
C!!                      STATE VARIABLES                        !!
C!!-------------------------------------------------------------!!
C!! Y( 1)= Power                    Y( 2)= # of fissions        !!
C!! Y( 3)= DNP Concentration Gr1  Y( 4)= DNP Concentration Gr2  !!
C!! Y( 5)= DNP Concentration Gr3  Y( 6)= DNP Concentration Gr4  !!
C!! Y( 7)= DNP Concentration Gr5  Y( 8)= DNP Concentration Gr6  !!
C!! Y( 9)= Bulk temperature/Model I ---------]                   !!
C!!                                         ]-----Model II      !!
C!!       Net energy generated/Model III ---]                   !!
C!! Y(10)= Cnt. temperature Nd.1                                !!
C!!                                                             !!
C!!!!!!!!!!!!!!!!!!!!!!!!!!!!!!!!!!!!!!!!!!!!!!!!!!!!!!!!!!!!!!!!!
      IMPLICIT REAL*8 (A-H,O-Z)
      CHARACTER CFLGO*4
      DIMENSION Y(NEQ),YDOT(NEQ),AMDA(6),B(6)
      DIMENSION TPSW1(35,10),TPSW2(45,6)
      COMMON /TTPSW/ TPSW1,TPSW2
      COMMON /WPGEN/AMDA,B,CFLGO, IFLGC,IFLGS, PI,G, M, EPSIL,GEN,
     >SOURCE, ENRIC, DIN1, DIN2,THCNT, DIUP,DIDW, PL,BL, WW0, WLR,
     >TMP0, HGT0, PDNS0, REF0, DNS0, REACTOT,REACEX, REACFB,PRESS,
     >WMSS, DT,TMST,ZMUO2, HFTCA,BT,TCON,RHODENS,RHOHEIG, RHODOPP,
     >RHOREFL,WCON,REFHGT, PMSS,VOL,THETA,X, DOUT1, DOUT2,SPL,SPS,
     >S, S1, S2, TSTOP, TERA ,POWA,STEA,TOPA, BOTA,TCA,PRESS0,EF0,
     >TQT,WMSN,TWMSS,TOUT,IFLGM,IEDIT, IFLGE, IFLGW, ICNTF,IFTRAP,
     >ICHMS,WMQT,DTMS,VOLST,FRVOL,IFLGD, DELTA,R1,R2,R3,DSW,TMPW ,
     >CREAC,CPW,HFG,IFLGX,YOLD,WMSS0,IFLGB,IFLGA,IFLGU, ZNU,PRSFN,
     >SUBMUL,IDCP,EF20,CMSS
      COMMON /WPM3/AVAEN,AVAENW,EXEN
      COMMON /WPM1/SOR, CPS, SMSS, COEP, VOLI,ALF,U1,U2,QUAL,AIRM,
     >PAIR,PH2O,TAIR1,PAIR1,VV,CCRT
C
C Heat generated by fission
      QGEN=EPSIL*Y(1)
C
C Heat loss to air by natural convection
C ---#Cylinder
      IF (IFLGC.GE.1.AND.IFLGC.LE.2) THEN
      HBAR=VCYMB(TCON,TCA,G,BL,DOUT1,IFLGC)
      ELSE IF (IFLGC.EQ.3) THEN
      HBAR=VCYSK(TCON,TCA,G,BL,DOUT1)
C ---#Cone
      ELSE IF (IFLGC.GE.4.AND.IFLGC.LE.6) THEN
      HBAR=VCNWR(TCON,TCA,G,S,THETA,IFLGC)
      END IF
      QFC1=HBAR*(POWA+STEA)*(TCON-TCA)
C ---#Horizontal plate facing upward
      QFC2=TOPA*(HPAUP(TCON,TCA,DIUP,G))*(TCON-TCA)
C ---#Horizontal plate facing downward
      QFC3=BOTA*(HPADW(TCON,TCA,DIDW,G))*(TCON-TCA)
C ---#Total
```

Subroutine FWP (cont.)

```
      QFC=QFC1+QFC2+QFC3
C
C Heat loss to surroundings by radiation
      QRAD = GSTBS(TCON,TCA,EMMC(TCON))
C Heat loss by conduction through the container wall
      QCON = ((TCCNT(TCON)*(POWA+STEA+TOPA+BOTA)*(TCON-TMPW))/DELTA)
C
C Heat gain by water leaking into blender
      IF (TOUT.LE.TQT.AND.(IFLGM.EQ.2.OR.IFLGM.EQ.3)) THEN
      QWIN=WLR*HFTCA
      ELSE
      QWIN=0.D+0
      END IF
C
C Heat balance on powder
      QPW=QWIN+QGEN-QCON
      IF (IFLGM.EQ.1) THEN
C ---#0-htc model
      TTHC=(CPFP(TMPW,ZMUO2)*PMSS)
      ELSEIF (IFLGM.EQ.2.OR.IFLGM.EQ.3) THEN
C ---#inf-htc model
      TTHC=1.D+0
      END IF
      YDOT(9)=(1/TTHC)*QPW
C
C Temperature on the imaginary inner node
      IF (IFLGM.EQ.2) THEN
C ---#inf-htc model(open system)
      IF (IFLGB.EQ.0.AND.IFLGX.NE.2) THEN
      TMPW=(Y(9)/((CPFP(TMPW,ZMUO2)*PMSS)+(((CPFSUB(PRESS,TMPW))
     >*1.D+3)*WMSS)))+TMPO
      TMPW=DMIN1(TMPW,TMST)
      END IF
      ELSEIF (IFLGM.EQ.1) THEN
C ---#0-htc model
      TMPW=Y(9)
      ELSEIF (IFLGM.EQ.3) THEN
C ---#inf-htc model(closed system)
      TMPW=TMST
      END IF
      IF (TMPW.LT.20.D+0) TMPW=20.D+0
C
C Delayed neutron precursor concentrations
      SUM=0.D+0
      DO 10 I=1,6
      YDOT(I+2)=(((B(I)*Y(1))/GEN)-(AMDA(I)*Y(I+2)))
      SUM=SUM+(AMDA(I)*Y(I+2))
 10   CONTINUE
C
C Update the geometric information
      CALL PRDCL(NEQ,Y)
C
C Feedback and external reactivities
      FRDNS=(RHODENS*((PDNS(TMPW,PDNSO))-DNSO))*BT
      FRHGT=(RHOHEIG*(PL-HGTO))*BT
      FRDPP=(RHODOPP*(TMPW-TMPO))*BT
      FRREF=(RHOREFL*(REFHGT-REFO))*BT
```

Subroutine FWP (cont.)

```
      RHOEX = REWPC(WCON,IFLGU)*BT
      REACEX=RHOEX/BT
      REACFB=(FRDNS+FRHGT+FRDPP+FRREF)/BT
      REACTOT=REACEX+REACFB
C
C Power and Integrated fission yield
      YDOT(1)=((RHOEX+FRDPP+FRHGT+FRDNS+FRREF-BT)*(Y(1)/GEN))+
     >SUM+SOURCE
      YDOT(2)=Y(1)
C
C Temperature on the outer surface of the container (Assuming
C 1 mesh point on a slab wall with an infinite height)
C --->Heat balance on container wall
      QCNT=QCON-QFC-QRAD
C --->Temperature of surface node
      YDOT(10)=(1/(SPCNT(TCON)*CMSS))*QCNT
C Temperature on the outer surface of container
      TCON=Y(10)
      IF (TCON.LT.20.D+0) TCON=20.D+0
      RETURN
      END
```

Subroutine PRDCL

```
      SUBROUTINE PRDCL(NEQ,Y)
C This subroutine contains statements executed periodically on
C every integration interval.
      IMPLICIT REAL*8 (A-H,O-Z)
      DIMENSION Y(NEQ),AMDA(6),B(6)
      CHARACTER CFLGO*4
      COMMON /WPGEN/AMDA,B,CFLGO, IFLGC,IFLGS, PI,G, M, EPSIL,GEN,
     >SOURCE, ENRIC, DIN1, DIN2,THCNT, DIUP,DIDW, PL,BL, WWO, WLR,
     >TMPO, HGTO, PDNSO, REFO, DNSO, REACTOT,REACEX, REACFB,PRESS,
     >WMSS, DT,TMST,ZMUO2, HFTCA,BT,TCON,RHODENS,RHOHEIG, RHODOPP,
     >RHOREFL,WCON,REFHGT, PMSS,VOL,THETA,X, DOUT1, DOUT2,SPL,SPS,
     >S, S1, S2, TSTOP, TERA ,POWA,STEA,TOPA, BOTA,TCA,PRESSO,EFO,
     >TQT,WMSN,TWMSS,TOUT,IFLGM,IEDIT, IFLGE, IFLGW, ICNTF,IFTRAP,
     >ICHMS,WMQT,DTMS,VOLST,FRVOL,IFLGD, DELTA,R1,R2,R3,DSW,TMPW ,
     >CREAC,CPW,HFG,IFLGX,YOLD,WMSSO,IFLGB,IFLGA,IFLGU, ZNU,PRSFN,
     >SUBMUL,IDCP,EF20,CMSS
C New geometrical information
C ---#Void fraction
      VOL=PMSS/PDNS(TMPW,PDNSO)
      ZMAXVOL=PMSS/1.097D+4
      ZMXWCON=(1.D+0-(PDNS(TMPW,PDNSO)/1.097D+4))
      VOIDF=ZMXWCON
C ---#Powder height
      IF (IFLGC.GT.0.AND.IFLGC.LE.3) THEN
      CALL FHCYL(VOL,DIN1,DOUT1,BL,PL,POWA,STEA,VOLST,PI)
      ELSE IF (IFLGC.GE.4.AND.IFLGC.LE.6) THEN
      CALL FHCONE(PL,DIN1,DOUT1,DIN2,VOL,THETA,X,
     >THCNT,SPL,SPS,S,S1,S2,TERA,POWA,DIDW,STEA,DIUP,VOLST,BL,PI)
      END IF
      IF (IFLGD.EQ.1) THEN
      FRVOL=(VOL*VOIDF)
      ELSE
      FRVOL=(VOL*VOIDF)+VOLST
      END IF
C Maximum water mass and volume,
C current water volume,
C upper reflector height,
C water content
      ZMXWMSS=ZMXWCON*VOL*DSW
      IF (WMSS.GE.ZMXWMSS) THEN
      ZMXWTV=ZMXWMSS/DSW
      WTV=WMSS/DSW
      REFWTV=WTV-ZMXWTV
      WCON=ZMXWMSS/VOL
      ELSE
      REFWTV=0.D+0
      WCON=WMSS/VOL
      END IF
      COEP=WMSS/ZMXWMSS
C ---#Reflector height
C      IF (IFLGC.GT.0.AND.IFLGC.LE.3) THEN
C      CALL FHCYREF(REFHGT,REFWTV,DIN1,PI)
C      ELSE IF (IFLGC.GE.4.AND.IFLGC.LE.6) THEN
C      CALL FHCNREF(REFHGT,REFID,DIN1,REFWTV,THETA,X,PI)
C      END IF
      RETURN
      END
```

Function HPAUP

```
      FUNCTION HPAUP(TBULK,TCA,DIUP,G)
C This  function  calculates the free convection heat transfer
C coefficient  of  a  heated horizontal surface  facing upward
C and immersed in air  or  other gas.  The below  correlations
C were given by Fisherden and Saunders at 1950.   (V)
      IMPLICIT REAL*8 (A-H,O-Z)
      IF (TBULK.LE.TCA) THEN
      HPAUP=0.D+0
      RETURN
      END IF
      TFILM=((TBULK+TCA)/(2.D+0))
      CALL PRPA(TFILM,DENSA,CPA,CKA,VISCA,COTEA)
      GR=(((DENSA**2.D+0)*G*((0.9D+0*DIUP)**3.D+0)*COTEA*(TBULK-
     >TCA))/(VISCA**2.D+0))
      PR=((VISCA*CPA)/(CKA))
      RA=GR*PR
      IF (RA.LT.8.D+6) THEN
C Laminar flow conditions ---  10+4<N(RA)<10E+7
      AC=0.54D+0
      AN=(1.D+0/4.D+0)
      ELSE IF (RA.GE.8.D+6.AND.RA.LE.1.D+11) THEN
C Turbulent and transition regions ---  8E+6>=N(RA)>1.E+11
      AC=0.15D+0
      AN=(1.D+0/3.D+0)
      ELSE
      WRITE(25,1)
 1    FORMAT(' ERROR(HPAUP)....N(RA) is out of range')
      STOP
      END IF
      ANUB=AC*((GR*PR)**AN)
      HPAUP=(CKA*ANUB)/(0.9D+0*DIUP)
      RETURN
      END
```

Function HPADW

```
      FUNCTION HPADW(TBULK,TCA,DIDW,G)
C This  function  calculates the free convection heat transfer
C coefficient  of  a heated horizontal surface facing downward
C and immersed in air  or  other gas.  The below  correlations
C were given by McAdams at 1954.                        (V)
      IMPLICIT REAL*8 (A-H,O-Z)
      IF (TBULK.LE.TCA) THEN
      HPADW=0.D+0
      RETURN
      END IF
      TFILM=((TBULK+TCA)/(2.D+0))
      CALL PRPA(TFILM,DENSA,CPA,CKA,VISCA,COTEA)
      GR=(((DENSA**2.D+0)*G*((0.9D+0*DIDW)**3.D+0)*COTEA*(TBULK-
     >TCA))/(VISCA**2.D+0))
      PR=((VISCA*CPA)/(CKA))
      RA=GR*PR
      IF (RA.LT.10.D+10) THEN
C Laminar flow conditions ---  10+5<N(RA)<10E+10
      AC=0.27D+0
      AN=(1.D+0/4.D+0)
      ELSE
      WRITE(25,1)
 1    FORMAT(' ERROR(HPADW)....N(RA) is out of range')
      STOP
      END IF
      ANUB=AC*((GR*PR)**AN)
      HPADW=(CKA*ANUB)/(0.9D+0*DIDW)
      RETURN
      END
```

Function VCYMB

```
      FUNCTION VCYMB(TBULK,TCA,G,SL,DOUT1,IFLGC)
C This  function  calculates the free convection heat transfer
C coefficient  of  a  vertical  cylinder  with  large diameter
C immersed in air or other gas.  For vertical cylinders, it is
C generally acceptable  to  use the correlation  for  vertical
C planes,provided the diameter of the cylinder is large enough
C so  that curvature is not a major factor.  (V)
      IMPLICIT REAL*8 (A-H,O-Z)
      IF (TBULK.LE.TCA) THEN
      VCYMB=0.D+0
      RETURN
      END IF
      TFILM=((TBULK+TCA)/(2.D+0))
      CALL PRPA(TFILM,DENSA,CPA,CKA,VISCA,COTEA)
      GR=(((DENSA**2.D+0)*G*(SL**3.D+0)*COTEA*(TBULK-TCA))/
     >(VISCA**2.D+0))
      PR=((VISCA*CPA)/(CKA))
      RA=GR*PR
      IF (IFLGC.EQ.1) THEN
C Churchill and Chu
      AMLT=1.D+0
      ELSEIF (IFLGC.EQ.2) THEN
C Correction factor for cylinders by Minkowycz and Sparrow
      AMLT1=((SL/(DOUT1*(GR**(1.D+0/4.D+0))))**9.D-1)
      AMLT=(1.D+0+(1.43D+0*AMLT1))
      END IF
      IF (RA.LT.1.D+9) THEN
C Sparrow  and  Gregg obtained  the following criterion for Pr
C values  of 0.72 and 1.00 for  a  difference in heat transfer
C of less than 5% from the flat plate solution.
      HLFG=35.D+0/(GR**(1.D+0/4.D+0))
      IF ((DOUT1/SL).LT.HLFG) THEN
      WRITE(25,1)
 1    FORMAT(1H0,' ERROR(VCYHW)....D/L ratio is out of range')
      STOP
      END IF
C Laminar flow conditions ---  N(GR)*N(PR)<10E+9
      A1=0.68D+0
      A2=0.670D+0
      A3=0.492D+0
      AN1=(1.D+0/4.D+0)
      AN2=(9.D+0/16.D+0)
      AN3=(4.D+0/9.D+0)
      AN4=1.D+0
C      ELSE IF (RA.GE.1.D+9.AND.RA.LT.1.D+12) THEN
      ELSE IF (RA.GE.1.D+9) THEN
C Turbulent and transition regions ---  10E+9>=N(GR)*N(PR)>1.E+12
C For transition region, correlation for turbulent region is used
C as an approximate,(somewhat less accurate).
      A1=0.825D+0
      A2=0.387D+0
      A3=0.492D+0
      AN1=(1.D+0/6.D+0)
      AN2=(9.D+0/16.D+0)
      AN3=(8.D+0/27.D+0)
      AN4=2.D+0
      ELSE
```

Function VCYMB (cont.)

```
      WRITE(25,2)
2     FORMAT(1H0,' ERROR(VCYHW)....N(RA) is out of range')
      STOP
      END IF
      ANUP1=A2*(RA**AN1)
      ANUP2=(1.D+0+((A3/PR)**AN2))**AN3
      ANU=((A1+(ANUP1/ANUP2))**AN4)*AMLT
      VCYMB=(CKA*ANU)/SL
      RETURN
      END
```

Function VCYSK

```
      FUNCTION VCYSK(TBULK,TCA,G,SL,DOUT1)
C This function calculates the laminar natural convection heat
C transfer coefficient over vertical cylinders immersed in air or
C other gas. Expression for the Nusselt number is derived for
C cylinders where D/L ratio is not large enough to ignore the
C effect of curvature and are given by Lefevre and Ede.   (V)
      IMPLICIT REAL*8 (A-H,O-Z)
      IF (TBULK.LE.TCA) THEN
      VCYSK=0.D+0
      RETURN
      END IF
      TFILM=((TBULK+TCA)/(2.D+0))
      CALL PRPA(TFILM,DENSA,CPA,CKA,VISCA,COTEA)
      GR=(((DENSA**2.D+0)*G*(SL**3.D+0)*COTEA*(TBULK-TCA))/
     >(VISCA**2.D+0))
      PR=((VISCA*CPA)/(CKA))
      RA=GR*PR
C       IF (RA.LT.1.D+9) THEN
      IF (RA.LT.1.D+12) THEN
      FCTERM1=((4.D+0*CKA)/(3.D+0*SL))*(((7.D+0*GR*(PR**2.D+0))/
     >(5.D+0*(20.D+0+(21.D+0*PR))))**2.5D-1)
      FCTERM2=((4.D+0*(2.72D+2+(3.15D+2*PR))*CKA)/(3.5D+1*
     >(6.4D+1+(6.3D+1*PR))*DOUT1))
      VCYSK=(FCTERM1+FCTERM2)
      ELSE
      WRITE(25,1)
 1    FORMAT(1H0,' ERROR(VCYSK)....Flow is not laminar')
      STOP
      END IF
      RETURN
      END
```

Function VCNWR

```
      FUNCTION VCNWR(TBULK,TCA,G,S1,THETA,IFLGC)
C This function calculates the natural convection heat transfer
C coefficient from  the sides of a cone. Equation  for  average
C Nusselt  number was predicted  by Kuiken  and  modified using
C the measurements of Oosthuizen and Donaldson   by   Rohsenow,
C Hartnett and Ganic. The verification data  were  obtained for
C air for  2E+7<RA<4E+8 and 1.75deg<THETA<5.75deg.  (V)
      IMPLICIT REAL*8 (A-H,O-Z)
      IF (TBULK.LE.TCA) THEN
      VCNWR=0.D+0
      RETURN
      END IF
      TFILM=((TBULK+TCA)/(2.D+0))
      CALL PRPA(TFILM,DENSA,CPA,CKA,VISCA,COTEA)
      PR=((VISCA*CPA)/(CKA))
      GR=(((DENSA**2.D+0)*G*(S1**3.D+0)*(COS(THETA))*COTEA*
     >(TBULK-TCA))/(VISCA**2.D+0))
      RA=GR*PR
      IF (RA.LT.1.D+9) THEN
      IF (IFLGC.EQ.4) THEN
C Kuiken
      CON1=0.564D+0
      CON2=0.412D+0
      CON3=0.020D+0
      EPS=(2.D+0/(((RA**(1.D+0/4.D+0))*TAN(THETA))))
      MULTP=(RA**(1.D+0/4.D+0))
      ELSE IF(IFLGC.EQ.5) THEN
C Oosthuizen and Donaldson
      CON1=0.63D+0
      CON2=0.4536D+0
      CON3=0.D+0
      EPS=(2.D+0/(((GR**(1.D+0/4.D+0))*TAN(THETA))))
      MULTP=(GR**(1.D+0/4.D+0))
      ELSE IF(IFLGC.EQ.6) THEN
C Rohsenow, Hartnett and Ganic
      CON1=0.69D+0
      CON2=0.412D+0
      CON3=0.02D+0
      EPS=(2.D+0/(((RA**(1.D+0/4.D+0))*TAN(THETA))))
      MULTP=(RA**(1.D+0/4.D+0))
      END IF
      ANUL=(((CON1)+(CON2*EPS)+(CON3*(EPS**2.D+0)))*MULTP)
      VCNWR=(CKA/S1)*ANUL
      RETURN
      ELSE IF (RA.GE.1.D+9.AND.RA.LT.1.D+12) THEN
C Prandtl number dependent Ctv contants. The following function is
C valid only for gases ( 0.1 > PR > 1.0 ).
      IF (PR.GE.0.1D+0.AND.PR.LE.1.0D+0) THEN
      CTV=((-0.0395076D+0*(PR**2.D+0))+(0.077902D+0*PR)+(0.067604D+0))
      ELSE
      WRITE(25,1)
 1    FORMAT(' ERROR(VCNWR)....Invalid N(PR) for air.')
      STOP
      END IF
C For fully turbulent heat transport, the Condition-Layer approximate
C predicts  the  following for heat transfer coefficient. ( The below
C equation is assumed to be valid also in the transition region )
```

Function VCNWR (cont.)

```
      ANUT=CTV*(RA**(1.D+0/3.D+0))
      VCNWR=(CKA/S1)*ANUT
      RETURN
      ELSE
      WRITE(25,2)
2     FORMAT(' ERROR(VCNWR)....N(RA) is out of range.')
      STOP
      END IF
      RETURN
      END
```

Subroutine WPINTGEN

```
      SUBROUTINE WPINTGEN(NEQ,Y)
C This subroutine  conducts the initial calculations.
      IMPLICIT REAL*8 (A-H,O-Z)
      DIMENSION AMDA(6),B(6),Y(NEQ)
      CHARACTER CFLGO*4
      COMMON /WPGEN/AMDA,B,CFLGO, IFLGC,IFLGS, PI,G, M, EPSIL,GEN,
     >SOURCE, ENRIC, DIN1, DIN2,THCNT, DIUP,DIDW, PL,BL, WW0, WLR,
     >TMP0, HGT0, PDNS0, REF0, DNS0, REACTOT,REACEX, REACFB,PRESS,
     >WMSS, DT,TMST,ZMUO2, HFTCA,BT,TCON,RHODENS,RHOHEIG, RHODOPP,
     >RHOREFL,WCON,REFHGT, PMSS,VOL,THETA,X, DOUT1, DOUT2,SPL,SPS,
     >S, S1, S2, TSTOP, TERA ,POWA,STEA,TOPA, BOTA,TCA,PRESS0,EF0,
     >TQT,WMSN,TWMSS,TOUT,IFLGM,IEDIT, IFLGE, IFLGW, ICNTF,IFTRAP,
     >ICHMS,WMQT,DTMS,VOLST,FRVOL,IFLGD, DELTA,R1,R2,R3,DSW,TMPW ,
     >CREAC,CPW,HFG,IFLGX,YOLD,WMSS0,IFLGB,IFLGA,IFLGU, ZNU,PRSFN,
     >SUBMUL,IDCP,EF20,CMSS
      COMMON /WPM3/AVAEN,AVAENW,EXEN
      COMMON /WPM1/SOR, CPS, SMSS, COEP, VOLI,ALF,U1,U2,QUAL,AIRM,
     >PAIR,PH2O,TAIR1,PAIR1,VV,CCRT
C
C Calculate uranium dioxide atomic mass given its enrichment
      ZMU=(ENRIC*2.350439D+2)+((1-ENRIC)*2.380508D+2)
      ZMUO2=ZMU+(2.0D+0*15.9994D+0)
C
C Cone inclined angle, container mass, initial
C damp powder and container volume.(GEOMETRIC CALCULATIONS)
      DOUT1=DIN1+(2.D+0*THCNT)
      DOUT2=DIN2+(2.D+0*THCNT)
      DIUPB=DIUP-(2.D+0*THCNT)
      DIDWB=DIDW-(2.D+0*THCNT)
      DELTA=THCNT
      IF (IFLGC.GE.4.AND.IFLGC.LE.6) THEN
C ==========
C I        I
C I  CONE  I
C I        I
C ==========
      X=(DOUT2/(DOUT1-DOUT2))*PL
      S2=SQRT((X**2.D+0)+((DOUT2/2.D+0)**2.D+0))
      S1=SQRT(((X+PL)**2.D+0)+((DOUT1/2.D+0)**2.D+0))
      S =SQRT(((X+BL)**2.D+0)+((DIUP/2.D+0)**2.D+0))
      SPL=S1-S2
      SPS=S -S1
      THETA=ATAN((DOUT1/2.D+0)/(PL+X))
C Volume including container (up to powder level)
      VOLT=(1.D+0/3.D+0)*PI*PL*(((DOUT2/2.D+0)**2.D+0)+
     >(DOUT2*DOUT1/4.D+0)+((DOUT1/2.D+0)**2.D+0))
C Volume excluding container (up to powder level)
      VOL=(1.D+0/3.D+0)*PI*PL*(((DIN2/2.D+0)**2.D+0)+
     >(DIN2*DIN1/4.D+0)+((DIN1/2.D+0)**2.D+0))
C Volume of the upper void space
      VOLST=(1.D+0/3.D+0)*PI*(BL-PL)*(((DIUPB/2.D+0)**2.D+0)+
     >(DIUPB*DIN1/4.D+0)+((DIN1/2.D+0)**2.D+0))
C Total volume of blender
      VOLGR=(1.D+0/3.D+0)*PI*BL*(((DIUPB/2.D+0)**2.D+0)+
     >((DIUPB/2.D+0)*(DIDWB/2.D+0))+((DIDWB/2.D+0)**2.D+0))
C Approximate total surface area of blender
      TOPA=(((DIUP/2.D+0)**2.D+0)*PI)
```

Subroutine WPINTGEN (cont.)

```
      BOTA=(((DIDW/2.D+0)**2.D+0)*PI)
      POWA=(PI*((DOUT1/2.D+0)+(DIDW/2.D+0))*SPL)
      STEA=(PI*((DIUP/2.D+0)+(DOUT1/2.D+0))*SPS)
      TERA=(((DIN1/2.D+0)**2.D+0)*PI)
      RMEFF=((VOLGR/(PI*BL))**(1.D+0/2.D+0))
      R1=RMEFF+DELTA
      R2=0.D+0
      R3=0.D+0
      ELSE IF (IFLGC.GT.0.AND.IFLGC.LE.3) THEN
C ==============
C I            I
C I  CYLINDER  I
C I            I
C ==============
      VOLT=(PI*((DOUT1/2.D+0)**2.D+0)*PL)
      VOL=(PI*((DIN1/2.D+0)**2.D+0)*PL)
      VOLST=(PI*((DIN1/2.D+0)**2.D+0)*(BL-PL))
      VOLGR=(PI*((DIUPB/2.D+0)**2.D+0)*BL)
      TOPA=(((DIUP/2.D+0)**2.D+0)*PI)
      BOTA=(((DIDW/2.D+0)**2.D+0)*PI)
      POWA=(PI*DOUT1*PL)
      STEA=(PI*DOUT1*(BL-PL))
      TERA=(((DIN1/2.D+0)**2.D+0)*PL)
      R1=(DIN1/2.D+0)
      R2=(DIN1/2.D+0)+DELTA
      R3=(DIN1/2.D+0)+(DELTA*2.D+0)
      END IF
C
C Container(SS304) volume and mass
      VOLCNT=(VOLT-VOL)+(TOPA*THCNT)+(BOTA*THCNT)
      CMSS=VOLCNT*DNSCNT(TMPE)
C
C Net energy generated or temperature at t=0
      IF (IFLGM.EQ.2.OR.IFLGM.EQ.3) THEN
      Y(9)=0.D+0
      ELSEIF (IFLGM.EQ.1) THEN
      Y(9)=TMP0
      END IF
C
C Bulk temperature
      TMPW=TMP0
C
C Free convection correlation consistency check
      CALL PRPA(20.D+0,DENSA,CPA,CKA,VISKA,COTEA)
      IF (IFLGC.GE.4.AND.IFLGC.LE.6) XX=S
      IF (IFLGC.GT.0.AND.IFLGC.LE.3) XX=BL
      PR=((VISKA*CPA)/(CKA))
      GR=(((DENSA**2.D+0)*G*(XX**3.D+0)*COTEA*((TMPW+10.D+0)-TCA))/
     >(VISKA**2.D+0))
      RA=GR*PR
      IF (DIN1.EQ.DIN2.AND.DOUT1.EQ.DOUT2) THEN
      CHKL=DOUT1/BL
      CHKR1=(35.D+0/(GR**(1.D+0/4.D+0)))
      CHKR2=(38.D+0/(GR**(1.D+0/4.D+0)))
      IF (IFLGC.GE.4.AND.IFLGC.LE.6) THEN
      WRITE(25,1)
1     FORMAT(1H0,' ERROR(WPINTGEN)....Wrong correlation for cylinder')
```

Subroutine WPINTGEN (cont.)

```
      STOP
      END IF
      IF (IFLGC.EQ.1.AND.CHKL.LT.CHKR1) THEN
      WRITE(26,2)
2     FORMAT(1H0,' WARNING(WPINTGEN)....Cyl. dimensions out of range')
      ELSE IF (IFLGC.EQ.2.AND.CHKL.LT.CHKR2) THEN
      WRITE(26,2)
      ELSE IF (IFLGC.EQ.3.AND.CHKL.GE.CHKR1) THEN
      WRITE(26,2)
      END IF
      ELSE IF (DIN1.GT.DIN2.AND.DOUT1.GT.DOUT2) THEN
      IF (IFLGC.GT.0.AND.IFLGC.LE.3) THEN
      WRITE(25,3)
3     FORMAT(' ERROR(WPINTGEN)....Wrong correlation for cone')
      STOP
      END IF
      ELSE
      WRITE(25,4)
4     FORMAT(' ERROR(WPINTGEN)....Invalid geometry input')
      END IF
      IF (PL.GT.BL) THEN
      WRITE(25,5)
5     FORMAT(' ERROR(WPINTGEN)....Powder level > Container heigth')
      STOP
      END IF
C
C Initialize
C ---#Mass of water(liquid+vapor)
      TWMSS=WW0*VOL
C ---#Initial mass of water(liquid+vapor)
      WMSS0=WW0*VOL
C ---#Powder mass
      PMSS=(PDNS(TMP0,PDNS0))*VOL
C
C Power, and fission yield at t=0
      Y(1)=(((PRSFN/ZNU)*1.D+1)*(2.02D+2*1.602D-13))*PMSS*SUBMUL
      Y(2)=0.D+0
C
C Initial delayed neutron precursor concentrations
      DO 10 I=1,M
      BT=BT+B(I)
      Y(I+2)=B(I)*Y(1)/AMDA(I)/GEN
 10   CONTINUE
C ---#Water ingress rate corresponding to a reactivity
C     addition rate
      WLR=RECIT(WLR,VOL,IFLGU)
C ---#Total pressure
      PRESS=PRESS0
C ---#Void fraction
      ZMAXVOL=PMSS/1.097D+4
      ZMXWCON=(1.D+0-(PDNS(TMP0,PDNS0)/1.097D+4))
      VOIDF=ZMXWCON
C ---#Reflector height
      REFHGT=REF0
C ---#Flags
      IFLGW=0
      IFLGE=1
```

Subroutine WPINTGEN (cont.)

```
      ICNTF=0
      IFLGX=0
C ---#Container outer surface temperature
      TCON=TMPO
C
C inf-htc model(closed system)
      IF (IFLGM.EQ.3) THEN
C ---#Density of liquid water
      DSW = DF(PSAT(TCA))
C ---#Initial water mass
      WMSN=TWMSS
C ---#Initial volume
      VOLI=VOL
C ---#Saturation temperature
      TMST=TCA
C ---#Partial vapor pressure
      PH2O=PSAT(TCA)
C ---#Partial air pressure
      PAIR=PRESS-PH2O
      PAIR1=PAIR
      TAIR1=(TCA+273.15D+0)
C ---#Free volume
      IF (IFLGD.EQ.1) THEN
      FRVOL=(VOL*VOIDF)
      ELSE
      FRVOL=(VOL*VOIDF)+VOLST
      END IF
C ---#Specific volume of water
C     (Constant specific volume process)
      VV=FRVOL/WMSN
C ---#Quality
C --- ---#Specific internal energy and specific volume of
C        saturated water at TCA
         CALL INTRPLT2(TCA,PRSS,SVF,SVG,EIF,EIG)
      IF (IFLGA.EQ.1) THEN
      SVF=VF(PSAT(TCA))
      SVG=VG(PSAT(TCA))
      END IF
         QUAL=(VV-SVF)/(SVG-SVF)
C ---#Mass of water in vapor phase
      SMSS=QUAL*WMSN
C ---#Mass of water in liquid phase
      WMSS=WMSN-SMSS
C ---#Mass of air(using the ideal gas approximation;pV=nRT)
C     Equivalent molecular weight for air = 28.97 kg/kg-mol
C     The gas constant for air
      TGCA =((8.31441D+3)/(2.897D+1))
      AIRM=(((PAIR*1.D+6)*(FRVOL))/(TGCA*(TCA+273.15D+0)))
C ---#Initial internal energy
      U1=((((1.D+0)-QUAL)*EIF)+(QUAL*EIG))*WMSN
      YOLD=0.D+0
C
C inf-htc model(open system)
      ELSEIF (IFLGM.EQ.2) THEN
C ---#Initial water mass
      WMSN=TWMSS
C ---#Mass of water in liquid phase
```

```
      WMSS=TWMSS
C ---#Mass of water in vapor phase
      SMSS=0.D+0
C ---#Quality
      QUAL=0.D+0
C ---#Initial volume
      VOLI=VOL
C ---#Saturation temperature
      TMST=TSAT(PRESS)
C ---#Initial properties of subcooled water
      CALL INTRPLT1(PRESS,DSLS,DSVS,HFGS,CPLS,VSLS,ZKLS,PRLS,
     >STS,CTES)
      HFG=HFGS
      CPW = ((CPFSUB(PRESS,TMPW))*1.D+3)
      DSW = DFSUB(PRESS,TMPW)
      YOLD=EF0
C
C 0-htc model
      ELSEIF (IFLGM.EQ.1) THEN
C ---#Mass of water in liquid phase
      WMSS=TWMSS
C ---#Density of liquid water
      DSW = DF(PSAT(TCA))
      END IF
C ---#Water content
      WCON=WMSS/VOL
C ---#External reactivity
      REACEX=REWPC(WCON,IFLGU)
C ---#Feedback reactivity
      REACFB=0.D+0
C ---#Total reactivity(Since feedback reactivity is zero)
      REACTOT=REACEX
C ---#Water mass if porous body is fully water saturated
      ZMXWMSS=ZMXWCON*VOL*DSW
      RETURN
      END
```

Function TCCNT

```
      FUNCTION TCCNT(TMPE)
C This subroutine calculates the specific heat of SS304(Annealed)
C given its temperature.  (Limited to the temperature range   21-
C 871 degrees celcius)
      IMPLICIT REAL*8 (A-H,O-Z)
      IF (TMPE.LT.2.1D+1) THEN
      TR=2.1D+1
      ELSEIF (TMPE.GT.8.71D+2) THEN
      TR=8.71D+2
      ELSE
      TR=TMPE
      END IF
      TCCNT= (( 8.168027D+0 )+
     >        ( 5.845912D-3 *((1.8D+0*TR)+32.D+0))+
     >        (-1.095476D-6 *(((1.8D+0*TR)+32.D+0)**2.D+0))+
     >        ( 2.469959D-10*(((1.8D+0*TR)+32.D+0)**3.D+0))
     >)*1.729577D+0
      RETURN
      END
```

Function SPCNT

```
      FUNCTION SPCNT(TMPE)
C This subroutine calculates the specific heat of SS304(Annealed)
C given its temperature. (Limited to the temperature range   21-
C 871 degrees celcius)
      IMPLICIT REAL*8 (A-H,O-Z)
      IF (TMPE.LT.2.1D+1) THEN
      TR=2.1D+1
      ELSEIF (TMPE.GT.8.71D+2) THEN
      TR=8.71D+2
      ELSE
      TR=TMPE
      END IF
      SPCNT= (( 1.102380D-1 )+
     >        ( 5.750184D-5 *((1.8D+0*TR)+32.D+0))+
     >        (-4.189060D-8 *(((1.8D+0*TR)+32.D+0)**2.D+0))+
     >        ( 1.369815D-11*(((1.8D+0*TR)+32.D+0)**3.D+0))
     >)*4.186800D+3
      RETURN
      END
```

Function DNSCNT

```
      FUNCTION DNSCNT(TMPE)
C This subroutine calculates  the  density of  SS304(Annealed)
C given its temperature. (Limited to the temperature range 38-
C 816 degrees celcius)
      IMPLICIT REAL*8 (A-H,O-Z)
      IF (TMPE.LT.3.8D+1) THEN
      TR=3.8D+1
      ELSEIF (TMPE.GT.8.16D+2) THEN
      TR=8.16D+2
      ELSE
      TR=TMPE
      END IF
      DNSCNT=((-1.603769D-2*((1.8D+0*TR)+32.D+0))+
     >5.025447D+2)*1.601846D-2*1.D+3
      RETURN
      END
```

Function PRPA

```
      SUBROUTINE PRPA(TMPE,DENSA,CPA,CKA,VISKA,COTEA)
C This subroutine calculates the density,specific heat,thermal
C conductivity, viscosity and coefficient of thermal expansion
C for air at atmospheric pressure for a given temperature.
C Tmin = -23.0 C, Tmax = 1027.0 C          (V)
      IMPLICIT REAL*8 (A-H,O-Z)
      IF (TMPE.LT.-2.3D+1) THEN
      TR=2.5015D+2
      ELSEIF (TMPE.GT.1.027D+3) THEN
      TR=1.30015D+3
      ELSE
      TR=TMPE+2.7315D+2
      END IF
C Density
      DENSA=((6.32611D-18*(TR**6.D+0))+(-3.35972D-14*(TR**5.D+0))+
     >(7.35676D-11*(TR**4.D+0))+(-8.57601D-8*(TR**3.D+0))+
     >(5.7247D-5*(TR**2.D+0))+(-2.1793D-2*TR)+(4.36348D+0))
C Specific heat
      CPA=((2.40236D-13*(TR**4.D+0))+(-9.60387D-10*(TR**3.D+0))+
     >(1.31534D-6*(TR**2.D+0))+(-5.19672D-4*TR)+(1.0656D+0))
C Thermal conductivity
      CKA=((-1.37853D-14*(TR**4.D+0))+(4.16364D-11*(TR**3.D+0))+
     >(-5.9969D-8*(TR**2.D+0))+(9.83911D-5*TR)+(9.45229D-4))
C Viscosity
      VISKA=(((-5.26671D-13*(TR**4.D+0))+(2.45986D-9*(TR**3.D+0))+
     >(-4.8643D-6*(TR**2.D+0))+(6.97124D-3*TR)+(1.35554D-1))*
     >1.D-5)
C Coefficient of thermal expansion
      COTEA=((7.71607D-15*(TR**4.D+0))+(-2.93729D-11*(TR**3.D+0))+
     >(4.22333D-8*(TR**2.D+0))+(-2.84058D-5*TR)+(8.8277D-3))
      RETURN
      END
```

Function DFSUB

```
      FUNCTION DFSUB(P,TMPE)
C This function calculates the density of light water
C in the subcooled liquid phase.   (V)
      IMPLICIT REAL*8 (A-H,O-Z)
      PS=PSAT(TMPE)
      PP=P
      TT=TMPE
      IF (P.LT.PS) THEN
      WRITE(25,1)
1     FORMAT(' ERROR(DFSUB)....Pressure less than saturation')
      STOP
      ELSEIF (P.GT.1.8D+1) THEN
      WRITE(25,2)
2     FORMAT(' ERROR(DFSUB)....Pressure greater than 18 MPa')
      STOP
      ELSEIF (TMPE.LT.0.D+0) THEN
      WRITE(25,3)
3     FORMAT(' ERROR(DFSUB)....Temperature less than 0 C')
      STOP
      ELSEIF (TMPE.LT.9.179D+1) THEN
      IF (TMPE.GE.0.D+0.AND.TMPE.LT.5.0D+1) THEN
      EQ1=((8.86359D-7*(PP**2.D+0))+(-5.08685D-4*PP)+(1.00019D+0))
      EQ2=((5.07715D-7*(PP**2.D+0))+(-4.50192D-4*PP)+(1.01214D+0))
      DFSUB=(1.D+0/(EQ1+(((TMPE)*(EQ2-EQ1))/(5.0D+1))))*1.D+3
      RETURN
      ELSEIF (TMPE.GE.5.0D+1.AND.TMPE.LT.1.D+2) THEN
      EQ2=((5.07715D-7*(PP**2.D+0))+(-4.50192D-4*PP)+(1.01214D+0))
      EQ3=((7.2989D-7*(PP**2.D+0))+(-5.11773D-4*PP)+(1.04358D+0))
      DFSUB=(1.D+0/(EQ2+(((TMPE-5.0D+1)*(EQ3-EQ2))/(5.0D+1))))*1.D+3
      RETURN
      ENDIF
      ELSEIF (TMPE.GT.357.03D+0) THEN
      WRITE(25,4)
4     FORMAT(' ERROR(DFSUB)....Temperature greater than 357.03 C')
      ENDIF
      DFSUB = DF(PS) + ( 170.0D+0 / (375.0D+0-TT) - 0.2D+0) * ( PP-PS )
      RETURN
      END
```

Function CPF

```
      FUNCTION CPF(P)
C This function calculates the specific heat of light water
C for a given pressure.       (V)
      IMPLICIT REAL*8 (A-H,O-Z)
      IF (P.LT.3.D-2) THEN
      WRITE(25,1)
1     FORMAT(' ERROR(CPF)....Pressure less than 0.03 MPa')
      STOP
      ELSEIF (P.GT.2.15D+1) THEN
      WRITE(25,2)
2     FORMAT(' ERROR(CPF)....Pressure greater than 21.5 MPa')
      STOP
      ELSEIF (P.GE.3.0D-2.AND.P.LE.6.71D-1) THEN
      CPF=2.47763D-1* P**5.704026D-1 +4.150D+0
      RETURN
      ELSEIF (P.GT.6.71D-1.AND.P.LE.2.606D+0) THEN
      CPF=1.795305D-1* P**8.967323D-1 +4.223D+0
      RETURN
      ELSEIF (P.GT.2.606D+0.AND.P.LE.6.489D+0) THEN
      CPF=9.359843D-2* P**1.239114D+0 +4.340D+0
      RETURN
      ELSEIF (P.GT.6.489D+0.AND.P.LE.1.1009D+1) THEN
      CPF=1.068888D-2* P**2.11376D+0 +4.740D+0
      RETURN
      ELSEIF (P.GT.1.1009D+1.AND.P.LE.1.4946D+1) THEN
      CPF=1.333058D-4* P**3.707294D+0 +5.480D+0
      RETURN
      ELSEIF (P.GT.1.4946D+1.AND.P.LE.1.8079D+1) THEN
      CPF=6.635658D-3* (P -1.0D+1)**3.223323D+0 +7.350D+0
      RETURN
      ELSE
      CPF= 4.6844786D-6*EXP(7.396875D-1*P) +1.0020D+1
      RETURN
      ENDIF
      RETURN
      END
```

Function CPFSUB

```
      FUNCTION CPFSUB(P,TMPE)
C This function calculates the heat capacity of light water
C in the subcooled liquid phase.  (V)
      IMPLICIT REAL*8 (A-H,O-Z)
      PS=PSAT(TMPE)
      PP=P
      TT=TMPE
      IF (P.LT.PS) THEN
      WRITE(25,1)
1     FORMAT(' ERROR(CPFSUB)....Pressure less than saturation')
      STOP
      ELSEIF (P.GT.1.8D+1) THEN
      WRITE(25,2)
2     FORMAT(' ERROR(CPFSUB)....Pressure greater than 18 MPa')
      STOP
      ELSEIF (TMPE.LT.0.D+0) THEN
      WRITE(25,3)
3     FORMAT(' ERROR(CPFSUB)....Temperature less than 0 deg C')
      STOP
      ELSEIF (TMPE.GT.3.5703D+2) THEN
      WRITE(25,4)
4     FORMAT(' ERROR(CPFSUB)....Temperature greater than 357.03 C')
      STOP
      ELSEIF (TMPE.LT.8.996D+1) THEN
      IF (TMPE.GE.0.D+0.AND.TMPE.LT.5.0D+1) THEN
      EQ1=((1.98473D-5*(PP**2.D+0))+(-5.40098D-3*PP)+(4.2174D+0))
      EQ2=((6.96083D-6*(PP**2.D+0))+(-2.34797D-3*PP)+(4.18119D+0))
      CPFSUB=EQ1+(((TMPE)*(EQ2-EQ1))/(5.0D+1))
      RETURN
      ELSEIF (TMPE.GE.5.0D+1.AND.TMPE.LT.1.D+2) THEN
      EQ2=((6.96083D-6*(PP**2.D+0))+(-2.34797D-3*PP)+(4.18119D+0))
      EQ3=((5.85375D-6*(PP**2.D+0))+(-2.25463D-3*PP)+(4.21585D+0))
      CPFSUB=EQ2+(((TMPE-5.0D+1)*(EQ3-EQ2))/(5.0D+1))
      RETURN
      ENDIF
      ENDIF
      CPFSUB = CPF(PS) + (1.8D-3-7.6D+1/(3.64D+2-TT)**1.8D+0)
     >*(PP-PS)
      RETURN
      END
```

Function CVAIR

```
      FUNCTION CVAIR(TMPE)
C This function calculates the heat capacity of air at constant
C volume(Cv) given its temperature and pressure. The  following
C computer  equations  are given  by T.F.Irvine,Jr., P.E.Liley.
C         Temperature  range  250 <= T <= 2000 deg K.
C       Maximum  absolute difference Cp=0.25%, Cv=0.31%
C       Average  absolute difference Cp=0.13%, Cv=0.17%
      IMPLICIT REAL*8 (A-H,O-Z)
      IF (TMPE.LT.-2.315D+1) THEN
      TR=2.5D+2
      ELSEIF (TMPE.GT.1.72685D+3) THEN
      TR=2.0D+3
      ELSE
      TR=TMPE+(2.7315D+2)
      END IF
      CPAIR=((0.103409D+1)+(-0.2848870D-3*TR)+
     >(0.7816818D-6*(TR**2.D+0))+(-0.4970786D-9*(TR**3.D+0))+
     >(0.1077024D-12*(TR**4.D+0)))
      CVAIR=((CPAIR-0.287040D+0)*(1.D+3))
      RETURN
      END
```

Function CPFP

```
      FUNCTION CPFP(TMPE,ZMUO2)
C This function calculates the heat capacity of uranium
C dioxide powder given its temperature and atomic mass. (V)
      IMPLICIT REAL*8 (A-H,O-Z)
      IF (TMPE.LT.2.5D+1) THEN
      TT=2.5D+1
      ELSEIF (TMPE.GT.1.227D+3) THEN
      TT=1.227D+3
      ELSEIF (TMPE.GE.2.5D+1.AND.TMPE.LE.1.227D+3) THEN
      TT=TMPE
      END IF
      CPFP=(19.2D+0+((1.62D+0/1.D+3)*(TT+2.7315D+2))-
     >((3.96D+0/1.D-5)/((TT+2.7315D+2)**2.D+0)))*(1.D+3/
     >ZMUO2)*(4.186D+0)
      RETURN
      END
```

Function PDNS

```
      FUNCTION PDNS(TMPE,PDNS0)
C This function calculates the density of stoichiometric uranium
C dioxide given its temperature and density at 0 deg C.     (V)
      IMPLICIT REAL*8 (A-H,O-Z)
      IF (TMPE.LT.0.D+0) THEN
      TT=0.D+0
      ELSEIF (TMPE.GT.2.846D+3) THEN
      TT=2.846D+3
      ELSEIF (TMPE.GE.0.D+0.AND.TMPE.LE.2.846D+3) THEN
      TT=TMPE
      END IF
      PDNS=(PDNS0/(1.D+0+(2.04D-5*TT)+(8.7D-9*(TT**2.D+0))))
      RETURN
      END
```

Function VF

```
      FUNCTION VF(P)
C This function calculates the specific volume of light water
C in the liquid phase at saturation for a given pressure.
C Pmin = 0.002, Pmax = 21.5 MPa       (V)
      IMPLICIT REAL*8 (A-H,O-Z)
      IF (P.LT.0.002D+0) THEN
      WRITE(25,1)
1     FORMAT(' ERROR(VF)....Pressure less than 0.002 MPa')
      STOP
      ELSEIF (P.GT.21.5D+0) THEN
      WRITE(25,2)
2     FORMAT(' ERROR(VF)....Pressure greater than 21.5 MPa')
      STOP
      ELSEIF (P.GE.0.002D+0.AND.P.LT.0.01468D+0) THEN
      VF=1.9118D-4 * P**0.546472D+0 + 0.0009947D+0
      RETURN
      ELSEIF (P.GE.0.01468D+0 .AND. P.LT.0.275D+0) THEN
      VF=1.380934D-4 * P**0.388715D+0 + 0.000987D+0
      RETURN
      ELSEIF (P.GE.0.275D+0 .AND. P.LE.1.0D+0) THEN
      VF=1.2746977D-4* P**0.4644339D+0 +0.001D+0
      RETURN
      ELSEIF (P.GT.1.0D+0 .AND. P.LE.3.88D+0) THEN
      VF=1.0476071D-4* P**0.5651090D+0 +0.001022D+0
      RETURN
      ELSEIF (P.GT.3.88D+0 .AND. P.LE.8.84D+0) THEN
      VF=3.2836717D-5* P +1.12174735D-3
      RETURN
      ELSEIF (P.GT.8.84D+0 .AND. P.LE.14.463D+0) THEN
      VF=3.3551046D-4 * EXP(0.058403566D+0 *P) +0.00085D+0
      RETURN
      ELSEIF (P.GT.14.463D+0 .AND. P.LT.18.052D+0) THEN
      VF= 3.1014626D-8* P**3.284754D+0 +0.00143D+0
      RETURN
      ELSEIF (P.GE.18.052D+0 .AND. P.LT.20.204D+0) THEN
      VF= 1.5490787D-11* P**5.7205D+0 +0.001605D+0
      RETURN
      ELSE
      VF= 4.1035988D-24* P**15.03329D+0 +0.00189D+0
      RETURN
      ENDIF
      RETURN
      END
```

Function VG

```
      FUNCTION VG(P)
C This function calculates the specific volume of light water
C in the gas phase at saturation for a given pressure.
C Pmin = 0.002, Pmax = 21.5 MPa       (V)
      IMPLICIT REAL*8 (A-H,O-Z)
      IF (P.LT.0.002D+0) THEN
      WRITE(25,1)
1     FORMAT(' ERROR(VG)....Pressure less than 0.002 MPa')
      STOP
      ELSEIF (P.GT.21.5D+0) THEN
      WRITE(25,2)
2     FORMAT(' ERROR(VG)....Pressure greater than 21.5 MPa')
      STOP
      ELSEIF (P.GE.0.002D+0 .AND. P.LT.0.2139D+0) THEN
      VG= 1.0D+0/ (5.0981616D+0 * P**0.936226D+0 - 0.00025D+0)
      RETURN
      ELSEIF (P.GE.0.2139D+0.AND.P.LT.1.112D+0) THEN
      VG= 1.0D+0/(5.126076D+0* P**0.9475862D+0 +0.012D+0)
      RETURN
      ELSEIF (P.GE.1.112D+0.AND.P.LT.3.932D+0) THEN
      VG= 1.0D+0/(4.630832D+0* P**1.038819D+0 +0.52D+0)
      RETURN
      ELSEIF (P.GE.3.932D+0.AND.P.LT.8.996D+0) THEN
      VG= 1.0D+0/(2.868721D+0* P**1.252148D+0 +3.80D+0)
      RETURN
      ELSEIF (P.GE.8.996D+0.AND.P.LT.14.628D+0) THEN
      VG= 1.0D+0/(0.5497653D+0* P**1.831182D+0 +18.111D+0)
      RETURN
      ELSEIF (P.GE.14.628D+0.AND.P.LE.18.21D+0) THEN
      VG=1.0D+0/(8.5791582D-3* P**3.176484D+0 +50.0D+0)
      RETURN
      ELSEIF (P.GT.18.21D+0.AND.P.LE.20.253D+0) THEN
      VG= 1.0D+0/( 3.5587113D-6* P**5.660939D+0 +88.0D+0)
      RETURN
      ELSE
      VG= 1.0D+0/( 3.558734D-16* P**13.03774D+0 +138.0D+0)
      RETURN
      ENDIF
      RETURN
      END
```

Function PSAT

```
      FUNCTION PSAT(T)
C This function calculates the saturation pressure of light water
C for a given temperature.      (V)
C Tmin = 18.0, Tmax = 373.0
      IMPLICIT REAL*8 (A-H,O-Z)
      IF (T .LT. 1.80D+1) THEN
      WRITE(25,1)
1     FORMAT(' ERROR(PSAT)....Temperature less than 18.0 C')
      STOP
      ELSEIF (T .GT. 3.730D+2) THEN
      WRITE(25,2)
2     FORMAT(' ERROR(PSAT)....Temperature greater than 373.0 C')
      STOP
      ELSEIF (T.GE.1.80D+1.AND.T.LT.5.6275D+1) THEN
      PSAT=((T+9.92D+1)/2.70121D+2)**7.406365D+0
      RETURN
      ELSEIF (T.GE.5.6275D+1.AND.T.LT.9.088D+1) THEN
      PSAT=((T+7.82D+1)/2.546831D+2)**6.4058216D+0
      RETURN
      ELSEIF (T.GE.9.088D+1.AND.T.LT.1.39781D+2) THEN
      PSAT=((T+5.70D+1)/2.362315D+2)**5.602972D+0
      RETURN
      ELSEIF (T.GE.1.39781D+2.AND.T.LT.2.03662D+2) THEN
      PSAT=((T+2.80D+1)/2.079248D+2)**4.778504D+0
      RETURN
      ELSEIF (T.GE.2.03662D+2.AND.T.LE.2.99407D+2) THEN
      PSAT=((T+5.0D+0)/1.850779D+2)**4.304376D+0
      RETURN
      ELSEIF (T.GT.2.99407D+2.AND.T.LT.3.55636D+2) THEN
      PSAT=((T+1.60D+1)/1.951819D+2)**4.460843D+0
      RETURN
      ELSE
      PSAT=((T+5.00D+1)/2.272963D+2)**4.960785D+0
      RETURN
      ENDIF
      RETURN
      END
```

Function TSAT

```
      FUNCTION TSAT(P)
C This function calculates the saturation temperature of light water
C for a given pressure.              (V)
C Pmin = 0.002, Pmax = 21.5 MPa
      IMPLICIT REAL*8 (A-H,O-Z)
      IF (P.LT.2.D-3) THEN
      WRITE(25,1)
1     FORMAT(' ERROR(TSAT)....Pressure less than 0.002 MPa')
      STOP
      ELSEIF (P.GT.2.15D+1) THEN
      WRITE(25,2)
2     FORMAT(' ERROR(TSAT)....Pressure graeter than 21.5 MPa')
      STOP
      ELSEIF (P.GE.2.D-3 .AND. P.LT.1.672D-2) THEN
      TSAT=2.70121D+2 * P**1.35019D-1 - 9.92D+1
      RETURN
      ELSEIF (P.GE.1.672D-2 .AND. P.LT.7.25D-2) THEN
      TSAT=2.546831D+2 * P**1.56108D-1 - 7.82D+1
      RETURN
      ELSEIF (P.GE.7.25D-2.AND.P.LE.3.59D-1) THEN
      TSAT=2.362315D+2* P**1.784767D-1 -5.70D+1
      RETURN
      ELSEIF (P.GT.3.59D-1.AND.P.LE.1.676D+0) THEN
      TSAT=2.079248D+2* P**2.092705D-1 -2.80D+1
      RETURN
      ELSEIF (P.GT.1.676D+0.AND.P.LE.8.511D+0) THEN
      TSAT=1.850779D+2* P**2.323217D-1 -5.0D+0
      RETURN
      ELSEIF (P.GT.8.511D+0.AND.P.LE.1.769D+1) THEN
      TSAT=1.951819D+2* P**2.241729D-1 - 1.60D+1
      RETURN
      ELSE
      TSAT= 2.272963D+2*P**2.01581D-1 - 5.00D+1
      RETURN
      ENDIF
      RETURN
      END
```

Function DF

```
      FUNCTION DF(P)
C This function calculates the density of light water in the
C liquid phase at saturation for a given pressure.
C Pmin = 0.002, Pmax = 21.5 MPa      (V)
      IMPLICIT REAL*8 (A-H,O-Z)
      PMIN =  0.002D+0
      PMAX = 21.5D+0
      IF (P .LT. PMIN) THEN
      WRITE(25,1)
1     FORMAT(' ERROR(DF)....Pressure less than 0.002 MPa')
      STOP
      ELSEIF (P .GT. PMAX) THEN
      WRITE(25,2)
2     FORMAT(' ERROR(DF)....Pressure greater than 21.5 MPa')
      STOP
      ELSEIF (P.GE.0.002D+0 .AND. P.LT.0.01468D+0) THEN
      DF=1.D+0/ (1.9118D-4 * P**0.546472D+0 + 0.0009947D+0)
      RETURN
      ELSEIF (P.GE.0.01468D+0 .AND. P.LT.0.275D+0) THEN
      DF=1.D+0/ (1.380934D-4 * P**0.388715D+0 + 0.000987D+0)
      RETURN
      ELSEIF (P.GE.0.275D+0.AND.P.LE.1.0D+0) THEN
      DF=1.D+0/(1.2746977D-4* P**0.4644339D+0 +0.001D+0)
      RETURN
      ELSEIF (P.GT.1.0D+0.AND.P.LE.3.88D+0) THEN
      DF=1.D+0/(1.0476071D-4* P**0.5651090D+0 +0.001022D+0)
      RETURN
      ELSEIF (P.GT.3.88D+0.AND.P.LE.8.84D+0) THEN
      DF=1.D+0/(3.2836717D-5* P +1.12174735D-3)
      RETURN
      ELSEIF (P.GT.8.84D+0.AND.P.LE.14.463D+0) THEN
      DF=1.D+0/(3.3551046D-4 * EXP(0.058403566D+0 *P) +0.00085D+0)
      RETURN
      ELSEIF (P.GT.14.463D+0.AND.P.LT.18.052D+0) THEN
      DF= 1.D+0/(3.1014626D-8* P**3.284754D+0 +0.00143D+0)
      RETURN
      ELSEIF (P.GE.18.052D+0.AND.P.LT.20.204D+0) THEN
      DF= 1.D+0/(1.5490787D-11* P**5.7205D+0 +0.001605D+0)
      RETURN
      ELSE
      DF= 1.D+0/(4.1035988D-24* P**15.03329D+0 +0.00189D+0)
      ENDIF
      RETURN
      END
```

Subroutine INTRPLT1

```
      SUBROUTINE INTRPLT1(PRSSM,DSL,DSV,HFG,CPL,VSL,ZKL,
     >PRL,ST,CTE)
C This subroutine interpolates  the  thermophysical properties of
C saturated water  such as  saturation temperature and  pressure,
C vapor and liquid densities,heat of vaporization,liquid specific
C heat, viscosity, thermal conductivity,  Prandtl number, surface
C tension and expansion coefficient.   (V)
      IMPLICIT REAL*8 (A-H,O-Z)
      DIMENSION TPSW1(35,10),TPSW2(45,6),TMPR(10)
      COMMON /TTPSW/ TPSW1,TPSW2
      I=2
      IF (PRSSM.LT.0.10133D+0) THEN
      WRITE(25,1)
1     FORMAT(' ERROR(INTRPLT1)....Pressure less than 0.10133 MPa')
      STOP
      ELSE IF (PRSSM.GT.22.12D+0) THEN
      WRITE(25,2)
2     FORMAT(' ERROR(INTRPLT1)....Pressure greater than 22.12 MPa')
      STOP
      END IF
      PRSS=PRSSM*1.D+1
10    IF (PRSS.GE.TPSW1(I-1,1).AND.PRSS.LT.TPSW1(I,1)) THEN
      DELP2=TPSW1(I-1,1)-PRSS
      DO 20 J=1,10
      DELP1=TPSW1(I-1,1)-TPSW1(I,1)
      DELR1=TPSW1(I-1,J)-TPSW1(I,J)
      DELR2=((DELP2*DELR1)/DELP1)
      TMPR(J)=(-1.D+0*(-TPSW1(I-1,J)+DELR2))
20    CONTINUE
      GO TO 30
      ELSE
      I=I+1
      IF (I.GT.35) THEN
      WRITE(25,3)
3     FORMAT(' ERROR(INTRPLT1)....Teperature greater than crit. temp.')
      STOP
      END IF
      GO TO 10
      END IF
30    DSL=(1.D+0/TMPR(2))
      DSV=(1.D+0/TMPR(3))
      HFG=TMPR(4)
      CPL=TMPR(5)
      VSL=TMPR(6)
      ZKL=TMPR(7)
      PRL=TMPR(8)
      ST=TMPR(9)
      CTE=TMPR(10)
      RETURN
      END
```

Subroutine INTRPLT2

```
      SUBROUTINE INTRPLT2(TMPE,PRSS,SVF,SVG,EIF,EIG)
C This subroutine interpolates  the  thermophysical properties of
C saturated water  such as  saturation pressure, vapor and liquid
C specific volumes, vapor and liquid internal egergies given  its
C temperature.
      IMPLICIT REAL*8 (A-H,O-Z)
      DIMENSION TPSW1(35,10),TPSW2(45,6),TMPR(6)
      COMMON /TTPSW/ TPSW1,TPSW2
      I=2
      IF (TMPE.LT.0.D+0) THEN
      WRITE(25,1)
1     FORMAT(' ERROR(INTRPLT2)....Temperature less than 0.deg C')
      STOP
      ELSE IF (TMPE.GT.3.7414D+2) THEN
      WRITE(25,2)
2     FORMAT(' ERROR(INTRPLT2)....Temp. greater than crit. temp')
      STOP
      END IF
10    IF (TMPE.GE.TPSW2(I-1,1).AND.TMPE.LT.TPSW2(I,1)) THEN
      DELP2=TPSW2(I-1,1)-TMPE
      DO 20 J=1,6
      DELP1=TPSW2(I-1,1)-TPSW2(I,1)
      DELR1=TPSW2(I-1,J)-TPSW2(I,J)
      DELR2=((DELP2*DELR1)/DELP1)
      TMPR(J)=(-1.D+0*(-TPSW2(I-1,J)+DELR2))
20    CONTINUE
      GO TO 30
      ELSE
      I=I+1
      IF (I.GT.45) THEN
      WRITE(25,3)
3     FORMAT(' ERROR(INTRPLT2)....Temp. greater than crit. temp')
      STOP
      END IF
      GO TO 10
      END IF
30    PRSS=TMPR(2)*1.D-1
      SVF=TMPR(3)*1.D-3
      SVG=TMPR(4)*1.D-3
      EIF=TMPR(5)*1.D+3
      EIG=TMPR(6)*1.D+3
      RETURN
      END
```

Function REWPC

```
      FUNCTION REWPC(WCON,IFLGU)
C This function calculates external Reactivity for a given
C water content.
      IMPLICIT REAL*8 (A-H,O-Z)
      WW=WCON*1.D-3
      IF (WW.LT.0.D+0) THEN
      WRITE(25,1)
1     FORMAT(' ERROR(REWPC)....Water content negative')
      STOP
      ELSEIF (WW.GT.7.973577D-1) THEN
      WRITE(25,2)
2     FORMAT(' ERROR(REWPC)....Water content > 0.797gr/cc')
      STOP
      ELSE
      IF (IFLGU.EQ.0) THEN
C External reactivity driving force function due to accidental
C water leakage into a 5000 kg cylindrical blender(D=106.92 cm,
C H=244.96 cm) containing uranium dioxide powder at 5 w/o U-235.
C The reactivity data set was calculated using Criticality Safety
C Analysis Sequence No.1(CSAS1X) of SCALE-4 system. (V)
C                  ***[Powder density=2.2g/cc]***
      REWPC=(-4.34888D+2+(8.39353D+3*WW)+(-8.16329D+4*(WW**2.D+0))+
     >(4.92226D+5*(WW**3.D+0))+(-1.904230D+6*(WW**4.D+0))+
     >(4.790320D+6*(WW**5.D+0))+(-7.775430D+6*(WW**6.D+0))+
     >(7.839210D+6*(WW**7.D+0))+(-4.458370D+6*(WW**8.D+0))+
     >(1.091800D+6*(WW**9.D+0)))
      ELSEIF (IFLGU.EQ.1) THEN
C External reactivity driving force function due to accidental
C water leakage into a 1106.52 kg cylindrical blender (D=80.00 cm,
C H=100.00 cm) containing uranium dioxide powder at 5 w/o U-235.
C The reactivity data set was calculated using Criticality Safety
C Analysis Sequence No.1(CSAS1X) of SCALE-4 system. (V)
C                  ***[Powder density=2.2g/cc]***
      REWPC=(-7.16295D+2+(9.81512D+3*WW)+(-6.32538D+4*(WW**2.D+0))+
     >(2.35277D+5*(WW**3.D+0))+(-5.22112D+5*(WW**4.D+0))+
     >(6.79929D+5*(WW**5.D+0))+(-4.78393D+5*(WW**6.D+0))+
     >(1.40132D+5*(WW**7.D+0)))
      ELSEIF (IFLGU.EQ.2) THEN
C External reactivity driving force function due to accidental
C water leakage into a 500.00 kg cylindrical blender (D=80.00 cm,
C H=100.00 cm) containing uranium dioxide powder at 5 w/o U-235.
C The reactivity data set was calculated using Criticality Safety
C Analysis Sequence No.1(CSAS1X) of SCALE-4 system. (V)
C                  ***[Powder density=1.0g/cc]***
      REWPC=(-1.6642D+3+(2.50627D+4*WW)+(-1.68985D+5*(WW**2.D+0))+
     >(6.33003D+5*(WW**3.D+0))+(-1.389600D+6*(WW**4.D+0))+
     >(1.773550D+6*(WW**5.D+0))+(-1.216520D+6*(WW**6.D+0))+
     >(3.46251D+5*(WW**7.D+0)))
      END IF
      END IF
      RETURN
      END
```

Function RECIT

```
      FUNCTION RECIT(WLR,VOL,IFLGU)
C This function calculates the constant water ingress rate
C corresponding to an initial reactivity addition rate.
      IMPLICIT REAL*8 (A-H,O-Z)
      WW=0.D+0
10    IF (IFLGU.EQ.0) THEN
      WW=(1.D+0/(-8.39353D+3))*(-4.34888D+2+(-8.16329D+4*
     >(WW**2.D+0))+ (4.92226D+5*(WW**3.D+0))+(-1.904230D+6*
     >(WW**4.D+0))+(4.790320D+6*(WW**5.D+0))+(-7.775430D+6*
     >(WW**6.D+0))+(7.839210D+6*(WW**7.D+0))+(-4.458370D+6*
     >(WW**8.D+0))+(1.091800D+6*(WW**9.D+0)))
       ELSEIF(IFLGU.EQ.1) THEN
      WW=(1.D+0/(-9.81512D+3))*(-7.16295D+2+(-6.32538D+4*
     >(WW**2.D+0))+(2.35277D+5*(WW**3.D+0))+(-5.22112D+5*
     >(WW**4.D+0))+(6.79929D+5*(WW**5.D+0))+(-4.78393D+5*
     >(WW**6.D+0))+(1.40132D+5*(WW**7.D+0)))
       ELSEIF(IFLGU.EQ.2) THEN
      WW=(1.D+0/(-2.50627D+4))*(-1.6642D+3+(-1.68985D+5*
     >(WW**2.D+0))+(6.33003D+5*(WW**3.D+0))+(-1.389600D+6*
     >(WW**4.D+0))+(1.773550D+6*(WW**5.D+0))+(-1.216520D+6*
     >(WW**6.D+0))+(3.46251D+5*(WW**7.D+0)))
       END IF
      IF (ABS(WWOLD-WW).LT.1.D-5) THEN
      WW1=WW
      WWOLD=WW
      GO TO 20
      ELSE
      WWOLD=WW
      GO TO 10
      END IF
20    IF (IFLGU.EQ.0) THEN
       WW=(1.D+0/(-8.39353D+3))*(-WLR+(-4.34888D+2+(-8.16329D+4*
     >(WW**2.D+0))+ (4.92226D+5*(WW**3.D+0))+(-1.904230D+6*
     >(WW**4.D+0))+(4.790320D+6*(WW**5.D+0))+(-7.775430D+6*
     >(WW**6.D+0))+(7.839210D+6*(WW**7.D+0))+(-4.458370D+6*
     >(WW**8.D+0))+(1.091800D+6*(WW**9.D+0))))
       ELSEIF(IFLGU.EQ.1) THEN
      WW=(1.D+0/(-9.81512D+3))*(-WLR+(-7.16295D+2+(-6.32538D+4*
     >(WW**2.D+0))+(2.35277D+5*(WW**3.D+0))+(-5.22112D+5*
     >(WW**4.D+0))+(6.79929D+5*(WW**5.D+0))+(-4.78393D+5*
     >(WW**6.D+0))+(1.40132D+5*(WW**7.D+0))))
       ELSEIF(IFLGU.EQ.2) THEN
      WW=(1.D+0/(-2.50627D+4))*(-WLR+(-1.6642D+3+(-1.68985D+5*
     >(WW**2.D+0))+(6.33003D+5*(WW**3.D+0))+(-1.389600D+6*
     >(WW**4.D+0))+(1.773550D+6*(WW**5.D+0))+(-1.216520D+6*
     >(WW**6.D+0))+(3.46251D+5*(WW**7.D+0))))
       END IF
      IF (ABS(WWOLD-WW).LT.1.D-5) THEN
      WW2=WW
      GO TO 30
      ELSE
      WWOLD=WW
      GO TO 20
      END IF
30    RECIT=((WW2-WW1)*1.D+3*VOL)
      RETURN
      END
```

Function GSTBS

```
      FUNCTION GSTBS(TEMP,TCA,EPS1)
C This function calculates the rate of radiant heat exchange
C between diffuse-grey surface to blackbody surrounding. (V)
      IMPLICIT REAL*8 (A-H,O-Z)
      IF (TEMP.GE.1.027D+3) THEN
      TT1=(1.027D+3)+(2.7315D+2)
      ELSE IF (TEMP.LE.0.D+0) THEN
      TT1=2.7315D+2
      ELSE
      TT1=TEMP+(2.7315D+2)
      END IF
      TT2=TCA+2.7315D+2
      SBC=5.67032D-8
      GSTBS=(SBC*EPS1*((TT1**4.D+0)-(TT2**4.D+0)))
      RETURN
      END
```

Function EMMC

```
      FUNCTION EMMC(TEMP)
C This function calculates the emmisivity of the container
C material for a given temperature.                    (V)
      IMPLICIT REAL*8 (A-H,O-Z)
C Emmisivity for alloyed(%8Ni-%18Ch) Steel  is equal to 0.35
C at 500 deg C.(assumed to be true for SS304 -Highly alloyed
C stainless steel with %8Ni-%18Ch- and constant with respect
C to temperature)
      TT=TEMP
      EMMC=0.35D+0
      RETURN
      END
```

Subroutine FHCYL

```
      SUBROUTINE FHCYL(VOL,DIAM,DOUT,BLEV,PLEV,PA,SA,VOLST,PI)
C This subroutine updates the geometric information
C for a cylindrical shaped system.          (V)
      IMPLICIT REAL*8 (A-H,O-Z)
      PLEV=(VOL/(PI*((DIAM/2.D+0)**2.D+0)))
C Lateral surface area
      IF (PLEV.GE.BLEV) THEN
      PLEV=BLEV
      PA=(PI*DOUT*BLEV)
      SA=0.D+0
      VOLST=0.D+0
      ELSE
      PA=(PI*DOUT*PLEV)
      SA=(PI*DOUT*(BLEV-PLEV))
      VOLST=(PI*((DIAM/2.D+0)**2.D+0)*(BLEV-PLEV))
      END IF
      RETURN
      END
```

Subroutine FHCONE

```
      SUBROUTINE FHCONE(HGT,DIAM1,DIAMO1,DIAM2,VOL,THETA,X,
     >THCNT,SPL,SPS,S,S1,S2,TERA,POWA,DIDW,STEA,DIUP,VOLST,BL,PI)
C This subroutine updates the geometric information
C for a conical shaped system.          (V)
      IMPLICIT REAL*8 (A-H,O-Z)
      DD1=DIAM1
      DD2=DIAMO1
      DIUPB=DIUP-(2.D+0*THCNT)
      SMVOL=(1.D+0/3.D+0)*PI*((DIAM2/2.D+0)**2.D+0)*X
      FLVOL=VOL+SMVOL
      FLHGT=(((FLVOL*3.D+0)/(PI*((TAN(THETA))**2.D+0)))**
     >(1.D+0/3.D+0))
      DIAM1=2.D+0*(SQRT((FLVOL*3.D+0)/(PI*FLHGT)))
      DIAMO1=DIAM1+(2.D+0*THCNT)
      HGT=FLHGT-X
      IF (HGT.GE.BL) THEN
      HGT=BL
      DIAM1=DD1
      DIAMO1=DD2
      SPL=S-S2
      SPS=0
      TERA=(((DIAM1/2.D+0)**2.D+0)*PI)
      POWA=(PI*((DIAMO1/2.D+0)+(DIDW/2.D+0))*SPL)
      STEA=0.D+0
      VOLST=0.D+0
      ELSE
      S1=SQRT(((X+HGT)**2.D+0)+((DIAMO1/2.D+0)**2.D+0))
      SPL=S1-S2
      SPS=S -S1
      TERA=(((DIAM1/2.D+0)**2.D+0)*PI)
      POWA=(PI*((DIAMO1/2.D+0)+(DIDW/2.D+0))*SPL)
      STEA=(PI*((DIUP/2.D+0)+(DIAMO1/2.D+0))*SPS)
      VOLST=(1.D+0/3.D+0)*PI*(BL-HGT)*(((DIUPB/2.D+0)**2.D+0)+
     >(DIUPB*DIAM1/4.D+0)+((DIAM1/2.D+0)**2.D+0))
      END IF
      RETURN
      END
```

Subroutine WPM1DYN

```
      SUBROUTINE WPM1DYN(NEQ,Y)
C This subroutine contains statements executed periodically on
C every communication interval for Model 1.
      IMPLICIT REAL*8 (A-H,O-Z)
      CHARACTER CFLGO*4
      DIMENSION AMDA(6),B(6),Y(NEQ)
      DIMENSION TPSW1(35,10),TPSW2(45,6)
      COMMON /TTPSW/ TPSW1,TPSW2
      COMMON /WPGEN/AMDA,B,CFLGO, IFLGC,IFLGS, PI,G, M, EPSIL,GEN,
     >SOURCE, ENRIC, DIN1, DIN2,THCNT, DIUP,DIDW, PL,BL, WW0, WLR,
     >TMP0, HGT0, PDNS0, REF0, DNS0, REACTOT,REACEX, REACFB,PRESS,
     >WMSS, DT,TMST,ZMUO2, HFTCA,BT,TCON,RHODENS,RHOHEIG, RHODOPP,
     >RHOREFL,WCON,REFHGT, PMSS,VOL,THETA,X, DOUT1, DOUT2,SPL,SPS,
     >S, S1, S2, TSTOP, TERA ,POWA,STEA,TOPA, BOTA,TCA,PRESS0,EF0,
     >TQT,WMSN,TWMSS,TOUT,IFLGM,IEDIT, IFLGE, IFLGW, ICNTF,IFTRAP,
     >ICHMS,WMQT,DTMS,VOLST,FRVOL,IFLGD, DELTA,R1,R2,R3,DSW,TMPW ,
     >CREAC,CPW,HFG,IFLGX,YOLD,WMSS0,IFLGB,IFLGA,IFLGU, ZNU,PRSFN,
     >SUBMUL,IDCP,EF20,CMSS
      COMMON /MXM/ ZPWMX,ZTMMX,ZNFMX,ZPRMX,ZWMMX,ZQLMX,ZSMMX,
     >             TPWMX,TTMMX,TNFMX,TPRMX,TWMMX,TQLMX,TSMMX
C
C Output results
C ---#Check if "SUBROUTINE F" is skipped by LSODE;
C     If answer is "YES" then update geometrical and reactivity
C     information.
      IF (IFTRAP.EQ.1) THEN
      IF (ICNTF.EQ.0.AND.TOUT.NE.DT) THEN
      CALL PRDCL(NEQ,Y)
      FRDNS=(RHODENS*((PDNS(TMPW,PDNS0))-DNS0))*BT
      FRHGT=(RHOHEIG*(PL-HGT0))*BT
      FRDPP=(RHODOPP*(TMPW-TMP0))*BT
      FRREF=(RHOREFL*(REFHGT-REF0))*BT
      RHOEX = REWPC(WCON,IFLGU)*BT
      REACEX=RHOEX/BT
      REACFB=(FRDNS+FRHGT+FRDPP+FRREF)/BT
      REACTOT=REACEX+REACFB
      ELSE
      ICNTF=0
      END IF
      END IF
C
C ---#Output results
      IF (IFLGE.EQ.1) THEN
      IF (TOUT.EQ.DT) THEN
      CALL WPOUT(NEQ, 0.D+0,IFLGW, Y, REACTOT, REACEX,REACFB,PRESS,
     >PH2O,PAIR,WMSS,SMSS,TCON,TMPW, CREAC,WMSN,VOLI,CFLGO)
      ELSE
      CALL WPOUT(NEQ,(TOUT-DT),IFLGW,Y,REACTOT,REACEX,REACFB,PRESS,
     >PH2O,PAIR,WMSS,SMSS,TCON,TMPW,CREAC, WMSN, VOLI,CFLGO)
      END IF
      END IF
C
C Stop water ingress if time is greater that TQT
      IF (TOUT.GT.TQT.AND.IFLGW.EQ.0) THEN
      IFLGW=1
      CREAC=REACEX
      IF (ICHMS.EQ.1) DT=DT*1.D+1
```

Subroutine WPM1DYN (cont.)

```
      END IF
C
C If IFLGW=1, stop water ingress at T = TQT
C         =0, continue adding water
      IF (IFLGW.EQ.1) THEN
      TTT=TQT
      ELSE
      TTT=TOUT
      END IF
C
C Calculate the total mass of ingress water
      WNAD=WLR*TTT
C
C Stop water ingress if total water mass is greater that WMQT
      IF (WNAD.GE.WMQT.AND.IFLGW.EQ.0) THEN
      IFLGW=1
      TQT=TOUT
      CREAC=REACEX
      IF (ICHMS.EQ.1) DT=DT*1.D+1
      END IF
C
C Total water mass=water added+initial water mass
      WMSS=WNAD+TWMSS
C
      RETURN
      END
```

Subroutine SCRNMKR

```
      SUBROUTINE SCRNMKR(IFLGM,WMSS,WLR,IEDIT,WMQT,IFTRAP,TQT,
     >TSTOP,ICHMS,IFLGC)
C This subroutine resets the computer screen.
      IMPLICIT REAL*8 (A-H,O-Z)
      DO JJ=1,5
      PRINT*
      END DO
      PRINT*,' ================================================
     >======================='
      PRINT*
      PRINT*,'    SSSSS    KK    KK  IIIIII  NN       NN   AAAAA
     >A   TTTTTTTT  HH    HH'
      PRINT*,'   SSSSSSS   KK   KK     II    NNN      NN  AAAAAA
     >AA     TT     HH    HH'
      PRINT*,'   SS   SS   KK  KK      II    NNNN     NN  AA
     >AA     TT     HH    HH'
      PRINT*,'   SS        KK KK       II    NN NN    NN  AA
     >AA     TT     HH    HH'
      PRINT*,'    SSSSS    KKK         II    NN  NN   NN  AAAAAA
     >AA     TT     HHHHHHHH'
      PRINT*,'     SSSSS   KKK         II    NN   NN  NN  AAAAAA
     >AA     TT     HHHHHHHH'
      PRINT*,'        SS   KK KK       II    NN    NN NN  AA
     >AA     TT     HH    HH'
      PRINT*,'   SS   SS   KK  KK      II    NN     NNNN  AA
     >AA     TT     HH    HH'
      PRINT*,'   SSSSSSS   KK   KK     II    NN      NNN  AA
     >AA     TT     HH    HH'
      PRINT*,'    SSSS    KK    KK  IIIIII  NN       NN  AA
     >AA     TT     HH    HH'
      PRINT*
      PRINT*,' ================================================
     >======================='
      PRINT*,'                  <<< By Benan BASOGLU - October 19
     >91 >>>'
      PRINT*
      IF (IFLGM.EQ.1) THEN
      PRINT*,'                        $$$  WET POWDER : MODEL  I  $$$'
      ELSEIF (IFLGM.EQ.2) THEN
      PRINT*,'                        $$$  WET POWDER : MODEL II  $$$'
      ELSEIF (IFLGM.EQ.3) THEN
      PRINT*,'                        $$$  WET POWDER : MODEL III $$$'
      END IF
      PRINT*
      BBB=((WMSS/WLR)/60.D+0)
      DDD=((WMQT/WLR)/60.D+0)
 5    WRITE(*,10) '  WIR:',WLR,   '   PIT:',BBB,    '  IEDIT:',
     >IEDIT ,' ICHMS:',ICHMS
      WRITE(*,10) '  TWI:',WMQT,  '   TIT:',BBB+DDD,' IFTRAP:',
     >IFTRAP,'   TQT:',INT(TQT)
      WRITE(*,10) '  IWM:',WMSS,  '   TWM:',WMSS+WMQT,'  IFLGC:',
     >IFLGC,' TSTOP:',INT(TSTOP)
      PRINT*
      PRINT*
10    FORMAT(A6,F10.4,3X,A7,F10.4,3X,A8,I5,8X,A7,I6)
      RETURN
      END
```

VITA

Benan Başoğlu was born in Ankara, Türkiye, on January 30, 1967. He attended İrfan Baştuğ elementary school (Ankara) for two years. He transferred to T.E.D. Ankara Lisesi (Ankara) and graduated from elementary, junior high, and high school in June 1978, June 1981, and June 1984, respectively. The following August he entered Hacettepe University (Ankara) where he received a Bachelor of Science Degree in Nuclear Engineering in June 1988. He worked for one year as a research assistant at the Hacettepe University.

In August 1989, he accepted a graduate scholarship at the University of Cincinnati (Ohio) and came to the United States to study in Nuclear Engineering. Mr. Başoğlu transferred to University of Tennessee, Knoxville in August 1990 accepting a research assistantship.

He received the Master of Science degree in Nuclear Engineering in August, 1992. Since that time, he has pursued the degree of Doctor of Philosophy in Nuclear Engineering.